JOC The Journal of Organic Chemistry

Article

Bu4NI Catalyzed Radical Induced Regioselective N-Alkylations and Arylations of Tetrazoles Using Organic Peroxides/Peresters

Suresh Rajamanickam, Chitranjan Sah, Bilal Ahmad Mir, Subhendu Ghosh, Garima Sethi, Vinita Yadav, Sugumar Venkataramani, and Bhisma K. Patel

J. Org. Chem., **Just Accepted Manuscript** • DOI: 10.1021/acs.joc.9b02875 • Publication Date (Web): 07 Jan 2020

Just Accepted

is published by the American Chemical Society. 1155 Sixteenth Street N.W., Washington, DC 20036

Bu_4NI Catalyzed Radical Induced Regioselective *N*-Alkylations and Arylations of Tetrazoles Using Organic Peroxides/Peresters

Suresh Rajamanickam,[†] Chitranjan Sah,[‡] Bilal Ahmad Mir,[†] Subhendu Ghosh,[†] Garima Sethi,[§] Vinita Yadav,[†] Sugumar Venkataramani,[‡]* and Bhisma K. Patel[†]*

[†]Department of Chemistry, Indian Institute of Technology Guwahati, Guwahati-781039, India

[‡]Department of Chemical Sciences, Indian Institute of Science Education and Research (IISER) Mohali, Sector 81, SAS Nagar, Knowledge City, Manauli-140306, India

[§]School of Chemical Sciences, Department of Chemistry, Central University of Haryana, Haryana-123031, India

Fax: (+91)361-26909762, E-mail: patel@iitg.ac.in

RECEIVED DATE (will be automatically inserted after the manuscript is accepted).

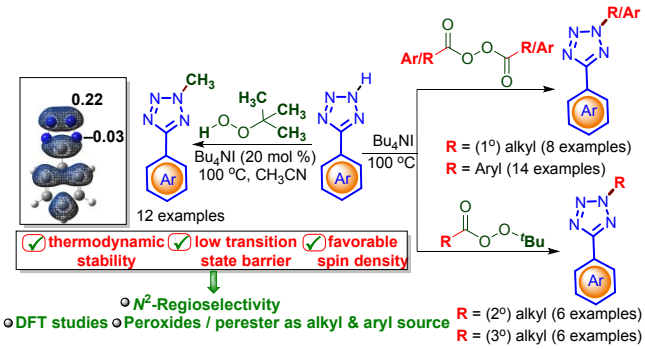

ABSTRACT: A Bu_4NI-catalyzed regioselective N^2-methylation, N^2-alkylation and N^2-arylation of tetrazoles have been achieved using *tert*-butyl hydroperoxide (TBHP) as the methyl, alkyl diacyl peroxides as the primary alkyl, alkyl peresters as the secondary and tertiary alkyls and aryl diacyl peroxides as the arylating sources. These reactions proceed without pre-functionalization of tetrazole and in the absence of any metal catalysts. Here, peroxides serve the dual role of oxidants as well as alkylating or arylating agents. Based on DFT calculations, it was found that spin density, transition state barriers (kinetic control) and thermodynamic stability of the products (thermodynamic control) play essentials roles in the observed regioselective during *N*-alkylation. This radical-mediated process is amenable to a broad range of substrates and provides products in moderate to good yields.

INTRODUCTION

Nitrogen center radicals (NCRs) are far less explored than the carbon center radicals due to the absence of an operationally simple process for their generations. Most of the NCRs are generated under a harsh and potentially explosive reaction conditions.[1] Historically, Hofmann-Löffler-Freytag reaction produce NCR via the homolytic cleavage of a *N*–halogen bond, forming an intramolecular C–N bond by abstracting a γ-hydrogen atom.[2] Very recently, a NCR is generated via a photo-induced cleavage of a N–X bond (where X = halogen or oxygen).[3] Even though, these processes are milder but are not economical. Thus, the search for alternative protocols for the direct conversion of N–H bonds in general and azoles in particular, to their corresponding NCRs under a mild condition is challenging. Transformation of azole N–H into a NCR and trapping it with appropriate coupling partners would lead to valuable target molecules. Barring a single report on the functionalization of an amide with an azole, there is no other report on nitrogen center azole radicals.[4]

Tetrazole based *N*-heterocyclic compounds have been investigated extensively owing to its usage in biology, pharmaceuticals, and material sciences.[5] Tetrazoles have found applications as ligands,[6] in agriculture as herbicides, and fungicides[7] and as a stabilizer in photography.[8] Due to their similar *p*Ka values, they serve as metabolically stable bioisosteres of carboxylic acid surrogates in medicinal chemistry.[9] For example, biphenyl tetrazoles are key intermediates for the preparation of multibillion-dollar angiotensin-II receptor antagonist, a class of high blood pressure agents such as valsartan, losartan, candesartan, and irbesartan (Figure 1).[10a-d] Whereas, pemirolast is an antiallergic, and azosemide is a diuretic drug (Figure 1).[10e,f] In the above-mentioned drugs, the tetrazole moiety is present in its free NH form. Among tetrazole derivatives, *N*–alkylated tetrazoles are important synthetic targets as they are found in bioactive compounds, chemical intermediates, and energy-intensive materials.[11] Recently, a *N*–methylated tetrazole core, tedizolid phosphate (Sivextro) has been approved by the US FDA for the treatment of acute bacterial skin and skin structure infections caused by susceptible gram-positive pathogens, including MRSA (Methicillin-Resistant Staphylococcus Aureus), MSSA (Methicillin-Sensitive Staphylococcus Aureus), VRE (Vancomycin-Resistant Enterococci) and Hi (Haemophilus influenza) bacterial strains (Figure 1).[12] Similarly, *N*-arylated tetrazoles HM30181 derivatives are potent and selective inhibitors of breast cancer resistance protein (BCRP/ABCG2) (Figure 1).[13]

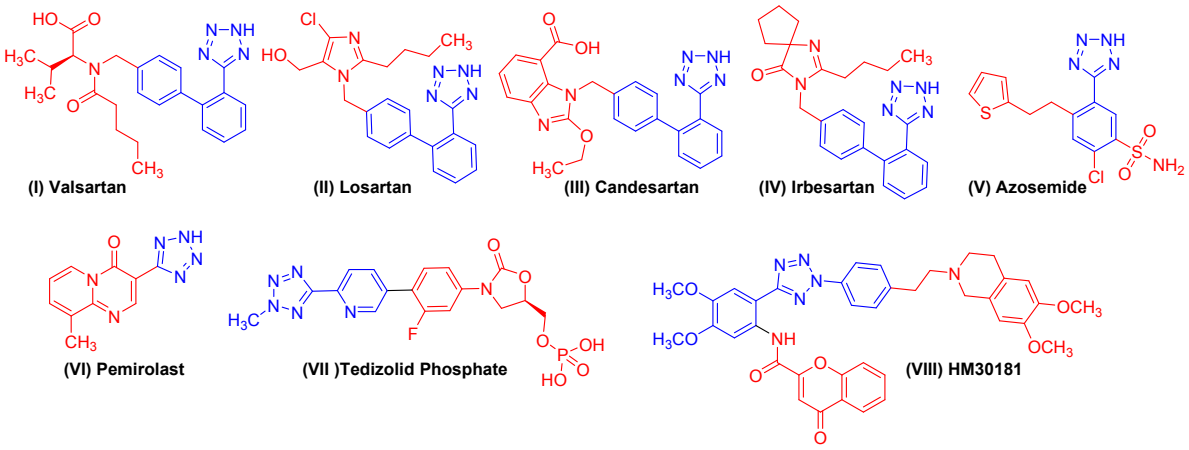

Figure 1. Representative biologically active tetrazole containing molecules.

The classical method for the synthesis of *N*-alkylated tetrazole is via the nucleophilic substitution reaction of tetrazole with an alkyl halide in the presence of a base. Due to the existence of two isomeric forms viz. 5-phenyl-1*H*-tetrazole or N^1 (**1x**) and 5-phenyl-2*H*-tetrazole or N^2 (**1**) (Scheme 1, Table 1) the selective alkylation of tetrazole is highly challenging as it is reported to give a mixture of regioisomeric products.[12d,e,14a,b] The silylated or stannylated derivatives of tetrazoles are alkylated regioselectively using chloroformates or cyanoformates via the *in situ* generated urethanes, which rearranges to a *N*-alkyl product with concurrent loss of carbon dioxide.[14c] Regioselective metal-fee alkylation of tetrazole is accomplished using cheap and readily available methylarenes,[14d,e] ethers[14e-g] via oxidative couplings. On the other hand, the regioselective N^2-arylation of tetrazole has been carried out by coupling tetrazole with an aryl boronic acid under Cu catalysis.[15] Alternatively, a Cu(II)-catalyzed *N*-arylation is accomplished by coupling pre-functionalized tetrazoles such as *N*-tributylstannyl or its *N*-sodium salt with a diaryliodonium salt. While the former gave a single regioisomer (N^2-arylation), the latter yielded a mixture of regioisomers.[16] No doubt the metal-catalyzed reactions are advantageous but are not always appreciated in the synthesis of pharmaceuticals, owing to the difficulties in the removal of traces of transition-metal residues from the final product. Therefore, it is essential to develop a regioselective metal-free protocol for the *N*-arylation of tetrazole. Recently, *tert*-butyl hydroperoxide (TBHP),[17] diacyl peroxides,[18a-d] and alkyl perester[18b-f] have been utilized for various alkylation procedures. TBHP has been successfully employed as an oxidant cum methyl source for the oxidative esterification of benzylic alcohols, aryl carbaldehydes, and aryl carboxylic acids {Scheme 1(i)}.[17]

Scheme 1. Radical Mediated Alkylation Strategies

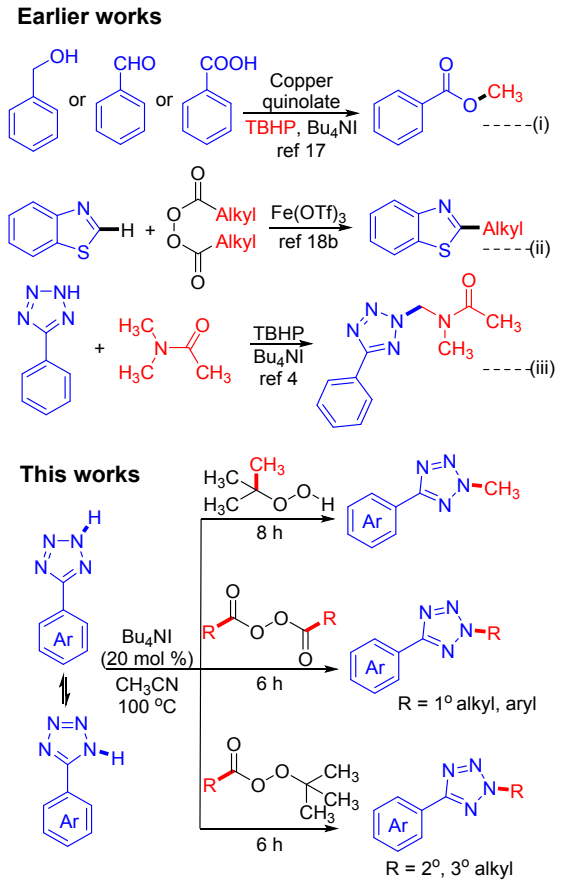

Alkyl radicals are generated from diacyl peroxides via the homolytic cleavage of peroxide bond followed by the extrusion of carbon dioxide (CO_2). These alkyl radicals are trapped with various reacting partners leading to useful products. Several fluoroalkanes have been prepared by treating diacyl peroxides with *N*-fluorobenzene sulfonimide under thermal or photochemical conditions.[18a] Synthesis of 2-alkyl benzothiazoles has been accomplished via a Fe-catalyzed decarboxylative C–H alkylation of benzothiazoles using diacyl peroxides {Scheme 1(ii)}.[18b] A radical-mediated coupling between a tetrazole and a *N*,*N*-dialkyl formamide leads to an exclusive formation of a N^2-alkylated tetrazole without giving any traces of N^1-alkylation {Scheme 1(iii)}.[4] Thus, it would be interesting to investigate whether regioselective N^2-alkylation of tetrazole can be achieved using TBHP as the methyl and diacyl peroxides/peresters as the alkyl sources.

RESULTS AND DISCUSSION

We initiated our exploration by examining the reaction between an aryl tetrazole (**1**) and *tert*-butyl hydroperoxide (TBHP) in decane (5–6 M) (3 equiv), in the presence of tetrabutylammonium iodide (Bu_4NI) (20 mol %) at 100 °C in DMSO. Interestingly, the reaction provided a *N*–methylated product in 39% yield (Table 1, entry 1), which is based on mass spectrometry and IR, ^1H and ^{13}C NMR spectroscopic analysis of the product (**1a**). However, whether the product obtained is a N^1 or a N^2 isomer it could not be ascertained. Incidentally, the reported melting point of the methylated N^1-isomer i.e., 1-methyl-5-phenyl-1*H*-tetrazole is 103–104 °C, whereas, the N^2-isomer i.e., 2-methyl-5-phenyl-2*H*-tetrazole (**1a**) melts at 49–50 °C.[19a] The melting point of the isolated compound was found to be 50–52 °C, which is in close agreement with the reported methylated N^2-isomer. Further, all the spectroscopic data (IR, ^1H and ^{13}C NMR) of the isolated compound (**1a**) is in agreement with the literature reported one, thereby confirming its structure to be a N^2-isomer, i.e., 2-methyl-5-phenyl-2*H*-tetrazole (**1a**).[19b-e] To obtain a satisfactory yield of the product (**1a**) various important reaction parameters such as solvents, catalysts, methylating source, and the temperature was tuned. By switching the oxidant from TBHP (in decane) to an aqueous TBHP (aq TBHP) (70% in water) (3 equiv) an improvement in the yield (47%) of (**1a**) was observed (Table 1, entry 2). Some other commercially available oxidants such as di-*tert*-butyl peroxide (DTBP) and *tert*-butyl peroxybenzoate (TBPB) were also examined under identical reaction conditions. While DTBP failed to give any trace of the product, the oxidant TBPB provided only 19% yield of (**1a**) along with numerous side products (Table 1, entries 3 and 4). The reaction was found to be extremely solvent dependent. As can be seen from Table 1, solvents such as DMF, DCE, MeOH were detrimental to the reaction (Table 1, entries 5–7). Pleasingly, the use of acetonitrile (CH_3CN) provided the desired methylated product (**1a**) in 60% yield (Table 1, entry 8). The reaction proceeds better in solvents such as $(CH_3)_2SO$, CH_3CN (Table 1, entries 2 and 8). Thus, it is possible that the methyl group present in $(CH_3)_2SO$ or CH_3CN might be serving as the possible source of the methyl group in the product (**1a**). To ascertain this, two reactions were carried out independently in deuterated DMSO-d_6 and CD_3CN solvents under otherwise identical reaction conditions (Table 1, entries 9 and 10). However, the isolated *N*-methyl tetrazole (**1a**) was found to be devoid of any deuterated methyl (CD_3) group, thereby suggesting neither the DMSO nor CH_3CN as the possible source of the methyl group. Thus, the methyl group is originating from the oxidant TBHP in this reaction. The reaction when performed in normal acetonitrile provided a low

yield of the product (**1a**) (41%) possibly because of the quenching of radicals by the dissolved oxygen in acetonitrile (Table 1, entry 11).

Table 1. Screening of the Reaction Conditions[a,b]

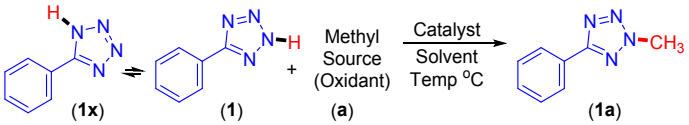

entry	oxidant (equiv)	catalyst (mol %)	solvent	yield (%)
1	dec. TBHP (3)	Bu_4NI (20)	DMSO	39
2	aq TBHP (3)	Bu_4NI (20)	DMSO	47
3	DTBP (3)	Bu_4NI (20)	DMSO	n.d.
4	TBPB (3)	Bu_4NI (20)	DMSO	19
5	aq TBHP (3)	Bu_4NI (20)	DMF	n.d.
6	aq TBHP (3)	Bu_4NI (20)	DCE	n.d.
7	aq TBHP (3)	Bu_4NI (20)	MeOH	n.d.
8	**aq TBHP (3)**	**Bu_4NI (20)**	**CH_3CN**	**60**
9	aq TBHP (3)	Bu_4NI (20)	DMSO-d_6	45
10	aq TBHP (3)	Bu_4NI (20)	CD_3CN	59
11[c]	aq TBHP (3)	Bu_4NI (20)	CH_3CN	41
12	aq TBHP (3)	Bu_4NF (20)	CH_3CN	n.d.
13	aq TBHP (3)	Bu_4NCl (20)	CH_3CN	19
14	aq TBHP (3)	Bu_4NBr (20)	CH_3CN	26
15	aq TBHP (3)	KI (20)	CH_3CN	50
16	aq TBHP (3)	NaI (20)	CH_3CN	42
17	aq TBHP (3)	I_2 (20)	CH_3CN	n.r.
18	aq TBHP (2)	Bu_4NI (20)	CH_3CN	53
19	aq TBHP (4)	Bu_4NI (20)	CH_3CN	62
20	aq TBHP (3)	Bu_4NI (10)	CH_3CN	48
21	aq TBHP (3)	Bu_4NI (30)	CH_3CN	62
22[d]	aq TBHP (3)	Bu_4NI (20)	CH_3CN	47
23[e]	aq TBHP (3)	Bu_4NI (20)	CH_3CN	61
24	aq TBHP (3)	--	CH_3CN	n.r.
25	--	Bu_4NI (20)	CH_3CN	n.r.

[a]Reaction conditions: 5-phenyl-2*H*-tetrazole (**1**) (1 mmol), solvent (2 m 100 °C under degassed condition. [b]Isolated yield after 8 h. [c]N acetonitrile without dried and degassed (AR grade). [d]At 90 °C. [e]At 11 n.d. = not detected. n.r. = no reaction.

Next a genre of quaternary ammonium salts such as Bu_4NF, Bu_4NCl and Bu_4NBr were tested, but all were found to be ineffective compared to Bu_4NI for this transformation (Table 1, entries 12–14). Other inorganic iodo salts such as KI and NaI when used in lieu of Bu_4NI, gave the product (**1a**) in 50% and 42% yields respectively, whereas I_2 failed to give any product (Table 1, entries 15–17). By

decreasing the quantity of aq TBHP from 3 to 2 equivalents, the product (**1a**) yield dropped from 60 to 53% but remained practically unchanged (62%) when 4 equivalents of TBHP was used (Table 1, entries 18 and 19). Similarly, by decreasing the quantity of catalyst Bu_4NI loading from 20 to 10 mol %, marginally reduced the yield (48%) of (**1a**) whereas, a higher catalyst loading (30 mol %) did not improve the yield any further (Table 1, entries 20 and 21). On decreasing the reaction temperature (90 °C), the yield of (**1a**) dropped to 47% but an increase in the temperature (110 °C), there was no significant improvement in the product yield 61% (Table 1, entries 22 and 23). Control experiments carried out in the absence of the catalyst (Bu_4NI) or oxidant (TBHP), failed to provide the desired product (**1a**) (Table 1, entries 24 and 25). After several optimizations (Table 1), it was found that a combination of aqueous TBHP (3 equiv), Bu_4NI (20 mol %) at 100 °C in CH_3CN solvent was found to be the most optimum for this *N*-methylation protocol (Table 1, entry 8).

Having established an optimized reaction condition, we set out to investigate the substrate scope of this metal-free regioselective *N*-methylation of aryl tetrazoles and the results are summarized in Scheme 2. This methodology was found to be highly successful for electron-neutral tetrazole (**1**) and a biphenyl tetrazole (**2**) providing their *N*-methylated tetrazoles (**1a**) and (**2a**) in 60% and 66% yields, respectively (Scheme 2). Similarly, aryl tetrazoles bearing electron-donating groups such as *p*-CH_3 (**3**), *p*-OCH_3 (**4**), *p*-*tert*-butyl (**5**) and *m*-OCH_3 (**6**) on the phenyl moiety of the tetrazole reacted smoothly to provide the expected products (**3a**, 61%), (**4a**, 59%), (**5a**, 64%) and (**6a**, 60%) in modest yields. Moderately electron-withdrawing halo substituents namely, *p*-Br (**7**), *p*-Cl (**8**), and *o*-Cl (**9**) irrespective of their position of attachments in the phenyl ring remained unaffected giving their *N*-methylated products (**7a**, 65%), (**8a**, 66%) and (**9a**, 61%). Further synthetic elaborations such as Suzuki coupling, Buchwald–Hartwig amination can be carried out at these halo sites of the products (**7a**–**9a**), if desired. The compound (**7a**) was crystallized from a supersaturated solution of chloroform by the slow evaporation method. The structure of the product (**7a**) and its regioselectivity has been unambiguously confirmed by X-ray crystallography (Scheme 2) (see the Supporting Information).

Scheme 2. Substrate Scope for *N*-Methylation of Aryl Tetrazoles[a,b]

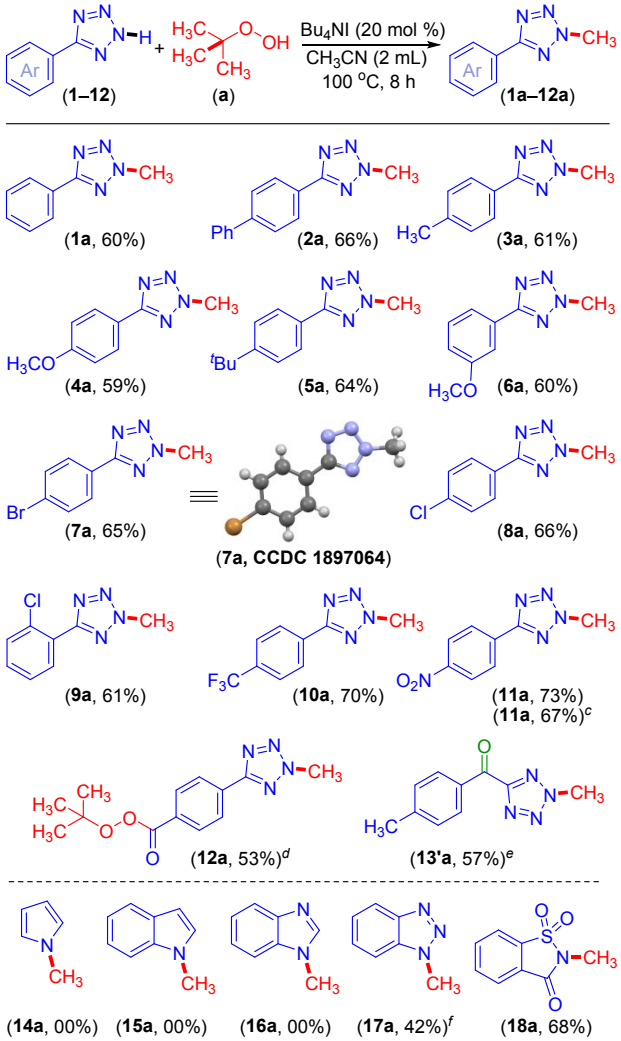

[a]Reaction conditions: aryl tetrazole (1 mmol), Bu_4NI (20 mol %) and aq TBHP (**a**) (3 equiv) at 100 °C in CH_3CN (2 mL) under degassed condition. [b]Isolated yields after 8 h. [c]Isolated yield reported for 8 mmol (1.53 g) scale. [d]4-(2*H*-tetrazol-5-yl)benzaldehyde was used as the starting material with 5 equivalents of aq TBHP. [e]5-(4-methylbenzyl)-2*H*-tetrazole was used as starting material with 5 equivalents of aq TBHP, 30 mol % of Bu_4NI. [f]1*H*-benzo[*d*][*1,2,3*]triazole (1 mmol), Bu_4NI (30 mol %) and aq TBHP (**a**) (4 equiv) at 120 °C in CH_3CN (2 mL) under degassed condition for 12 h.

Aryl rings of tetrazole possessing strongly electron-withdrawing substituents such as *p*-CF_3 (**10**) and *p*-NO_2 (**11**) delivered the corresponding *N*-methylated products (**10a**, 70%) and (**11a**, 73%) in good yields. To evaluate the potential and scope of this radical-induced *N*-methylation reaction, (**11**) and (**a**)

were reacted on 8 mmol scale (1.56 g), which provided 67% of the product 2-methyl-5-(4-nitrophenyl)-2*H*-tetrazole (**11a**) (Scheme 2). Tetrazole possessing an electron-withdrawing formyl group (**12**) was found to be extremely sensitive to the reaction. Under the standard reaction condition i.e., using 3 equivalents of TBHP, the expected *N*-methylated tetrazole was associated with peresterification at the aldehydic site and less than 10% yield of the product (**12a**) could be isolated. Such esterification of aldehydes using TBHP is well documented in the literature.[20] By increasing the quantity of TBHP to 5 equivalents, the *N*-methylated peresterified product (**12a**) was isolated in 53% yield. The formation of product (**12a**) supports a radical-mediated reaction pathway. It is well known that the aryl methyl groups are susceptible to oxidation under TBHP condition.[14d,e] But in the substrate (**3**), the methyl group remained intact and the alkylation took place at the tetrazole N–H site. This is because all the three equivalents of TBHP are used up during this transformation. Interestingly, a benzylic tetrazole viz. 5-[(4-methylphenyl)]-2*H*-tetrazole (**13**), when reacted with TBHP (**a**) gave *N*-methylated product (**13′a**) with concurrent oxidation at the benzylic position (Scheme 2).

To ascertain nature of the mechanism, when a reaction of 5-phenyl-2*H*-tetrazole (**1**) with TBHP (**a**) was performed in the presence of a radical quencher 2,2,6,6-tetramethylpiperidine *N*-oxide (TEMPO) (**b**) (2 equiv) under an identical reaction condition, only traces (9%) of N^2-methylated tetrazole (**1a**) was Isolated. However, the formation of a *O*-methylated TEMPO adduct (**ab**) could be detected by HRMS analysis of the reaction mixture (Scheme 3A). This trapping experiment confirms the generation of a methyl radical from TBHP in the medium. The use of cumene peroxide (**c**) *in lieu* of *tert*-butyl hydroperoxide (TBHP) may provide either a methylated tetrazole (**1a**) or a phenylated tetrazole (**1n**) (Scheme 3B). Interestingly, the treatment of cumene peroxide (**c**) with 5-phenyl-2*H*-tetrazole (**1**) provided an equimolar mixture of N^2-methylated product (**1a**) and acetophenone (**c′′**) without giving any trace of N^2-phenylated product (**1n**) (Scheme 3B). This observation suggests that the cleavage of a methyl radical from the intermediate 2-phenyl-2-propoxy radical is more favorable as it generates a stable secondary benzylic radical.[21] On the other hand, cleavage leading to a phenyl radical would leave behind a less stable isopropoxy radical, which is unfavorable. Next, a reaction of 5-phenyl-2*H*-tetrazole (**1**) was carried out with another radical scavenger 1,1-diphenylethylene (DPE) (**d**) (Scheme 3C). The reaction provided a 1,1-diphenyl-2-(5-phenyl-2*H*-tetrazol-2-yl)ethan-1-ol (**1d**) in 60% isolated yield. Thereby confirming the generation of nitrogen centered radical from tetrazole during the reaction.

Scheme 3. Control Experiments to Confirm the Radical Nature of the Reaction

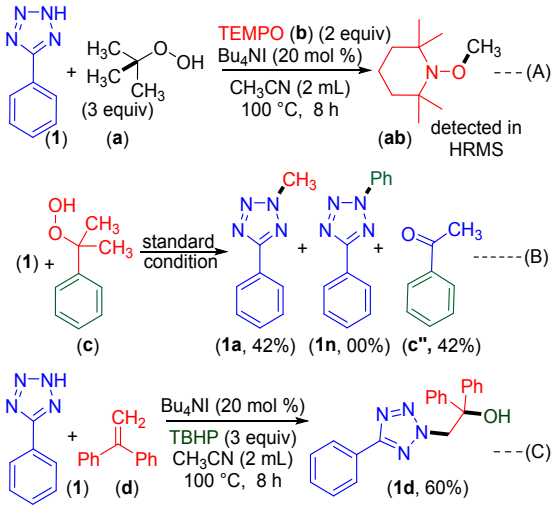

In order to understand the origin of regioselectivity in tetrazole, computations have been performed at DFT level. A preliminary potential energy surface (PES) scan calculations by varying the N=C–C=C dihedral angle of phenyl tetrazole in the increments of 10° revealed a planar structure as minima for both the isomeric tetrazoles 5-phenyl-2*H*-tetrazole (**1**) and 5-phenyl-1*H*-tetrazole (**1x**) as well as their corresponding radical isomers (**1′** and **1x′**) (Figure 2a).[22a] Indeed, the generation of radicals from N^2-H-tetrazole (**1**) and N^1-H-tetrazole (**1x**) were expected to give two distinguishable *N*-centered radicals (**1′**) and (**1x′**) via homolytic cleavage of N–H bonds. However, both of these lead to the same tetrazole radical (**1′**), which was basically a π-radical (indistinguishable) (Figure 2). This was further confirmed by inspecting the spin density and singly occupied molecular orbital (SOMO) (*vide infra*) [(Figure 2 (d)]. The scan showed maxima at 90 degrees for all the three species viz. (**1**), (**1x**) and the radical (**1′**), and the rotational energy barriers were estimated to be 5.4, 3.6 and 15.6 kcal/mol, respectively. The higher rotational barrier about N=C–C=C for radical (**1′**) also favor a coplanar orientation of the tetrazole ring relative to the phenyl ring (Figure 2). The true minima for each species have been optimized based on the PES scan calculations, and the resulting structures were further used for the estimation of bond dissociation energies (BDE).[22b]. The N–H BDE value corresponding to homolytic bond scission was found to be 97.2 and 99.5 kcal/mol for (**1x**) and (**1**), respectively. Presumably, the steric release between N–H (tetrazole) and the *ortho* C–H (phenyl) in (**1x**) could be responsible for lowering in BDE (Figure 2b).

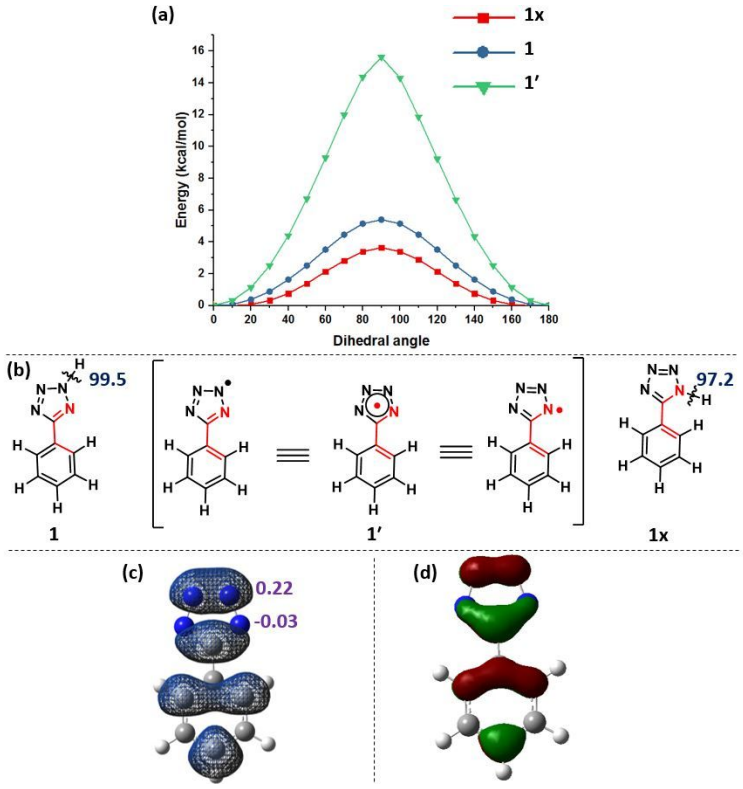

Figure 2. (a) Potential Energy Surfaces (PES) of **1, 1x** and **1′**; (b) Bond Dissociation Energy (BDEs) of **1** and **1x** (in kcal/mol); (c) Spin density and (d) Singly Occupied Molecular Orbital (SOMO) of the radical **1′** (isovalue 0.05). (All the computations have been performed at (U)B3LYP/cc-pVTZ level of theory).

In order to obtain further insights into regioselectivity, spin densities have been inspected for the *N*-centered radicals **1′** (Figure 2c). The spin densities in the radicals also confirmed that the spin is delocalized over the π-orbitals. Interestingly, the spin density was found to be more localized at the N^2-centered radical (**1′**) (0.22) compared to the N^1-centered radical (**1x'**) (-0.03) (Figure 2c). Once again, the SOMO of the tetrazolyl radical (**1′**) confirmed the π-radical character of it (Figure 2d). The larger spin density accounts for the higher reactivity at the N^2-site than at the N^1-in tetrazole. This could be one of the reasons for the regioselective product formation at the N^2 position.

Apart from spin density (Figure 2c), the regioselectivity at N^2-tetrazolyl (**1′**) compared to N^1-tetrazolyl (**1x′**) can also be explained on the basis of activation barriers for the reactions. In this regard, the transition states have been computed for the alkylation reaction with TBHP at N^1- and N^2-positions

of the tetrazolyl radical (**1′**). Computations predicted a barrier of 38.0 kcal/mol for the N^1-methylation, whereas for the N^2-methylation it is 32.6 kcal/mol. Further, the N^2-methylated product (**1a**) is both kinetically and thermodynamically more favored than the N^1-methylated product (**1xa**) by 5.4 and 6.1 kcal/mol, respectively (Figure 3, Table 2). The lower energy barrier for N^2-methylation of (**1′**) is due to marginal entropy preference as well as lower enthalpy contribution, which is also consistent with its positive spin density value (0.22) at the N^2-center (Figure 3). The thermodynamic stability of the N^2-methylated product can be due to the release of the steric factor arising between the methyl group and the phenyl C–H at the *ortho* position.

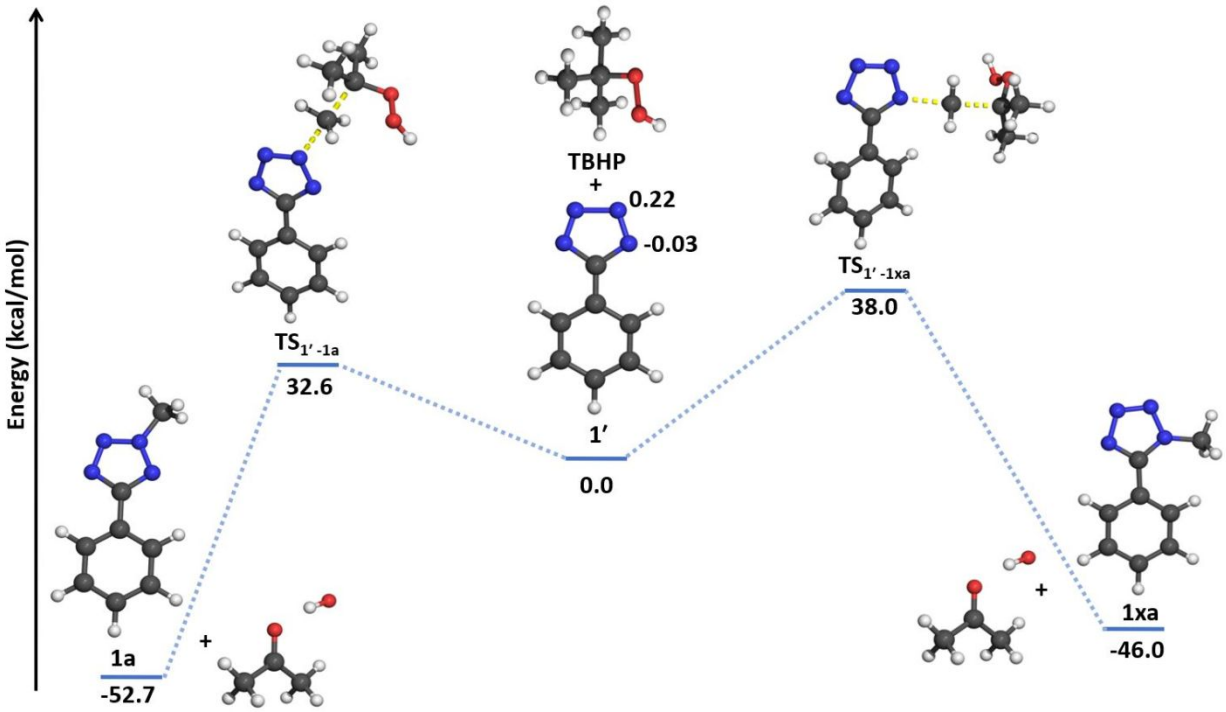

Figure 3. Energy profile in the N^1- and N^2-methylation of tetrazole radical (**1′**) with TBHP (All the reactants, products and transition states have been optimized at (U) B3LYP/cc-pVTZ level of theory).

After demonstrating the compatibility of a variety of aryl and alkyl tetrazoles and understanding the N^2-regioselectivity, other heterocycles possessing NH sites such as pyrrole (**14**), indole (**15**), benzimidazole (**16**) and benzotriazole (**17**) were tested (Scheme 2). All these azoles failed to give any *N*-methylated products even in a trace. To understand the failure behind *N*-methylation for these *N*-heterocycles (**14**–**17**) and N^2-regioselectivity of tetrazole (**1**), it is essential to understand the detailed mechanism of *N*-methylation.

Scheme 4. Proposed Mechanism for *N*–Methylation of Aryl Tetrazole

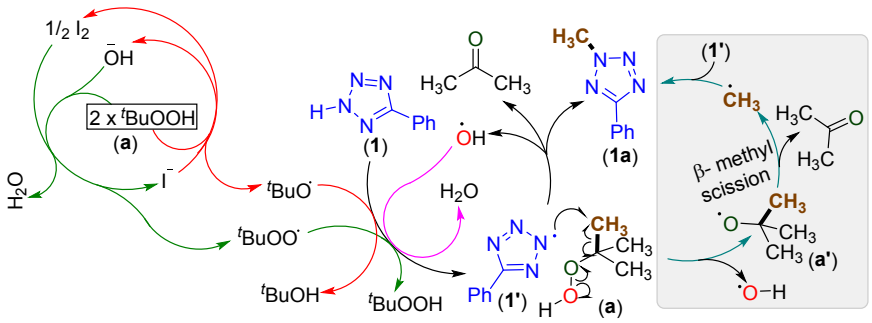

Initially, the oxidation of iodide (I^-) by TBHP (**a**) afforded a *tert*-butoxyl radical, iodine and a hydroxyl anion (Scheme 4, red arrows). The *in situ* generated iodine reacts with another molecule of TBHP and hydroxyl ion to generate a *tert*-butylperoxy radical and a molecule of water (Scheme 4, green arrows).[23] Any one of these radicals can abstract a hydrogen atom from the tetrazole N–H (**1**), to provide a persistent nitrogen-centered radical (**1′**). In order to obtain additional insights, computations have been performed for the H-abstraction reactions in creating NCR from the 5-phenyl-2*H*-tetrazole (**1**) and 5-phenyl-1*H*-tetrazole (**1x**) using iodine atom and *tert*-butoxy radical. Based on the results, we predicted a very low barrier for the *H*-abstraction by *tert*-butoxyl radical (1.9 kcal/mol) in the case of (**1**) (Figure S5).[24] Based on the barriers, it is very clear that the hydrogen abstraction is most likely happened through the *tert*-butyloxy radical as indicated in the Scheme 4 (See computational details in the SI-Figure S5). The concerted reaction between the tetrazolyl radical (**1′**) with TBHP led to a *N*-methylated product (**1a**) along with the formation of a molecule of acetone and an OH radical. Apart from this, possible concerted mechanism between the tetrazolyl radical and TBHP in the regioselective methylation, an alternative pathway through *β*-methyl scission from the *tert*-butoxyl radical (**a′**) leading to the fragments acetone and methyl radical, followed by a radical recombination step to the regioselective product has also been considered (Scheme 4). The barrier for such fragmentation of *tert*-butoxyl radical has been estimated to be 11.8 kcal/mol (Figure S7). However, our attempts in locating the corresponding transition states for the recombination step or a conceted "*β*-methyl scission–radical coupling" reaction were unsuccessful. The OH radical so generated may abstract a proton from the tetrazole to generate a tetrazolyl radical (**1′**), which may participate in the further reaction (Scheme 4, magenta arrow).

In yet another control experiment, TBHP was treated with TEMPO (in the absence of TBAI) in CD_3CN under an identical reaction conditions in a sealed tube. The ^{13}C NMR of the crude reaction

mixture confirmed the generation of a TEMPO methyl adduct (**ab**, Scheme S1) and acetone which was ascertained by the appearance of a carbonyl signals at 210.4 ppm. Thus, instead of a tetrazole radical (**1′**) the persistant radical TEMPO can also abstact a CH_3 group from the TBHP either via a concerted fashion (black arrows) or via β-methyl scission pathway (in the gray rectangle box). Thus, we concluded that both the concerted reaction between NCR and the TBHP, as well as the radical combination between the NCR and methyl radical formed through a β-methyl scission of ^{t}BuO/ *tert*-butoxyl radical (in the grey rectangular) might equally be plausible pathways (Scheme 4). Furthermore, the factors such as lower barrier (kinetic favourability), higher spin density (higher reactivity) and less steric factor (thermodynamic favourability) lead to higher regioselectivity in the N^2-alkylation.

Having understood the regioselective N^2-methylation in aryl tetrazoles the next objective is to find out the reason for the unsuccessful *N*- methylation for azoles (**14**–**17**) (Scheme 2). The spin density, activation barriers and thermodynamic stability of the products for all these *N*-heterocycles (**14**–**17**) were calculated at **(U)**B3LYP/cc-pVTZ level of theory. Based on the calculations, we concluded that all the three factors viz. high electron spin density around the nitrogen atom, lower activation barrier and higher thermodynamic stability of the products were found to be responsible for the *N*-alkylation. A negative spin density of -0.13 at the nitrogen center for the pyrrolyl radical (**14′**) suggests a complete π–delocalization of radical electron, which enhances the stability and lowers the reactivity.[25a-c] Despite having a moderately positive spin density values of 0.27, 0.13/0.42, and 0.20/0.47, at different nitrogen centers for the *N*-centered indolyl (**15′**), benzimidazolyl (**16′**), and benzotriazolyl (**17′**) radicals, respectively (Figure 4). The reactions failed in all these cases. Presumably, the delocalization of the spin (or the radical character in the fused ring system) along with a higher reaction barrier may hinder the reactivity in all these cases. In this regard, we compared the activation barriers for the *N*-methylation of all these species have also been estimated computationally (Table 2).

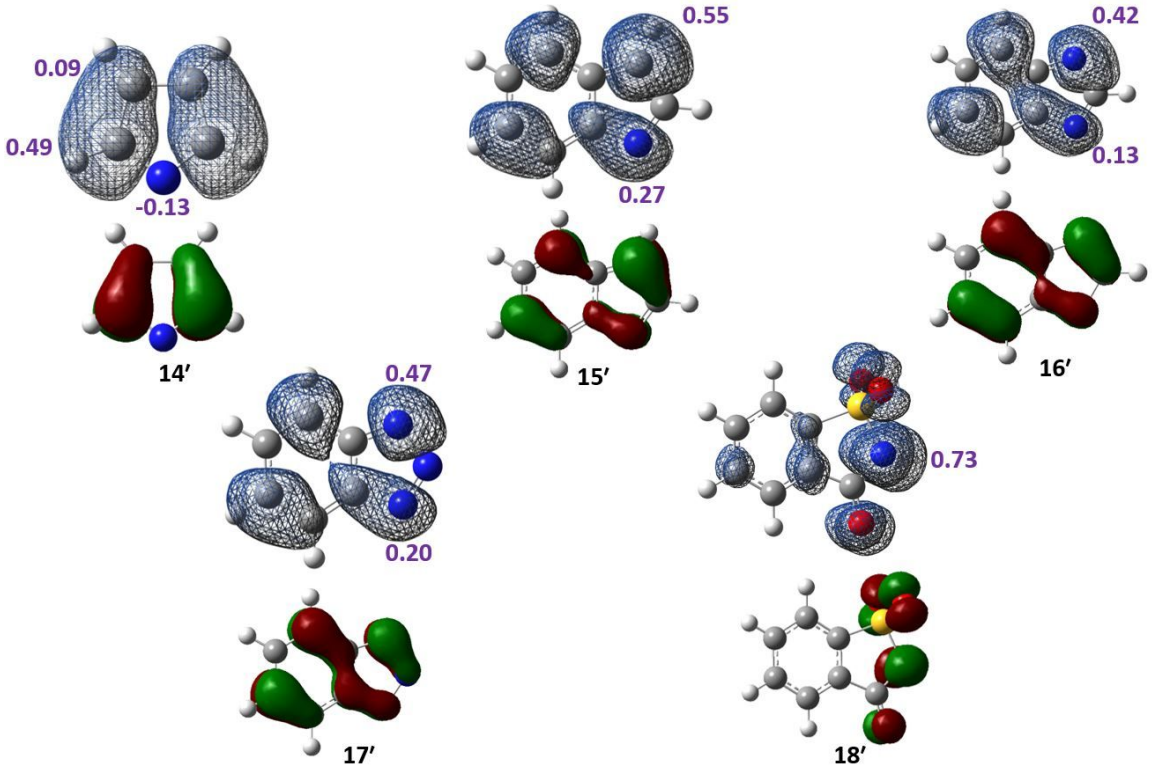

Figure 4. Spin densities and SOMO of various azole radicals **14′–18′** (Computations are performed at (U)B3LYP/cc-pVTZ level of theory; The MOs are rendered at an isovalue 0.05).

A high activation barrier of 51.1 and 42.7 kcal/mol, respectively were computed for indolyl (**15′**) and benzimidazolyl (**16′**) radicals compared to a barrier of 32.6 kcal/mol for N^2-tetrazolyl radical (**1′**), which could be the reason behind their reluctance to participate in the reaction. As can be seen from Table 2, all the anticipated products **14a**–**17a** showed higher stability relative to their respective reactants indicating thermodynamically favorable reactions. In spite of favorable spin density 0.20 and high thermodynamic stability (-53.3), benzotriazolyl radical (**17′**) failed to react under the present reaction condition, which can be due to higher activation barrier (35.2 kcal/mol) compared to N^2-tetrazolyl (**1′**) (32.6 kcal/mol). Interestingly, by carrying out the reaction at a higher temperature (120 ^{o}C) and high catalyst loading (30 mol %) leads to 42% of the product (**17a**). A radical-mediated oxidative imidation of ketones with saccharin (**18**) has been achieved using a combination of TBHP and Bu_4NI.[25d] A higher positive spin density value 0.73 of saccharin encouraged us to test the feasibility of similar *N*-methylation on saccharin (**18**). Interestingly *N*-methylation of saccharin (**18**) (Scheme 2) could be accomplished in 68% yield under the standard reaction condition. For this reaction, obtaining the kinetic barrier through the location transition state failed even after multiple

attempts. However, the larger spin density value (0.73) at the *N*-centre of saccharin radical (**18′**) and the inspection of its SOMO confirmed a more localization of the radical character at the *N*-center that can be attributed to its higher reactivity.

Table 2. Computed thermodynamic and kinetic parameters corresponding to the *N*-methylation reactions using TBHP for the various *N*-heterocycles.

reactant	product	thermodynamic parameters[a,b]		kinetic parameters[a,b,c]			
		relative energy	**ΔG^{o}**	**E_a**	**$\Delta G^{\ddagger}$**	**$\Delta H^{\ddagger}$**	**$\Delta S^{\ddagger}$**
(1′)–*N*²	**(1a)**	–52.7	–57.6	32.6	42.2	32.9	–31.0
(1′)–*N*¹	**(1xa)**	–46.6	–51.2	38.0	48.0	38.3	–32.6
(14′)	**(14a)**	–42.0	–47.0	50.3	60.1	50.7	–31.7
(15′)	**(15a)**	–38.9	–43.3	51.1	61.9	51.6	–34.6
(16′)	**(16a)**	–47.3	–51.5	42.7	52.9	43.1	–32.9
(17′)	**(17a)**	–53.3	–57.5	35.2	45.7	35.4	–34.4
(18′)	**(18a)**	–50.9	–61.0	-	-	-	-

[a]The thermodynamic (between products and reactants) and kinetic (between transition states and the reactants) parameters, were calculated at (U)B3LYP/cc-pVTZ level of theory; [b]All the energy values are expressed in kcal/mol; [c]$\Delta S^{\ddagger}$ values are expressed in cal/mol.K.

So far, we have delineated the *N*-methylating capability of commercially available *tert*-butyl hydroperoxide as the methyl source. Unfortunately, the higher alkyl analogs of similar reagents for ethylation, propylation etc. are neither commercially available nor they can be easily synthesized. One of the reagents, 2-hydroperoxy-2-methylpentane (**e**) is commercially available, which can be the source of both methyl and propyl radicals. Assuming similar stability of their corresponding alkyl (methyl or propyl) radicals there is 2/3rd probability of methylation and 1/3rd probability of propylation (Scheme 5). Can this reagent deliver regioselective propylation (if the radical stability is higher than the methyl radical) under the present reaction condition? When 5-phenyl-2*H*-tetrazole (**1**) was treated with 2-hydroperoxy-2-methylpentane (**e**) *in lieu* of TBHP under an otherwise identical condition provided both *N*-methylated (**1a**, 20%) and *N*-propylated (**1e**, 43%) products (Scheme 5).

Scheme 5. Regioselective Alkylation using Unsymmetrical Peroxide[a,b]

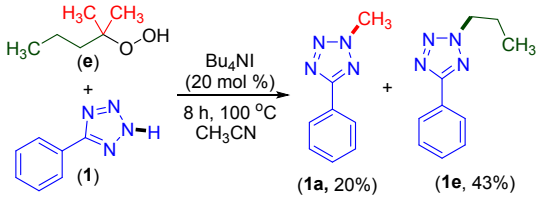

[a]Reaction conditions: 5-phenyl-2*H*-tetrazole (**1**) (1 mmol), Bu_4NI (20 mol %) and 2-hydroperoxy-2-methylpentane (**e**) (3 equiv) at 100 °C in CH_3CN (2 mL) under degassed condition. [b]Isolated yields after 8 h.

The success of this *N*-alkylation reaction is in general dependent on the generation of nitrogen centered radicals (NCR), as well as alkyl radicals. The higher homologs of alkyl radicals can be generated via the homolytic cleavage of a diacyl peroxide followed by the extrusion of carbon dioxide (CO_2).[18a-g] The long-chain *N*-alkylation of tetrazoles could be achieved by minor modification of the just established methylation protocol (Scheme 2). When the reaction was carried out using 1 equivalent of diacyl peroxide i.e., dihexanoyl peroxide (**f**), it provided 56% yield of (**1f**) (Scheme 6). However, the yield improved up to 74% using two equivalents of the peroxide (**f**). Many of the diacylperoxides are commercially not available and can be prepared by treating alkyl carboxylic acids with DCC, H_2O_2, DMAP in methylene chloride.[26] It would be advantageous if the same can be generated *in situ*. Thus, in a one-pot strategy all diacyl peroxide precursors (hexanoic acid, DCC, H_2O_2, DMAP), tetrazole and TBAI were added in a 1:1 mixture of DCM and CH_3CN and the reaction was allowed to proceed. The reaction did not give any trace of the *N*-alkylated product (**1f**). In another approach initially diacyl peroxide i.e., dihexanoyl peroxide (**f**) was generated *in situ* via a DCC mediated dehydrative condensation with hydrogen peroxide, which was used directly after simple filtration (without further purification). It leads to the formation of product 2-pentyl-5-phenyl-2*H*-tetrazole (**1f**) in 61% yield, which is 13% lower than when pure isolated peroxide (**f**) was used. Thus, we have used pure isolated diacylperoxides throughout the reaction. After few optimization reactions, it was found that the use of hexanoic peroxyanhydride (**f**) (2 equiv) and Bu_4NI (20 mol %) was necessary to achieve a decent yield (74%) of the N^2-alkylation (pentanylation) of aryl tetrazole (**1f**). The results of various other alkylations are portrayed in Scheme 6.

Scheme 6. Substrate Scope for *N*-Alkylation of Aryl Tetrazoles[a,b]

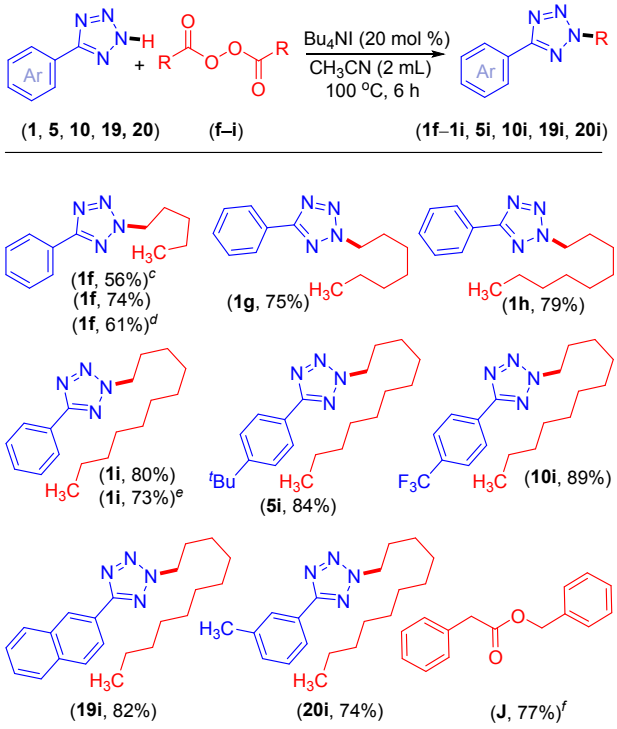

[a]Reaction conditions: aryl tetrazole (1 mmol), Bu_4NI (20 mol %) and alkyl diacyl peroxide (2 equiv) at 100 °C in CH_3CN under degassed condition (2 mL). [b]Isolated yield after 6 h. [c]One equivalent of dihexanoyl peroxide was used. [d]*In situ* generated dihexanoyl peroxide, simply filtered used for the reaction without purification. [e]Isolated yield reported for 8 mmol (1.17 g) scale. [f]2-phenylacetic peroxyanhydride was used as the starting material.

Treatment of alkyl peroxyanhydrides, such as octanoic (**g**), decanoic (**h**) and dodecanoic (**i**) with 5-phenyl-2*H*-tetrazole (**1**) smoothly afforded their anticipated N^2-heptanyl (**1g**, 75%), N^2-nonyl (**1h**, 79%) and N^2-undecanyl (**1i**, 80%) products (Scheme 6). To further explore the synthetic potential of this peroxyanhydrides mediated regioselective N^2-alkylation strategy, a variety of substituted aryl tetrazoles were investigated. Aryl tetrazoles substituted with electron-releasing group on *para*-position, namely *p-tert*-butyl (**5**), and electron-withdrawing *p*-CF_3 (**10**) groups, all successfully provided their corresponding N^2-undecylated products (**5i**, 84%), and (**10i**, 89%) in good yields. A 5-(naphthalen-2-yl)-2*H*-tetrazole (**19**) with dodecanoic peroxyanhydride (**i**) gave the targeted compound (**19i**) in synthetically useful yield (82%) (Scheme 6). Further, a *meta*-methyl substituted tetrazole successfully provide its N^2-undecanyl product (**20i**) in 74% yield. Judging from the trends in the yields of all the

preceding set of substrates in Scheme 6, long chain alkyl peroxyanhydrides delivered higher yields than short chain alkyl peroxyanhydrides. In an attempt to synthesize N^2-benzylated tetrazole following a similar strategy, tetrazole (**1**) was reacted with 2-phenylacetic peroxyanhydride (**j**), which failed to give any benzylated product. Under the reaction condition, the 2-phenylacetic peroxyanhydride decomposed to give a benzyl 2-phenylacetate (**J**) product (Scheme 6). Such decomposition of 2-phenylacetic peroxyanhydride (**J**) is well documented in the literature.[27]

After multiple attempts, secondary and tertiary alkyl diacyl peroxides could not be prepared as they tend to decompose even under extreme care.[28] On the other hand, Hongli Bao group have used secondary and tertiary alkyl peresters as 2° or 3° alkyl radical synthons in various systems instead of peroxides, as they are relatively easier to synthesize.[18c-g] Interestingly, the reaction between 5-phenyl-2*H*-tetrazole (**1**) and *tert*-butyl 2-ethylhexaneperoxoate (**k**) under the optimized reaction condition smoothly provided secondary N^2-alkylated tetrazole (**1k**). To demonstrate the versatility of this regioselective N^2-alkylation a variety of tetrazoles were tested. As can be seen from Scheme 7, aryl tetrazoles bearing electron-donating (*p*-OMe) (**4**) and electron-withdrawing [*o*-Cl (**9**), *p*-CF_3 (**10**), and *p*-NO_2 (**11**)] substituents afforded their corresponding products (**4k**, 71%), (**9k**, 73%), (**10k**, 82%), and (**11k**, 85%) in good to excellent yields. Apart from aryl tetrazoles, a thiophene attached tetrazole i.e., 5-(thiophen-2-yl)-2*H*-tetrazole (**21**) also underwent N^2-alkylation with perester (**k**) giving the corresponding product (**21k**) in 74% yield (Scheme 7). After regioselective installation of a secondary alkyl group onto aryl tetrazoles, we wish to install tertiary alkyl groups. Under the identical reaction conditions treatment of *tert*-butyl-2,2-dimethylpropaneperoxoate (**l**) with phenyl tetrazole (**1**) furnished the corresponding N^2-*t*-butylated product (**1l**) in 87% yield. Two other tetrazoles, one possessing an EDG, *p*-OMe (**4**) and another an EWG group *p*-NO_2 (**11**), both successfully underwent *t*-butylation at the N^2-position giving products (**4l**) and (**11l**) in 81% and 92% yields, respectively. Following this strategy, a tricyclic adamantyl group was successfully incorporated into a variety of aryl tetrazoles (**1**), (**10**), and (**11**) providing tertiary N^2-adamantyl tetrazoles (**1m**, 85%), (**10m**, 89%), and (**11m**, 90%), respectively (Scheme 7).

Scheme 7. Substrate Scope for *N*-Secondary and Tertiary Alkylation of Aryl Tetrazoles[a,b]

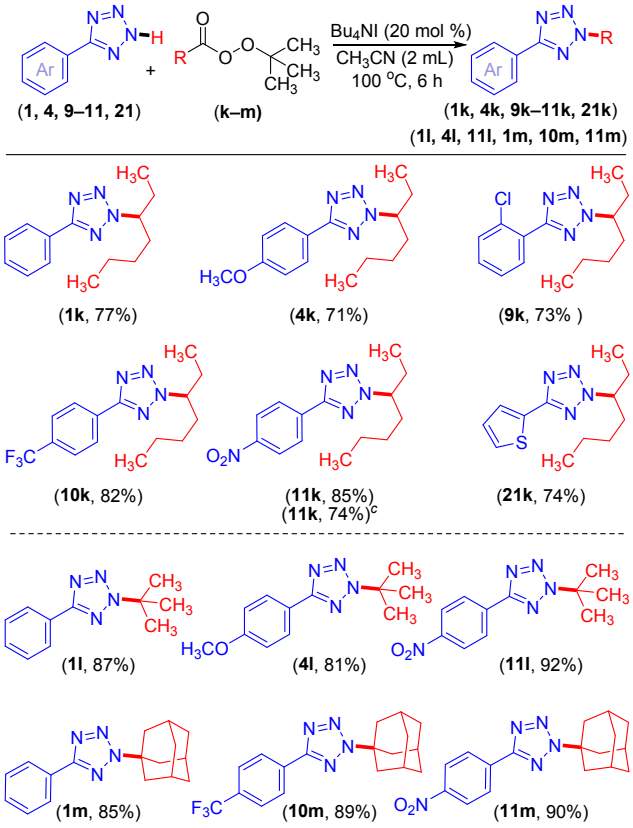

[a]Reaction conditions: aryl tetrazole (1 mmol), Bu_4NI (20 mol %) and *tert*-butyl alkylperoxoate (2 equiv) at 100 °C in CH_3CN under degassed condition (2 mL). [b]Isolated yield after 6 h. [c]Isolated yield reported for 8 mmol (1.53 g) scale.

A Pd(II) catalyzed *ortho*-arylation of directing arene has been successfully demonstrated using aroyl peroxyanhydride via a decarboxylative radical pathway.[29] After the efficacious alkylation using alkyl peroxyanhydrides ($(RCO)_2OO$) (Scheme 6) and taking cues from the *ortho*-arylation, we were encouraged to attempt various N^2-arylation using a number of aroyl peroxyanhydrides. Employing benzoic peroxyanhydride (**n**) as the aryl surrogate, its reaction with 5-phenyl-2*H*-tetrazole (**1**) under the optimized reaction condition afforded the N^2-phenyl substituted tetrazole (**1n**) in a satisfactory yield of 61% (Scheme 8). Similarly, aryl tetrazoles bearing various electron-donating *p*-CH_3 (**3**), *m*-OMe (**6**) and electron-withdrawing *p*-Br (**7**), *o*-Cl (**9**), *p*-CF_3 (**10**), and *p*-NO_2 (**11**) groups, all lead to their regioselective N^2-phenylation products (**3n**, 58%), (**6n**, 54%), (**7n**, 62%), (**9n**, 56%), (**10n**, 65%), and (**11n**, 67%) in modest yields, when treated with benzoic peroxyanhydride (**n**) (Scheme 8). Besides, aryl tetrazoles, 5-(thiophen-2-yl)-2*H*-tetrazole (**21**) also smoothly underwent coupling with benzoic

peroxyanhydride (**n**) exhibiting good compatibility providing the product (**21n**) in 63% yield. A *di*-substituted 5-(2-bromo-4-methylphenyl)-2*H*-tetrazole (**22**) reacted successfully with benzoic peroxyanhydride (**n**) giving its *N*-phenylated tetrazole (**22n**).

Scheme 8. Substrate Scope for *N*-Arylation of Aryl Tetrazoles[a,b]

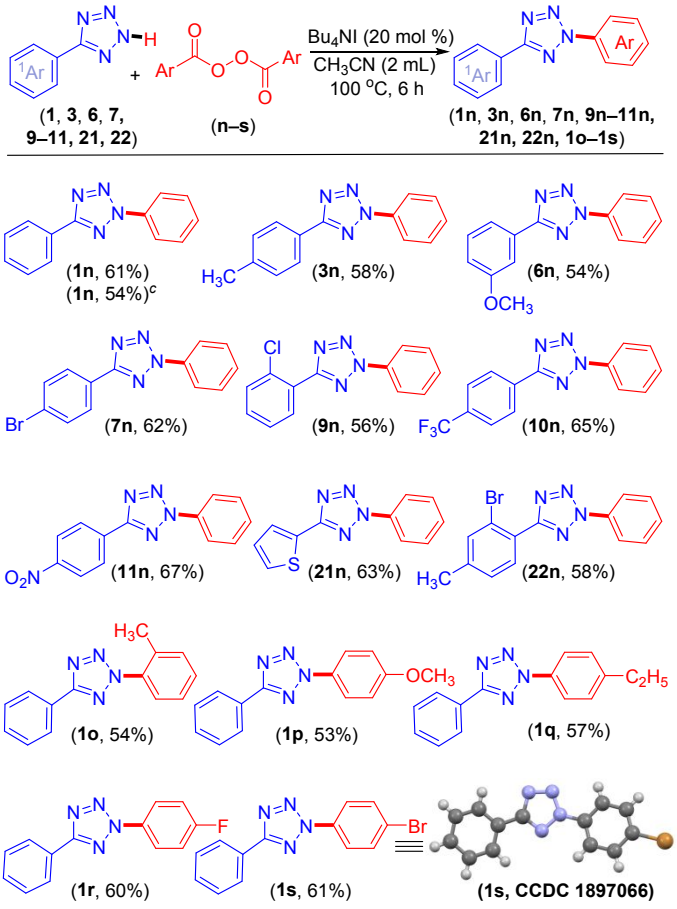

[a]Reaction conditions: aryl tetrazole (1 mmol), Bu_4NI (20 mol %) and diaryl acyl peroxide (2 equiv) at 100 °C in CH_3CN under degassed condition (2 mL). [b]Isolated yield after 6 h. [c]Isolated yield reported for 10 mmol (1.46 g scale).

To further demonstrate the synthetic utility of this protocol, a diverse array of aryl peroxyanhydrides (**o**–**s**) were examined. Benzoic peroxyanhydrides bearing electron-releasing groups, such as *o*-methyl (**o**), *p*-methoxy (**p**), and *p*-ethyl (**q**) all reacted competently with 5-phenyl-2*H*-tetrazole (**1**), furnishing their respective N^2-arylated products (**1o**, 54%) (**1p**, 53%) and (**1q**, 57%) in modest yields. The scope of this decarboxylative *N*-arylation reaction was further extended to benzoic peroxyanhydrides possessing electron-withdrawing

halogen functionality such as *p*-F (**r**) and *p*-Br (**s**) both lead to their respective arylation products (**1r**) and (**1s**) in 60 and 61% yields (Scheme 8). The compound (**1s**) was crystallized from a supersaturated solution of chloroform by the slow evaporation method. Here also, the N^2 regioselectivity of the arylation product (**1s**) was unequivocally confirmed by X-ray crystallographic analysis (Scheme 8) (see the Supporting Information). As can be seen from Scheme 8, no absolute correlation could be drawn from the yields of the product obtained with the presence of either electron-donating or electron-withdrawing groups present in any of the reacting partners.

To gain insight into the reaction pathway of this N^2-regioselective alkylation and arylation, a series of control experiments were conducted. At first, to ascertain the nature of the mechanism, a reaction between 5-phenyl-2*H*-tetrazole (**1**) and dodecanoic peroxyanhydride (**i**) under the standard condition was performed in the presence of radical scavenger 2,2,6,6-tetramethylpiperidin-1-yl)oxyl (TEMPO, 1.2 equiv). The TEMPO-undecanyl adduct (**bi**, 72%) along with 15% of the N^2-undecanylated product (**1i**) was isolated {Scheme 9 (D)}. This result confirms the radical nature of the reaction.

Scheme 9. Control Experiments to Confirm the Radical Nature of the Reaction

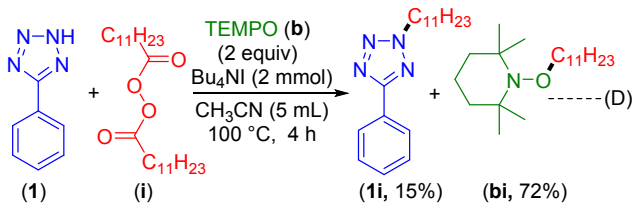

In general, the oxidation of (I^-) with benzoyl peroxide (**n**) leads to a benzoate anion ($PhCOO^-$) and a phenyl hypoiodate (PhCOOI).[30a,b] To check the active role of benzoate anion ($PhCOO^-$) and phenyl hypoiodate (PhCOOI) in the reaction, four different reactions were carried out. A reaction of 5-phenyl-2*H*-tetrazole (**1**), with a stoichiometric amount of benzoate anion (sodium benzoate) and iodine in DMSO (in CH_3CN sodium benzoate is insoluble) failed to provide the desired product (**1n**) thereby suggesting benzoate ion not to be the active species in the reaction {Scheme 10 (E)}. However, reactions between the *in situ* generated phenyl hypoiodate (PhCOOI) or acyl hypoiodate ($C_{11}H_{23}COOI$)[31a-d] upon treatment with 5-phenyl-2*H*-tetrazole (**1**) provided the phenylated product (**1n**) and undecylated product (**1i**) {Scheme 10 (F–H)} thereby implying the active involvement of hypoiodate species.

Scheme 10. Control Experiments to Confirm Involvement of Hypoiodate Species

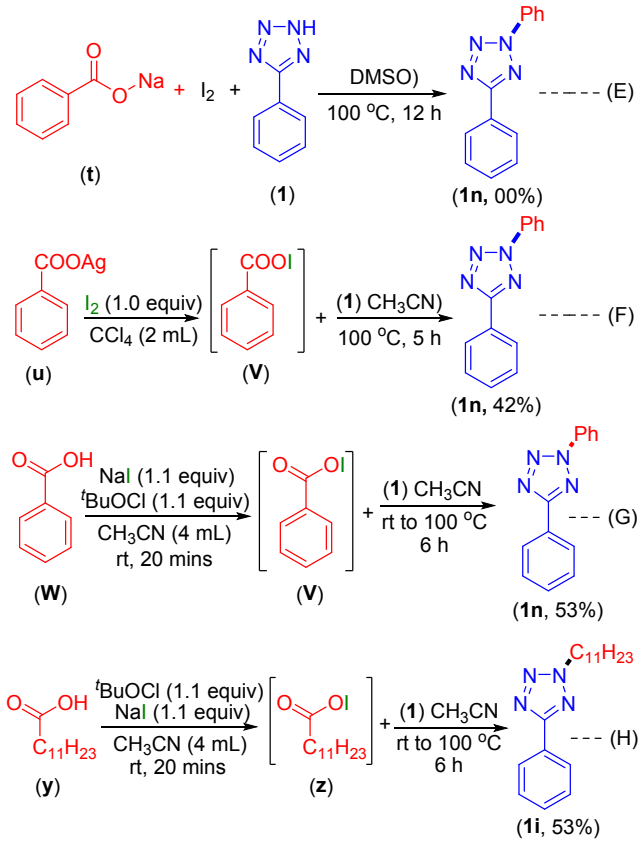

Naked phenyl radicals are not stable enough to participate in this reaction. It is possible that the reaction may proceed either via a decarbonylation or a decarboxylation path. Accordingly, two additional controlled experiments were carried out to ascertain the mechanistic path Failure to detect carbon monoxide by $PdCl_2$-PMA strip test rule out any decarbonylation path (Figure S1, see the Supporting Information).[31e,f] On the other hand, the evolution of CO_2 as confirmed by lime water test (Figure S2, see the Supporting Information) suggest a decarboxylation path. To reassertain, the possible decarboxylation path, 5-(*m*-tolyl)-2*H*-tetrazole (**20**) was treated with benzoic peroxyanhydride (**n**) and Bu_4NI at a lower temperature (80 °C). After 4 h the reaction was stopped and an intermediate (**20n′**) was isolated in 73% yield, which was confirmed to be 5-(*m*-tolyl)-2*H*-tetrazol-2-yl benzoate (**20n′**). When the isolated product (**20n′**) was further heated at 100 °C in acetonitrile for 3 h, it provided the product 2-phenyl-5-(*m*-tolyl)-2*H*-tetrazole (**20n**) in 51% yield with concurrent evolution of CO_2 thereby confirming a decarboxylative path {Scheme 11 (I)}. Based on the results of control

experiments (Schemes 9–11) and cues from the literature,[30,31] a plausible mechanism has been proposed as depicted in Scheme 12.

Scheme 11. Control Experiments to Confirm the Decarboxylation Path

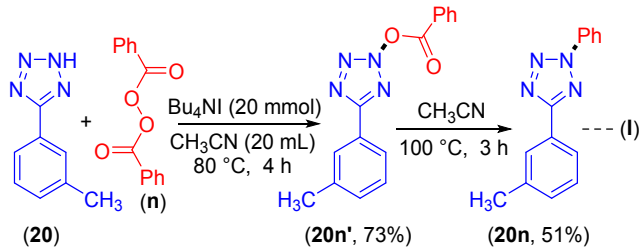

So far as the phenylation using benzoyl peroxide is concerned, a mechanism as shown in Scheme 12 is proposed. The oxidation of iodide (I^-) by benzoyl peroxide (**n**) afforded a benzoate anion (**IV**) and a hypoiodate species PhCOOI (**V**). Formation of a similar intermediate has been proposed by Tokumaru, K.[30a] Subsequently, the *in situ* generated PhCOOI (**V**) collapse to PhCOO (**VI**) and iodine radicals. Similar homolytic cleavage is well documented in the literature[32] The iodine radical then abstract the tetrazole N–H to furnish a persistent nitrogen-centered radical (**20′**) and releasing a molecule of HI. The liberated HI reacts with the benzoate anion (**IV**) to provide benzoic acid (**w**) as the byproduct, liberating the I^- for the subsequent cycle. The coupling between the tetrazole nitrogen radical (**20′**) and a PhCOO radical (**VI**) would form a 5-(*m*-tolyl)-2*H*-tetrazol-2-yl benzoate intermediate (**20n'**). When the reaction was carried out at a lower temperature (80 °C) it was possible to isolate and characterize the intermediate (**20n'**). But at a higher temperature (100 °C) the intermediate (**20n'**) undergoes extrusion of carbon dioxide leading to the formation of product (**20n**). For understanding whether this observation is controlled by the kinetic or thermodynamic factors, computations have been attempted at the estimation of barriers. However, the transition state could not be located even after several attempts. On calculating the energy difference between the product of decarboxylation reaction with respect to the intermediate (**20n'**), we estimated a value of -57.4 kcal/mol indicating a high thermodynamic favorability of the product (**20n**).

Scheme 12. Proposed Mechanism for Radical Induced *N*–Arylation of Aryl Tetrazole

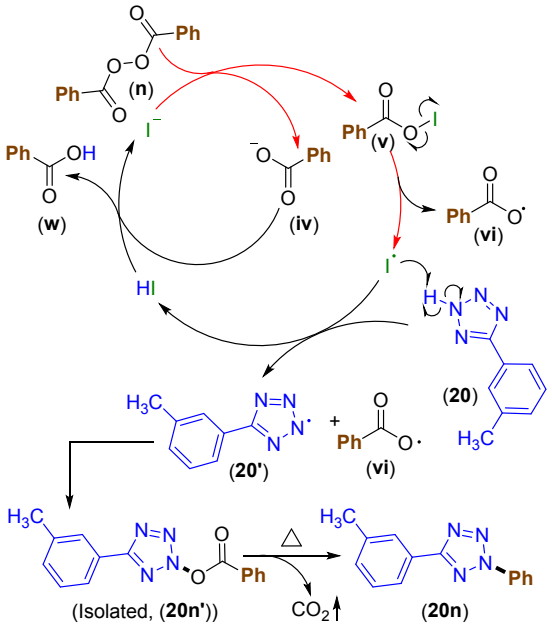

In this manuscript, we have provided a solution to the long-standing problem of regioselective N^2-alkylation, and arylation of tetrazoles, which is otherwise associated with the formation of a mixture of N^1 and N^2-isomers. This is achieved via the generation of nitrogen centered radical (NCR) in the presence of iodides and organic peroxides/peresters. Here, the organic peroxides/peresters serve the dual role of oxidants and alkyl or aryl sources. While *tert*-butyl hydroperoxide (TBHP) is the source of methyl group, alkyl diacyl peroxides as the primary alkyl, alkyl peresters as the secondary and tertiary alkyls and aryl diacyl peroxides as the arylating sources. These reactions proceed under a metal-free condition without the requirement of any pre-functionalization. Based on the control experiments carried out a concerted radical mechanism has been proposed. Barring an aldehyde functionality that forms a perester with peroxide several other functional groups are well-tolerated giving products in modest to good yields. The experimental findings, in particular the regioselectivity in the N^2-alkylation and the proposed mechanism have been confirmed by several control experiments, and also supported by the computations. Through DFT calculations, the estimated spin density, activation barriers for the reactions and thermodynamic parameters of the reactants and products clearly demonstrated the involvement of both kinetic and thermodynamic control in the regioselectivity.

EXPERIMENTAL SECTION

General information:

All the reagents were commercial grade and purified according to the established procedures. All the reactions were carried out in oven-dried glassware under a degassed atmosphere. Highest commercial quality reagents were purchased and were used without further purification unless otherwise stated. Aryl tetrazoles were prepared according to the literature procedure.[33a,b] Reactions were monitored by thin layer chromatography (TLC) on a 0.25 mm silica gel plates ($60F_{254}$) visualized under UV illumination at 254 nm. Organic extracts were dried over anhydrous sodium sulfate (Na_2SO_4). Solvents were removed using a rotary evaporator under reduced pressure. Column chromatography was performed to purify the crude product on silica gel 60–120 mesh using a mixture of hexane and ethyl acetate as eluent. All the isolated compounds were characterized by ^1H, $^{13}C\{^1H\}$ NMR and IR spectroscopic (HRMS-spectrometric) techniques. NMR spectra for all the samples were recorded in deuterochloroform ($CDCl_3$) or deuterated dimethyl sulfoxide (DMSO-*d*6). ^1H, $^{13}C\{^1H\}$ were recorded in 600 (151) or 400 (101) MHz spectrometer and were calibrated using tetramethylsilane or residual undeuterated solvent for ^1H NMR, deuterochloroform for ^{13}C NMR as an internal reference {$Si(CH_3)_4$: 0.00 ppm or $CHCl_3$: 7.26 ppm for ^1H NMR, 77.16 ppm for ^{13}C NMR or $(CH_3)_2SO$: 2.50 ppm for ^1H NMR, 39.52 ppm for ^{13}C NMR}. ^{19}F NMR was calibrated using hexafluorobenzene as internal standard. The chemical shifts are quoted in δ units, parts per million (ppm). ^1H NMR data is represented as follows: Chemical shift, multiplicity (s = singlet, d = doublet, t = triplet, q = quartet, p = pentat, m = multiplet, br = broad, dd = doublet of doublet, tt = triplet of triplet), integration and coupling constant(s) *J* in hertz (Hz). High resolution mass spectra (HRMS) were recorded on a mass spectrometer using electrospray ionization-time of flight (ESI-TOF) reflection experiments. FT-IR spectra were recorded in KBr or neat and reported in frequency of absorption (cm^{-1}). Compounds (**7a**) and (**1s**) both were crystallized from a supersaturated solution of chloroform by the slow evaporation method. [*Caution: peroxides are potentially explosive, so any peroxide involved reaction (as product or substrate) should be carried out with precautions!]*

Computational Details:

All the geometrical optimization for reactants, products and their corresponding transition states have been performed at density functional theory with B3LYP[34a] functional using cc-pVTZ[34b,c] basis set. The optimized geometries have been verified to minima/transition state[34d,e] by frequency calculations

(i.e., Zero and one imaginary frequency corresponding to minima and transition state, respectively)and the energies have been corrected for zero-point energy.[34f] For obtaining true minima; potential energy surface scan calculation have been performed by varying the N=C–C=C dihedral angle at every 10 degrees. Bond dissociation energy (BDE), transition state barrier and spin density calculations have been performed for the better understanding of regioselectivity. All these calculations were performed using Gaussian 09 suite of program.[34g]

General Procedure for the Synthesis of Alkyl Diacylperoxide (f–h).

These alkyl peroxides can be prepared following the literature procedure.[26] However, we have adopted the following modified procedure: To a 100 mL round bottom flask, the corresponding alkyl carboxylic acid (hexanoic acid) (1.16 g, 10 mmol, 1 equiv) was charged with an efficient magnetic stirring bar and diluted with methylene chloride (20 mL). The reaction vessel was immersed into a low temp bath (-15 °C). Then 1.2 equivalent of hydrogen peroxide (30% aqueous solution) (1.36 g, 1.22 mL) and 4-(dimethylamino)pyridine (0.12 g, 0.1 equiv) were added sequentially. After 15 minutes of stirring a solution of *N*,*N*′-dicyclohexylcarbodiimide (DCC, 2.47 g, 1.2 equiv) in methylene chloride (25 mL) was added dropwise into the reaction mixture. The resulting mixture was allowed to stir continuously for 3 h. Then, the crude reaction mixture was directly loaded into a short silica column and purified using methylene chloride as the eluent to afford 1.52 g of hexanoic peroxyanhydride (**f**) (66% yield).

General Procedure for the Synthesis of perester (k–m).

These alkyl peroxides can be prepared following the literature procedure.[18e] However, we have adopted the following modified procedure: To a 100 mL round bottom flask, the corresponding alkyl carboxylic acid (2-ethylhexanoic acid) (2.88 g, 20 mmol, 1 equiv) was charged with an efficient magnetic stirring bar and diluted with methylene chloride (25 mL). The reaction vessel was immersed into a low temp bath (-15 °C). Then 0.1 equivalent of 4-(dimethylamino)pyridine (0.24 g, 2.0 mmol) and 70% aq TBHP (24 mmol, 1.2 equiv) were added sequentially. After 15 minutes of stirring a solution of *N*,*N*′-dicyclohexylcarbodiimide (3.09 g, 15 mmol, 0.75 equiv) in methylene chloride (25 mL) was added dropwise into the reaction mixture. The resulting mixture was allowed to stir continuously for 3.5 h. Then, the crude reaction mixture was directly loaded into a short silica column

and purified using 3% of ethyl acetate in hexane as the eluent to afford *tert*-butyl 2-ethylhexaneperoxoate (**k**) (2.80 g, 65% yield).

General Procedure for the Synthesis of Aryl Diacylperoxide (o–s).

These compounds can be prepared following the literature procedure as reported.[35a] However, we have adopted the following modified procedure: To a 25 mL round bottom flask hydrogen peroxide (0.58 mL, 0.57 equiv, 30% aqueous solution) and sodium hydroxide (0.51 g, 1.27 equiv) were added in an ice bath for 20 minutes with vigorous stirring to generate sodium hydroperoxide. Separately, in another 100 mL round bottom flask was charged with 4-methoxybenzoyl chloride (1.70 g, 10 mmol, 1.0 equiv) and diethyl ether (30 mL). Then, the reaction mixture was immersed into a low temperature ice bath (-10 °C). The generated sodium hydroperoxide was added dropwise to the flask containing 4-methoxybenzoyl chloride over a period of 20 minutes and was allowed to stir for two hours. The resulting white precipitate was collected, washed sequentially with water (3 x 10 mL) and diethyl ether (3 x 10 mL). The solid product was recrystallized from cold acetone and water (1:3 v/v, 10 mL) provided 2.57 g of 4-methoxybenzoic peroxyanhydride (**p**) (85% yield).

General Procedure for the Synthesis of 2-Methyl-5-phenyl-2*H*-tetrazole (1a) from 5-Phenyl-2*H*-tetrazole (1).

To an oven-dried Schlenk tube equipped with a magnetic stir bar 5-phenyl-2*H*-tetrazole (146 mg, 1 mmol, 1.0 equiv), tetrabutylammonium iodide (Bu_4NI) (74 mg, 20 mol %), acetonitrile (2 mL) and an aqueous solution of TBHP (70%) (**a**) (411 μL, 3 equiv) was slowly added using a micropipette at room temperature. The resulting reaction mass was degassed using the freeze-pump-thaw method. Then the reaction mass was brought to room temperature. Maintaining the inert atmosphere, it was transferred to an oil bath and the temperature was raised to 100 °C from room temperature by increasing the temperature at the rate of 5 °C per minute and maintained for 8 h. The reaction mixture was removed from the oil bath and cooled to room temperature. The solvent acetonitrile was removed under reduced pressure. The reaction mixture was admixed with ethyl acetate (3 x 10 mL) and transferred into a separating funnel. The ethyl acetate layer was washed sequentially with 5% solution of sodium thiosulphate (2 x 10 mL) and brine solution (1 x 10 mL). The combined organic layer was dried over anhydrous Na_2SO_4, filtered and concentrated in *vacuo*. After the removal of the solvent, the crude product so obtained was purified over a column of silica gel using 5% ethyl acetate in hexane as the

eluent afforded pure 2-methyl-5-phenyl-2*H*-tetrazole (**1a**) (96 mg, yield 60%). The identity and purity of the product were confirmed by spectroscopic analysis.

General Procedure for the Synthesis of 2-Pentyl-5-phenyl-2*H*-tetrazole (1f) from 5-Phenyl-2*H*-tetrazole (1).

To an oven-dried Schlenk tube, charged with a stirring bar were added 5-phenyl-2*H*-tetrazole (**1**) (146 mg, 1 mmol, 1.0 equiv), tetrabutylammonium iodide (Bu_4NI) (74 mg, 20 mol %), and hexanoic peroxyanhydride (**f**) (460 mg, 2 mmol, 2 equiv). The reaction mass was degassed using a vacuum pump. Then dry and degassed acetonitrile (2 mL) was added to the reaction. Maintaining the inert atmosphere, the reaction mixture was heated at 100 ^oC for 6 h. After completion of the reaction. The reaction mixture was cooled to room temperature. The acetonitrile was removed from the reaction mixture using a rotary evaporator under reduced pressure. Then, the reaction mass was diluted with ethyl acetate (3 x 10 mL) and transferred to a separating funnel. The ethyl acetate layer was washed sequentially with 5% solution of sodium thiosulphate (2 x 10 mL) and brine solution (1 x 10 mL). The combined organic layer was dried over anhydrous Na_2SO_4, filtered and concentrated in *vacuo.* After removal of the solvent, the crude reaction mixture was purified over a column of silica gel using 4% ethyl acetate in hexane as the eluent afforded pure 2-pentyl-5-phenyl-2*H*-tetrazole (**1f**) (160 mg, yield 74%). The identity and purity of the product were confirmed by spectroscopic analysis.

General Procedure for the Synthesis of 2-(heptan-3-yl)-5-phenyl-2*H*-tetrazole (1k) from 5-Phenyl-2*H*-tetrazole (1).

To an oven-dried Schlenk tube, charged with a stirring bar were added 5-phenyl-2*H*-tetrazole (**1**) (146 mg, 1 mmol, 1.0 equiv), tetrabutylammonium iodide (Bu_4NI) (74 mg, 20 mol %), and *tert*-butyl 2-ethylhexaneperoxoate (**k**) (432 mg, 2 mmol, 2 equiv). The reaction mass was degassed using a vacuum pump. Then dry and degassed acetonitrile (2 mL) was added to the reaction. Maintaining the inert atmosphere, it was transferred to an oil bath and the temperature was raised to 100 °C from room temperature by increasing the temperature at the rate of 5 °C per minute and maintained for 6 h. After completion of the reaction, the reaction mixture was cooled to room temperature. The acetonitrile solvent was removed from the reaction mixture using a rotary evaporator under reduced pressure. Then, the reaction mass was admixed with ethyl acetate (2 x 25 mL) and transferred to a separating funnel. The ethyl acetate layer was washed sequentially with 5% solution of sodium thiosulphate (2 x 30 mL) and brine solution (1 x 20 mL). The combined organic layer was dried over anhydrous

Na_2SO_4, filtered and concentrated in *vacuo*. After removal of the solvent, the crude reaction mixture was purified over a column of silica gel using 2% ethyl acetate in hexane as the eluent to afforded pure 2-(heptan-3-yl)-5-phenyl-2*H*-tetrazole (**1k**) (188 mg, yield 77%).

General Procedure for the Synthesis of 2,5-Diphenyl-2*H*-tetrazole (1n) from 5-Phenyl-2*H*-tetrazole (1).

To an oven-dried Schlenk tube, charged with a stirring bar were added 5-phenyl-2*H*-tetrazole (**1**) (146 mg, 1 mmol, 1.0 equiv), tetrabutylammonium iodide (Bu_4NI) (74 mg, 20 mol %), benzoic peroxyanhydride (**n**) (484 mg, 2 mmol, 2 equiv). The reaction mass was degassed using a vacuum pump. Then dry and degassed acetonitrile (2 mL) was added to the reaction. Maintaining the inert atmosphere, the reaction mixture was heated at 100 °C for 6 h. The reaction mixture was cooled to room temperature. The acetonitrile was removed from the reaction mixture using a rotary evaporator under reduced pressure. Then, the reaction mass was admixed with ethyl acetate (30 mL) and transferred to a separating funnel. The ethyl acetate layer was washed sequentially with 5% solution of sodium thiosulphate (2 x 15 mL) and brine solution (1 x 10 mL). The combined organic layer was dried over anhydrous Na_2SO_4, filtered and concentrated in *vacuo*. After removal of the solvent, the crude reaction mixture was purified over a column of silica gel using 6% ethyl acetate in hexane as the eluent afforded pure 2,5-diphenyl-2*H*-tetrazole (**1n**) (135 mg, yield 61%). The identity and purity of the product were confirmed by spectroscopic analysis.

Gram scale procedure for the synthesis of (11a).

To an oven-dried 100 mL Schlenk round bottom flask equipped with a magnetic stir bar 5-(4-nitrophenyl)-2*H*-tetrazole (**11**) (1.53 g, 8 mmol, 1.0 equiv), tetrabutylammonium iodide (Bu_4NI) (591 mg, 1.60 mmol), acetonitrile (20 mL) and an aqueous solution of TBHP (70%) (**a**) (3.3 mL, 3 equiv) was slowly added using a micropipette at room temperature. The resulting reaction mass was degassed using the freeze-pump-thaw method. Then the reaction mass was brought to room temperature. Maintaining the inert atmosphere, it was transferred to an oil bath and the temperature was raised to 100 °C from room temperature by increasing the temperature at the rate of 5 °C per minute and maintained for 10 h. The reaction mixture was removed from the oil bath and cooled to room temperature. The solvent acetonitrile was removed under reduced pressure. The reaction mixture was admixed with ethyl acetate (2 x 80 mL) and transferred into a separating funnel. The ethyl acetate layer was washed sequentially with 5% solution of sodium thiosulphate (2 x 80 mL) and brine solution (1 x

80 mL). The combined organic layer was dried over anhydrous Na_2SO_4, filtered and concentrated in vacuo. After removal of the solvent, the crude product so obtained was purified over a column of silica gel using 6% ethyl acetate in hexane as the eluent afforded pure 2-methyl-5-(4-nitrophenyl)-2*H*-tetrazole (**11a**) (1.10 g, yield 67%).

Gram scale procedure for the synthesis of (1i).

To an oven-dried 100 mL Schlenk round bottom flask, charged with a stirring magnetic bar 5-phenyl-2H-tetrazole (**1**) (1.17 g, 8 mmol, 1.0 equiv), tetrabutylammonium iodide (Bu_4NI) (591 mg, 1.6 mmol), and dodecanoic peroxyanhydride (**i**) (6.38 g, 16 mmol, 2 equiv). The reaction mass was degassed using a vacuum pump. Then dry and degassed acetonitrile (20 mL) was added to the reaction. Maintaining the inert atmosphere, it was transferred to an oil bath and the temperature was raised to 100 °C from room temperature by increasing the temperature at the rate of 5 °C per minute and maintained for 7 h. After completion of the reaction. The reaction mixture was cooled to room temperature. The acetonitrile solvent was removed from the reaction mixture using a rotary evaporator under reduced pressure. Then, the reaction mass was admixed with ethyl acetate (2 x 60 mL) and transferred to a separating funnel. The ethyl acetate layer was washed sequentially with 5% solution of sodium thiosulphate (2 x 40 mL) and brine solution (1 x 50 mL). The combined organic layer was dried over anhydrous Na_2SO_4, filtered and concentrated in vacuo. After removal of the solvent, the crude reaction mixture was purified over a column of silica gel using 3% ethyl acetate in hexane as the eluent to afforded pure 5-phenyl-2-undecyl-2*H*-tetrazole (**1i**) (1.76 g, yield 73%).

Gram Scale Procedure for the Synthesis of (11k).

To an oven-dried 100 mL Schlenk round bottom flask, charged with a stirring magnetic bar 5-(4-nitrophenyl)-2*H*-tetrazole (**11**) (1.53 g, 8 mmol, 1.0 equiv), tetrabutylammonium iodide (Bu_4NI) (591 mg, 1.60 mmol), *tert*-butyl 2-ethylhexaneperoxoate (**k**) (3.46 g, 2 equiv). The reaction mass was degassed using a vacuum pump. Then dry and degassed acetonitrile (20 mL) was added to the reaction. Maintaining the inert atmosphere, it was transferred to an oil bath and the temperature was raised to 100 °C from room temperature by increasing the temperature at the rate of 5 °C per minute and maintained for 7 h. After completion of the reaction, the reaction mixture was cooled to room temperature. The acetonitrile solvent was removed from the reaction mixture using a rotary evaporator under reduced pressure. Then, the reaction mass was admixed with ethyl acetate (2 x 60 mL) and transferred to a separating funnel. The ethyl acetate layer was washed sequentially with 5% solution of

sodium thiosulphate (2 x 40 mL) and brine solution (1 x 50 mL). The combined organic layer was dried over anhydrous Na_2SO_4, filtered and concentrated in *vacuo*. After removal of the solvent, the crude reaction mixture was purified over a column of silica gel using 2% ethyl acetate in hexane as the eluent to afforded pure 2-(heptan-3-yl)-5-(4-nitrophenyl)-2*H*-tetrazole (**11k**) (1.71 g, yield 74%).

Gram scale procedure for the synthesis of (1n).

To an oven-dried Schlenk tube, charged with a stirring bar were added 5-phenyl-2*H*-tetrazole (**1**) (1.46 g, 10 mmol, 1.0 equiv), tetrabutylammonium iodide (Bu_4NI) (731 mg, 2 mmol, 0.2 equiv), benzoic peroxyanhydride (**n**) (4.84 g, 20 mmol, 2 equiv). The reaction mass was degassed using a vacuum pump. Then dry and degassed acetonitrile (20 mL) was added to the reaction mixture. Maintaining the inert atmosphere, it was transferred to an oil bath and the temperature was raised to 100 °C from room temperature by increasing the temperature at the rate of 5 °C per minute and maintained for 7.5 h. The reaction mixture was cooled to room temperature. The acetonitrile solvent was removed from the reaction mixture using a rotary evaporator under reduced pressure. Then, the reaction mass was admixed with ethyl acetate (2 x 50 mL) and transferred to a separating funnel. The ethyl acetate layer was washed sequentially with 5% solution of sodium thiosulphate (2 x 40 mL) and brine solution (1 x 40 mL). The combined organic layer was dried over anhydrous Na_2SO_4, filtered and concentrated in vacuo. After removal of the solvent, the crude reaction mixture was purified over a column of silica gel using 6% ethyl acetate in hexane as the eluent afforded pure 2,5-diphenyl-2*H*-tetrazole (**1n**) (1.20 g, yield 54%).

Procedure for free radical trapping experiments (bi).

To an oven-dried Schlenk tube equipped with a magnetic stirring bar 5-phenyl-2*H*-tetrazole (**1**) (146 mg, 1 mmol, 1.0 equiv), tetrabutylammonium iodide (Bu_4NI) (74 mg, 20 mol %), lauroyl peroxide (**i**) (797 mg, 2 equiv) and (2,2,6,6-tetramethylpiperidin-1-yl)oxyl (TEMPO) (**b**) (312 mg, 2 equiv) was added at room temperature. The reaction mass was degassed using a vacuum pump. Then dry and degassed acetonitrile (5 mL) was added to the reaction mixture. Maintaining the inert atmosphere, it was transferred to an oil bath and the temperature was raised to 100 °C from room temperature by increasing the temperature at the rate of 5 °C per minute and maintained for 4 h. The reaction mixture was cooled to room temperature. The acetonitrile solvent was removed from the reaction mixture using a rotary evaporator under reduced pressure. Then, the reaction mass was admixed with ethyl acetate (2 x 20 mL) and transferred to a separating funnel. The ethyl acetate layer was washed sequentially with 5% solution of sodium thiosulphate (2 x 20 mL) and brine solution (1 x 20 mL). The combined organic

layer was dried over anhydrous Na_2SO_4, filtered and concentrated in vacuo. After removal of the solvent, the crude reaction mixture was purified over a column of silica gel using 2% ethyl acetate in hexane as the eluent afforded pure 2,2,6,6-tetramethyl-1-(undecyloxy)piperidine (**bi**) (448 mg, yield 72%).

*Hexanoic peroxyanhydride (**f**):*[18d]

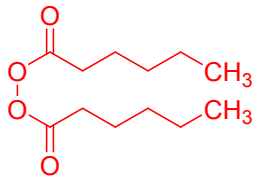

Colorless oil (1.52 g, 66% yield); ^{1}H NMR (600 MHz, $CDCl_3$): δ 2.41 (t, J = 7.5 Hz, 4H), 1.75–1.66 (m, 4H), 1.40–1.28 (m, 8H), 0.89 (t, J = 7.0 Hz, 6H); ^{13}C{^{1}H} NMR (151 MHz, $CDCl_3$): δ 169.4, 31.2, 30.1, 24.6, 22.3, 13.9.

*Octanoic peroxyanhydride (**g**):*[18d]

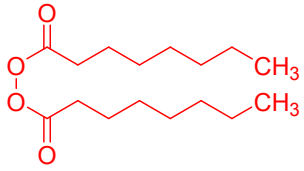

Colorless oil (2.29 g, 80% yield); ^{1}H NMR (400 MHz, $CDCl_3$): δ 2.42 (t, J = 7.5 Hz, 4H), 1.77–1.66 (m, 4H), 1.43–1.22 (m, 16H), 0.88 (t, J = 6.8 Hz, 6H); ^{13}C{^{1}H} NMR (101 MHz, $CDCl_3$): δ 169.4, 31.7, 30.2, 29.0, 28.9, 25.0, 22.7, 14.2.

*Decanoic peroxyanhydride (**h**):*

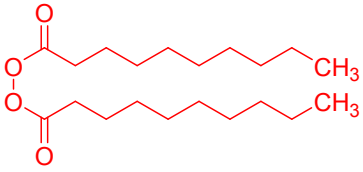

Gummy (2.98 g, 87% yield); ^{1}H NMR (400 MHz, $CDCl_3$): δ 2.42 (t, J = 7.5 Hz, 4H), 1.76–1.66 (m, 4H), 1.41–1.21 (m, 24H), 0.87 (t, J = 6.9 Hz, 6H); ^{13}C{^{1}H} NMR (101 MHz, $CDCl_3$): δ 169.4, 32.0, 30.2, 29.5, 29.3, 29.2, 29.1, 25.0, 22.8, 14.2.

*tert-Butyl 2-ethylhexaneperoxoate (**k**):*

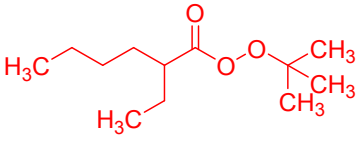

Colorless liquid (2.80 g, 65% yield); ^{1}H NMR (600 MHz, $CDCl_3$): δ 2.16–2.09 (m, 1H), 1.56–1.47 (m, 2H), 1.44–1.38 (m, 1H), 1.35 (m, 1H), 1.19 (s, 9H), 1.16–1.11 (m, 4H), 0.79 (t, J = 7.5 Hz, 3H), 0.74 (t, J = 6.9 Hz, 3H); ^{13}C{^{1}H} NMR (151 MHz, $CDCl_3$): δ 173.7, 83.1, 45.2, 32.0, 29.7, 26.4, 25.7, 22.6, 14.0, 12.0.

*tert-Butyl 2,2-dimethylpropaneperoxoate (**l**):*[18e]

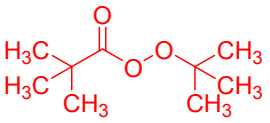

Colorless liquid (1.95 g, 56% yield); ^{1}H NMR (600 MHz, $CDCl_3$): δ 1.29 (s, 9H), 1.23 (s, 9H); ^{13}C{^{1}H} NMR (151 MHz, $CDCl_3$): δ 175.3, 83.6, 39.0, 27.4, 26.3.

*tert-Butyl adamantane-1-carboperoxoate (**m**):*[18e]

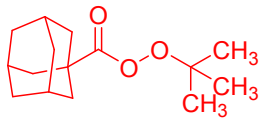

White solid (2.52 g, 50% yield); ^{1}H NMR (600 MHz, $CDCl_3$): δ 1.99 (s, 3H), 1.92 (s, 6H), 1.72–1.65 (m, 6H), 1.28 (s, 9H); ^{13}C{^{1}H} NMR (151 MHz, $CDCl_3$): δ 174.4, 83.5, 41.3, 39.0, 36.5, 28.0, 26.3.

*2-Methylbenzoic peroxyanhydride (**o**):*[29]

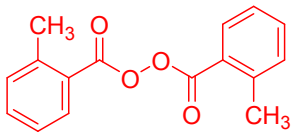

White solid (1.98 g, 73% yield); ^{1}H NMR (400 MHz, $CDCl_3$): δ 7.94 (d, J = 7.8 Hz, 2H), 7.48 (t, J = 7.6 Hz, 2H), 7.34–7.27 (m, 4H), 2.63 (s, 6H); ^{13}C{^{1}H} NMR (101 MHz, $CDCl_3$): δ 164.3, 140.6, 133.3, 131.9, 130.5, 126.1, 125.5, 21.2.

*4-Methoxybenzoic peroxyanhydride (**p**):*[29]

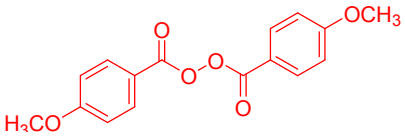

White solid (2.57 g, 85% yield); ^{1}H NMR (400 MHz, $CDCl_3$): δ 8.03 (d, J = 9.0 Hz, 4H), 6.98 (d, J = 9.0 Hz, 4H), 3.88 (s, 6H); ^{13}C{^{1}H} NMR (101 MHz, $CDCl_3$): δ 164.5, 163.1, 132.1, 117.9, 114.3, 55.7.

*4-Ethylbenzoic peroxyanhydride (**q**):*[35b]

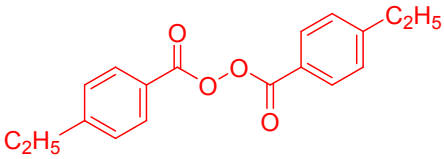

White solid (2.50 g, 84% yield); ^{1}H NMR (400 MHz, $CDCl_3$): δ 7.99 (d, J = 8.2 Hz, 4H), 7.32 (d, J = 8.2 Hz, 4H), 2.72 (q, J = 7.6 Hz, 4H), 1.26 (t, J = 7.6 Hz, 6H); ^{13}C{^{1}H} NMR (101 MHz, $CDCl_3$): δ 163.3, 151.5, 130.1, 128.5, 123.2, 29.2, 15.2.

*4-Fluorobenzoic peroxyanhydride (**r**):*[29]

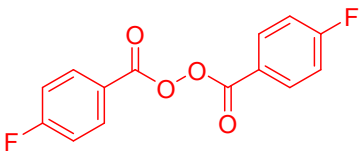

White solid (2.23 g, 80% yield); ^{1}H NMR (400 MHz, $CDCl_3$): δ 8.08–8.12 (m, 4H), 7.20 (t, J = 8.6 Hz, 4H); ^{13}C{^{1}H} NMR (101 MHz, $CDCl_3$): δ 166.7 (d, J = 257.6 Hz), 162.2, 132.7 (d, J = 9.7 Hz), 121.9 (d, J = 3.1 Hz), 164.4 (d, J = 22.4 Hz); ^{19}F NMR (377 MHz, $CDCl_3$): –102.3.

*4-Bromobenzoic peroxyanhydride (**s**):*[29]

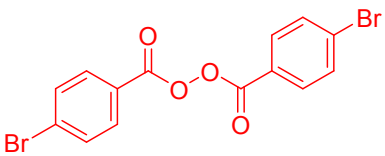

White solid (3.25 g, 81% yield); ^{1}H NMR (400 MHz, $CDCl_3$): δ 7.92 (d, J = 8.5 Hz, 4H), 7.66 (d, J = 8.5 Hz, 4H); ^{13}C{^{1}H} NMR (101 MHz, $CDCl_3$): δ 162.5, 132.5, 131.3, 129.9, 124.5.

*5-Phenyl-2H-tetrazole (**1**):*[33b]

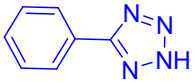

White solid (1.3 g, 89% yield); ^{1}H NMR (400 MHz, DMSO-d_6): δ 8.05–8.02 (m, 2H), 7.64–7.59 (m, 3H); ^{13}C{^{1}H} NMR (101 MHz, DMSO-d_6): δ 155.4, 131.3, 129.5, 127.1, 124.2.

*5-([1,1'-Biphenyl]-4-yl)-2H-tetrazole (**2**):*[33c]

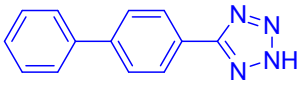

White solid (1.65 g, 74% yield); ^{1}H NMR (600 MHz, DMSO-d_6): δ 8.13 (d, J = 8.3 Hz, 2H), 7.93 (d, J = 8.3 Hz, 2H), 7.77 (d, J = 7.9 Hz, 2H), 7.52 (t, J = 7.5 Hz, 2H), 7.43 (t, J = 7.3 Hz, 1H); ^{13}C{^{1}H} NMR (101 MHz, DMSO-d_6): δ 155.1, 142.7, 138.9, 129.1, 128.2, 127.6, 127.5, 126.8, 123.1.

*5-(p-Tolyl)-2H-tetrazole (**3**):*[33b]

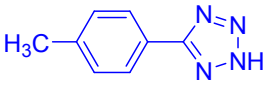

White solid (1.14 g, 71% yield); ^{1}H NMR (400 MHz, DMSO-d_6): δ 7.93 (d, J = 8.1 Hz, 2H), 7.42 (d, J = 8.0 Hz, 2H), 2.39 (s, 3H); ^{13}C{^{1}H} NMR (151 MHz, DMSO-d_6): δ 155.2, 141.3, 130.0, 126.9, 121.3, 21.1.

*5-(4-Methoxyphenyl)-2H-tetrazole (**4**):*[33d]

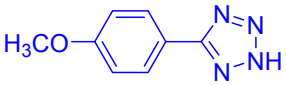

White solid (1.16 g, 66% yield); ^{1}H NMR (600 MHz, DMSO-d_6): δ 7.98 (d, J = 8.6 Hz, 2H), 7.16 (d, J = 8.6 Hz, 2H), 3.84 (s, 3H); ^{13}C{^{1}H} NMR (151 MHz, DMSO-d_6): δ 161.5, 128.7, 114.9, 55.5.

*5-(4-(tert-Butyl)phenyl)-2H-tetrazole (**5**):*[33c]

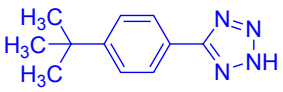

White solid (1.48 g, 73% yield); ^{1}H NMR (400 MHz, DMSO-d_6): δ 7.96 (d, J = 8.3 Hz, 2H), 7.62 (d, J = 8.3 Hz, 2H), 1.31 (s, 9H); ^{13}C{^{1}H} NMR (151 MHz, DMSO-d_6): δ 155.1, 154.1, 126.8, 126.3, 121.4, 34.8, 30.9.

*5-(3-Methoxyphenyl)-2H-tetrazole (**6**):*[33e]

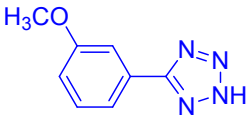

White solid (1.25 g, 71% yield); ^{1}H NMR (600 MHz, DMSO-d_6): δ 7.62 (d, J = 7.7 Hz, 1H), 7.58 (s, 1H), 7.52 (t, J = 8.0 Hz, 1H), 7.16 (d, J = 8.3 Hz, 1H), 3.85 (s, 3H); ^{13}C{^{1}H} NMR (151 MHz, DMSO-d_6): δ 159.8, 155.3, 130.6, 125.5, 119.2, 117.0, 112.1, 55.4.

*5-(4-Bromophenyl)-2H-tetrazole (**7**):*[33b]

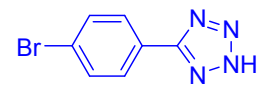

White solid (1.80 g, 80% yield); ^{1}H NMR (400 MHz, DMSO-d_6): δ 7.98 (d, J = 8.6 Hz, 2H), 7.82 (d, J = 8.6 Hz, 2H); ^{13}C{^{1}H} NMR (151 MHz, DMSO-d_6): δ 155.1, 132.5, 128.9, 124.8, 123.6.

*5-(4-Chlorophenyl)-2H-tetrazole (**8**):*[33b]

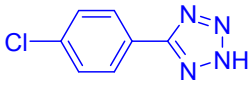

White solid (1.50 g, 83% yield); ^{1}H NMR (600 MHz, DMSO-d_6): δ 8.05 (d, J = 8.5 Hz, 2H), 7.69 (d, J = 8.5 Hz, 2H); ^{13}C{^{1}H} NMR (151 MHz, DMSO-d_6): δ 154.9, 136.0, 129.6, 128.8, 123.2.

*5-(2-Chlorophenyl)-2H-tetrazole (**9**):*[33d]

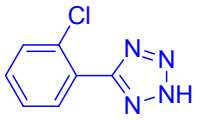

White solid (1.46 g, 81% yield); ^{1}H NMR (400 MHz, DMSO-d_6): δ 7.81 (d, J = 7.6 Hz, 1H), 7.71 (d, J = 8.0 Hz, 1H), 7.64 (t, J = 7.7 Hz, 1H), 7.56 (t, J = 7.5 Hz, 1H); ^{13}C{^{1}H} NMR (151 MHz, DMSO-d_6): δ 153.6, 132.7, 132.1, 131.8, 130.5, 127.9, 124.2.

*5-(4-(Trifluoromethyl)phenyl)-2H-tetrazole (**10**):*[33c]

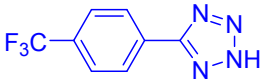

White solid (1.82 g, 85% yield); ^{1}H NMR (600 MHz, DMSO-d_6): δ 8.23 (d, J = 8.0 Hz, 2H), 7.95 (d, J = 8.0 Hz, 2H); ^{13}C{^{1}H} NMR (151 MHz, DMSO-d_6): δ 155.4, 131.1 (q, J = 32.16 Hz), 128.5, 127.8, 126.3 (d, J = 3.6 Hz), 123.8 (q, J = 272.55 Hz); ^{19}F NMR (565 MHz, DMSO-d_6): δ –61.45.

*5-(4-Nitrophenyl)-2H-tetrazole (**11**):*[33d]

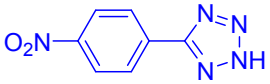

White solid (1.70 g, 89% yield); ^{1}H NMR (400 MHz, DMSO-d_6): δ 8.45 (d, J = 8.9 Hz, 2H), 8.30 (d, J = 8.9 Hz, 2H); ^{13}C{^{1}H} NMR (101 MHz, DMSO-d_6): δ 155.5, 148.6, 130.7, 128.1, 124.5.

*4-(2H-Tetrazol-5-yl)benzaldehyde (**12**):*[33c]

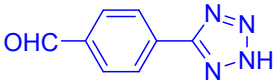

White solid (1.20 g, 69% yield); ^{1}H NMR (400 MHz, DMSO-d_6): δ 10.09 (s, 1H), 8.26 (d, J = 8.1 Hz, 2H), 8.11 (d, J = 8.2 Hz, 2H); ^{13}C{^{1}H} NMR (151 MHz, DMSO-d_6): δ 192.6, 174.5, 172.0, 137.5, 130.3, 127.5.

*5-(4-Methylbenzyl)-2H-tetrazole (**13**):*[33b]

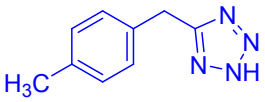

White solid (1.29 g, 74% yield); ^{1}H NMR (600 MHz, DMSO-d_6): δ 7.14 (bs, 4H), 4.22 (s, 2H), 2.26 (s, 3H); ^{13}C{^{1}H} NMR (151 MHz, DMSO-d_6): δ 155.9, 136.5, 133.4, 129.7, 128.9, 29.0, 21.1.

*5-(Naphthalen-2-yl)-2H-tetrazole (**19**):*[33d]

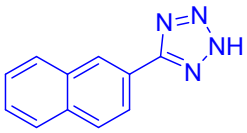

White solid (1.16 g, 76% yield); ^{1}H NMR (400 MHz, DMSO-d_6): δ 8.66 (s, 1H), 8.14 (m, 2H), 8.11–8.07 (m, 1H), 8.05–7.98 (m, 1H), 7.64 (m, 2H); ^{13}C{^{1}H} NMR (101 MHz, DMSO-d_6): δ 155.7, 133.9, 132.6, 129.2, 128.6, 127.9, 127.8, 127.2, 127.0, 123.7, 121.6.

*5-(m-Tolyl)-2H-tetrazole (**20**):*[33d]

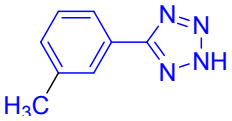

White solid (1.20 g, 75% yield); ^{1}H NMR (400 MHz, DMSO-d_6): δ 7.86 (s, 1H), 7.82 (d, J = 7.7 Hz, 1H), 7.46 (t, J = 7.6 Hz, 1H), 7.37 (d, J = 7.5 Hz, 1H), 2.38 (s, 3H); ^{13}C{^{1}H} NMR (101 MHz, DMSO-d_6): δ 155.5, 138.9, 132.0, 129.4, 127.5, 124.2, 124.1, 21.0.

*5-(Thiophen-2-yl)-2H-tetrazole (**21**):*[33f]

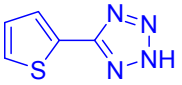

White solid (1.08 g, 71% yield); ^{1}H NMR (600 MHz, DMSO-d_6): δ 7.89 (d, J = 4.7 Hz, 1H), 7.80 (d, J = 2.8 Hz, 1H), 7.32 – 7.27 (m, 1H); ^{13}C{^{1}H} NMR (151 MHz, DMSO-d_6): δ 151.4, 130.3, 129.2, 128.5, 125.4.

*5-(2-Bromo-4-methylphenyl)-2H-tetrazole (**22**):*

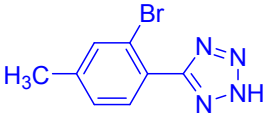

White solid (1.77 g, 74% yield); ^{1}H NMR (600 MHz, DMSO-d_6): δ 7.70 (s, 1H), 7.59 (d, J = 7.7 Hz, 1H), 7.39 (d, J = 7.1 Hz, 1H), 2.38 (s, 3H); ^{13}C{^{1}H} NMR (151 MHz, DMSO-d_6): δ 154.5, 143.2, 133.8, 131.6, 128.8, 123.4, 121.5, 20.5.

*2-Methyl-5-phenyl-2H-tetrazole (**1a**):*[19e]

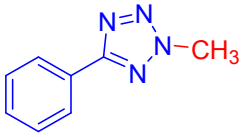

White solid (96 mg, 60% yield); R_f = 0.27 (0.5:9.5 EtOAc : hexane, Silica gel); mp 50–52 °C; ^{1}H NMR (600 MHz, $CDCl_3$): δ 8.14 (d, J = 7.8 Hz, 2H), 7.49 (t, J = 7.1 Hz, 3H), 4.41 (s, 3H); ^{13}C{^{1}H} NMR (151 MHz, $CDCl_3$): δ 165.4, 130.5, 129.1, 127.5, 126.9, 39.6; IR (KBr): 3071, 2956, 2926, 2853, 1718, 1449, 1190, 1048, 923, 792, 694 cm^{-1}; HRMS (ESI-TOF) m/z: $[M + H]^+$ Calcd for $C_8H_9N_4$ 161.0822; Found 161.0821.

*5-([1,1'-Biphenyl]-4-yl)-2H-tetrazole (**2a**):*[19e]

White solid (156 mg, 66% yield); R_f = 0.21 (0.5:9.5 EtOAc : hexane, Silica gel); mp 140–142 °C; ^{1}H NMR (600 MHz, $CDCl_3$): δ 8.21 (d, J = 8.3 Hz, 2H),

7.73 (d, J = 8.3 Hz, 2H), 7.65 (d, J = 7.3 Hz, 2H), 7.47 (t, J = 7.7 Hz, 2H), 7.39 (t, J = 7.4 Hz, 1H), 4.42 (s, 3H); $^{13}C\{^1H\}$ NMR (151 MHz, $CDCl_3$): δ 165.2, 143.2, 140.4, 129.0, 127.9, 127.7, 127.4, 127.3, 126.4, 39.7; IR (KBr): 3030, 2959, 2923, 1623, 1541, 1465, 1415, 1049, 847, 717, 643 cm^{-1}; HRMS (ESI-TOF) m/z: $[M + H]^+$ Calcd for $C_{14}H_{13}N_4$ 237.1135; Found 237.1137.

*2-Methyl-5-(p-tolyl)-2H-tetrazole (**3a**):*[19e]

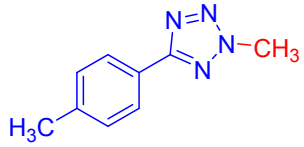

White solid (106 mg, 61% yield); R_f = 0.25 (0.5:9.5 EtOAc : hexane, Silica gel); mp 105–107 °C; ^1H NMR (600 MHz, $CDCl_3$): δ 8.02 (d, J = 8.1 Hz, 2H), 7.30 (d, J = 7.9 Hz, 2H), 4.39 (s, 3H), 2.42 (s, 3H); $^{13}C\{^1H\}$ NMR (151 MHz, $CDCl_3$): δ 165.5, 140.6, 129.8, 126.9, 124.7, 39.6, 21.6; IR (KBr): 3028, 2959, 2924, 2854, 1618, 1471, 1459, 1182, 1173, 1002, 844, 754, 677 cm^{-1}; HRMS (ESI-TOF) m/z: $[M + H]^+$ Calcd for $C_9H_{11}N_4$ 175.0978; Found 175.0980.

*5-(4-Methoxyphenyl)-2-methyl-2H-tetrazole (**4a**):*[19e]

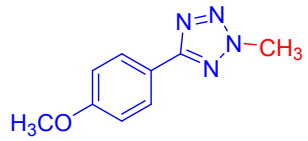

White solid (112 mg, 59% yield); R_f = 0.15 (2:8 EtOAc : hexane, Silica gel); mp 85–87 °C; ^1H NMR (600 MHz, $CDCl_3$): δ 8.07 (d, J = 8.9 Hz, 2H), 7.01 (d, J = 8.8 Hz, 2H), 4.38 (s, 3H), 3.87 (s, 3H); $^{13}C\{^1H\}$ NMR (151 MHz, $CDCl_3$): δ 165.3, 161.4, 128.4, 120.1, 114.4, 55.5, 39.6; IR (KBr): 3098, 2962, 2841, 1709, 1611, 1458, 1256, 1177, 1028, 846, 752, 611, 538 cm^{-1}; HRMS (ESI-TOF) m/z: $[M + H]^+$ Calcd for $C_9H_{11}N_4O$ 191.0927; Found 191.0932.

*5-(4-(tert-Butyl)phenyl)-2-methyl-2H-tetrazole (**5a**):*

White solid (138 mg, 64% yield); R_f = 0.28 (0.5:9.5 EtOAc : hexane, Silica gel); mp 88–90 °C; ^1H NMR (600 MHz, $CDCl_3$): δ 7.99 (d, J = 8.6 Hz, 2H), 7.44 (d, J = 8.5 Hz, 2H), 4.32 (s, 3H), 1.29 (s, 9H); $^{13}C\{^1H\}$ NMR (151 MHz, $CDCl_3$): δ 165.4, 153.8, 126.7, 126.0, 124.6, 39.6, 35.0, 31.4; IR (KBr): 3030, 2954, 2924, 2864, 1470, 1320, 1119, 1002, 843, 730, 682 cm^{-1}; HRMS (ESI-TOF) m/z: $[M + H]^+$ Calcd for $C_{12}H_{17}N_4$ 217.1448; Found 217.1447.

*5-(3-Methoxyphenyl)-2-methyl-2H-tetrazole (**6a**):*

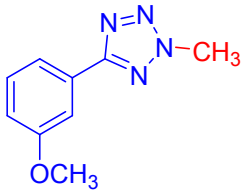

White Solid (114 mg, 60% yield); R_f = 0.21 (1.0:9.0 EtOAc : hexane, Silica gel); mp 80–82 °C; ^{1}H NMR (600 MHz, $CDCl_3$): δ 7.73 (d, J = 7.6 Hz, 1H), 7.68 (s, 1H), 7.40 (t, J = 7.9 Hz, 1H), 7.02 (dd, J = 8.3, 2.1 Hz, 1H), 4.41 (s, 3H), 3.89 (s, 3H); ^{13}C{^{1}H} NMR (151 MHz, $CDCl_3$): δ 165.3, 160.1, 130.2, 128.7, 119.4, 117.0, 111.5, 55.6, 39.6; IR (KBr): 3072, 2960, 2839, 1723, 1592, 1523, 1472, 1438, 1359, 1320, 1246, 1186, 1125, 1038, 859, 800, 754, 724, 688 cm^{-1}; HRMS (ESI-TOF) m/z: [M + H]$^+$ Calcd for $C_9H_{11}N_4O$ 191.0927; Found 191.0933.

*5-(4-Bromophenyl)-2-methyl-2H-tetrazole (**7a**):*[19e]

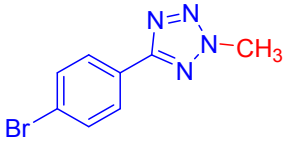

White solid (155 mg, 65% yield); R_f = 0.28 (0.5:9.5 EtOAc : hexane, Silica gel); mp 125–127 °C; ^{1}H NMR (600 MHz, $CDCl_3$): δ 8.01 (d, J = 8.5 Hz, 2H), 7.63 (d, J = 8.5 Hz, 2H), 4.40 (s, 3H); ^{13}C{^{1}H} NMR (151 MHz, $CDCl_3$): δ 164.6, 132.3, 128.41, 126.4, 124.8, 39.7; IR (KBr): 3033, 2951, 2918, 2850, 1605, 1442, 1135, 1015, 836, 745, 683 cm^{-1}; HRMS (ESI-TOF) m/z: [M + H]$^+$ Calcd for $C_8H_8{}^{79}BrN_4$ 238.9927; Found 238.9928.

*5-(4-Chlorophenyl)-2-methyl-2H-tetrazole (**8a**):*[19e]

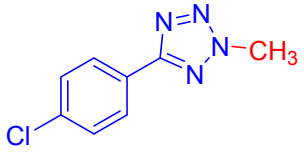

White solid (128 mg, 66% yield); R_f = 0.26 (0.5:9.5 EtOAc : hexane, Silica gel); mp 107–109 °C; ^{1}H NMR (600 MHz, $CDCl_3$): δ 8.08 (d, J = 8.6 Hz, 2H), 7.47 (d, J = 8.6 Hz, 2H), 4.40 (s, 3H); ^{13}C{^{1}H} NMR (151 MHz, $CDCl_3$): δ 164.6, 136.5, 129.4, 128.2, 126.0, 39.7; IR (KBr): 3032, 2949, 2851, 1601, 1515, 1453, 1361, 1198, 1091, 1009, 863 cm^{-1}; HRMS (ESI-TOF) m/z: [M + H]$^+$ Calcd for $C_8H_8{}^{35}ClN_4$ 195.0432; Found 195.0438.

*5-(2-Chlorophenyl)-2-methyl-2H-tetrazole (**9a**):*[19e]

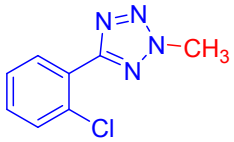

Colorless oil (118 mg, 61% yield); R_f = 0.27 (0.5:9.5 EtOAc : hexane, Silica gel); ^{1}H NMR (600 MHz, $CDCl_3$): δ 7.88 (d, J = 7.4 Hz, 1H), 7.47 (d, J = 7.6 Hz, 1H), 7.37–7.30 (m, 2H), 4.38 (s, 3H); ^{13}C{^{1}H} NMR (151 MHz, $CDCl_3$): δ 163.6, 133.2, 131.5, 131.3, 131.0, 127.1, 126.6, 39.8; IR (KBr): 3033, 2985, 2920, 2851, 1605, 1446, 1198, 1031, 844, 711,

640 cm^{-1}; HRMS (ESI-TOF) m/z: $[M + H]^+$ Calcd for $C_8H_7{}^{35}ClN_4$ 195.0432; Found 195.0434.

*2-Methyl-5-(4-(trifluoromethyl)phenyl)-2H-tetrazole (**10a**):*[19e]

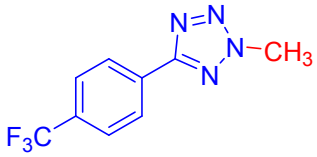

White solid (160 mg, 70% yield); R_f = 0.26 (0.5:9.5 EtOAc : hexane, Silica gel); mp 114–116 °C; ^1H NMR (600 MHz, $CDCl_3$): δ 8.27 (d, J = 8.1 Hz, 2H), 7.76 (d, J = 8.2 Hz, 2H), 4.43 (s, 3H); $^{13}C\{^1H\}$ NMR (151 MHz, $CDCl_3$): δ 164.2, 132.2 (q, J = 32.8 Hz), 130.8, 127.1, 126.0 (q, J = 3.8 Hz), 123.9 (q, J = 273 Hz), 39.7; ^{19}F NMR (377 MHz, $CDCl_3$): –65.908; IR (KBr): 3039, 2967, 2923, 2860, 1756, 1463, 1427, 1326, 1161, 1133, 1068, 1016, 851, 764, 723, 594 cm^{-1}; HRMS (ESI-TOF) m/z: $[M + H]^+$ Calcd for $C_9H_8F_3N_4$ 229.0696; Found 229.0699.

*2-Methyl-5-(4-nitrophenyl)-2H-tetrazole (**11a**):*[19e]

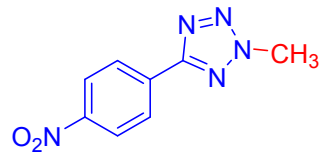

White solid (150 mg, 73% yield); R_f = 0.14 (0.5:9.5 EtOAc : hexane, Silica gel); mp 170–172 °C; ^1H NMR (600 MHz, $CDCl_3$): δ 8.39–8.32 (q, J = 9.0 Hz, 4H), 4.46 (s, 3H); $^{13}C\{^1H\}$ NMR (151 MHz, $CDCl_3$): δ 163.6, 149.0, 133.4, 127.8, 124.4, 39.9; IR (KBr): 3097, 3089, 3040, 2915, 2847, 1605, 1514, 1456, 1311, 1193, 1008, 864, 769, 690 cm^{-1}; HRMS (ESI-TOF) m/z: $[M + H]^+$ Calcd for $C_8H_8N_5O_2$ 206.0673; Found 206.0674.

*tert-Butyl 4-(2-Methyl-2H-tetrazol-5-yl)benzoperoxoate (**12a**):*

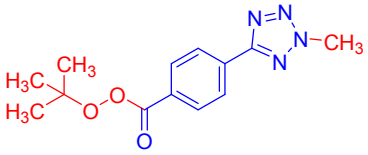

Gummy, (146 mg, 53% yield);R_f = 0.51 (1:9 EtOAc : hexane, Silica gel); ^1H NMR (600 MHz, $CDCl_3$): δ 8.27 (d, J = 8.3 Hz, 2H), 8.10 (d, J = 8.3 Hz, 2H), 4.46 (s, 3H), 1.46 (s, 9H); $^{13}C\{^1H\}$ NMR ($CDCl_3$, 101 MHz): δ 164.3, 164.0, 132.0, 129.9, 129.3, 127.0, 84.4, 39.8, 26.4; IR (KBr): 2985, 2924, 2848, 1746, 1617, 1456, 1181, 1018, 1005, 865, 690 cm^{-1}; HRMS (ESI-TOF) m/z: $[M + H]^+$ Calcd for $C_{13}H_{17}N_4O_3$ 277.1295; Found 277.1293.

*(2-Methyl-2H-tetrazol-5-yl)(p-tolyl)methanone (**13'a**):*

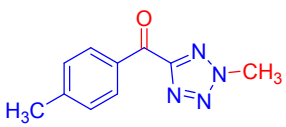

White solid (115 mg, 57% yield);R_f = 0.5 (3:7 EtOAc : hexane, Silica gel); mp 83–85 °C; ^1H NMR (600 MHz, $CDCl_3$): δ 8.24 (d, J = 8.2 Hz, 2H), 7.30 (d, J = 8.0 Hz, 2H), 4.46 (s, 3H), 2.41 (s, 3H); $^{13}C\{^1H\}$ NMR

(CDCl$_3$, 151 MHz): δ 182.1, 163.0, 145.6, 133.0, 130.9, 129.5, 40.1, 22.0; IR (KBr): 3048, 2921, 2855, 1657, 1596, 1449, 1360, 1228, 1170, 1033, 916, 837, 710, 656, 474 cm^{-1}; HRMS (ESI-TOF) m/z: [M + H]$^+$ Calcd for $C_{10}H_{11}N_4O$ 203.0927; Found 203.0928.

*1-Methyl-1H-benzo[d][1,2,3]triazole (**17a**):*[36a]

Reddish oil (56 mg, 42% yield); (56 mg, 42% yield); R_f = 0.42 (3:7 EtOAc : hexane, Silica gel); ^{1}H NMR (600 MHz, CDCl$_3$): δ 8.02 (d, J = 8.4 Hz, 1H), 7.51–7.44 (m, 2H), 7.34 (t, J = 8.0 Hz, 1H), 4.27 (s, 3H); ^{13}C{^{1}H} NMR (151 MHz, CDCl$_3$): δ 146.1, 133.6, 127.4, 123.9, 120.1, 109.2, 34.3; IR (KBr): 3055, 2919, 2858, 1606, 1452, 1380, 1265, 1198, 1108, 1019, 732, 586 cm^{-1}; HRMS (ESI-TOF) m/z: [M + H]$^+$ Calcd for C7H8N3 134.0713; Found 134.0715.

*2-Methylbenzo[d]isothiazol-3(2H)-one 1,1-dioxide (**18a**):*[36b]

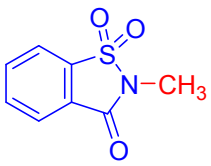

White solid (134 mg, 68% yield); R_f = 0.11 (0.5:9.5 EtOAc : hexane, Silica gel); mp 131–133 °C; ^{1}H NMR (600 MHz, CDCl$_3$): δ 8.07 (d, J = 7.4 Hz, 1H), 7.94 (d, J = 7.5 Hz, 1H), 7.88 (t, J = 7.4 Hz, 1H), 7.84 (t, J = 7.5 Hz, 1H), 3.28 (s, 3H); ^{13}C{^{1}H} NMR (151 MHz, CDCl$_3$): δ 158.9, 137.8, 134.8, 134.5, 127.8, 125.3, 121.2, 23.4; IR (KBr): 3094, 2920, 2852, 1738, 1463, 1320, 1178, 1057, 973, 889, 784, 676, 590 cm^{-1}; HRMS (ESI-TOF) m/z: [M + H]$^+$ Calcd for $C_8H_8NO_3S$ 198.0219; Found 198.0220.

*Acetophenone (**C''**):*

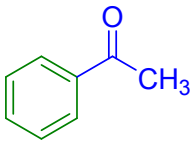

Colorless liquid (152 mg, 42% yield); R_f = 0.44 (0.5:9.5 EtOAc : hexane, Silica gel); ^{1}H NMR (600 MHz, CDCl$_3$): δ 7.96 (d, J = 7.2 Hz, 2H), 7.57 (t, J = 7.4 Hz, 1H), 7.47 (t, J = 7.7 Hz, 2H), 2.61 (s, 3H); ^{13}C{^{1}H} NMR (151 MHz, CDCl$_3$): δ 198.4, 137.2, 133.3, 128.7, 128.4, 26.8; IR (KBr): 3063, 2927, 1763, 1685, 1600, 1415, 1359, 1266, 1156, 1025, 997, 760, 691 cm^{-1}; HRMS (ESI-TOF) m/z: [M + H]$^+$ Calcd for C_8H_9O 121.0648; Found 121.0654.

*1,1-Diphenyl-2-(5-phenyl-2H-tetrazol-2-yl)ethan-1-ol (**1d**):*[4]

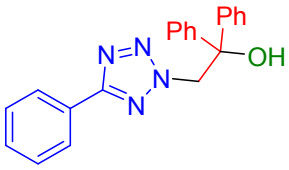

White solid (205 mg, 60% yield); R_f = 0.26 (1:9 EtOAc : hexane, Silica gel); mp 113–115 °C; ^{1}H NMR (600 MHz, $CDCl_3$): δ 8.15 (dd, J = 6.7, 3.0 Hz, 2H), 7.47 (dd, J = 5.0, 1.7 Hz, 3H), 7.39–7.31 (m, 6H), 7.18 (dd, J = 6.8, 2.9 Hz, 4H), 4.83 (d, J = 7.5 Hz, 2H), 3.90 (t, J = 7.6 Hz, 1H) (3.90 (t), D_2O exchangeable); ^{13}C{^{1}H} NMR (151 MHz, $CDCl_3$): δ 164.5, 139.2, 130.7, 129.0, 128.8, 128.6, 128.3, 127.1, 127.0, 78.8, 69.2; IR (KBr): 3433, 3397, 3059, 3033, 1942, 1600, 1464, 1447, 1409, 1367, 1307, 1193, 1084, 1013, 748, 735, 693 cm^{-1}; HRMS (ESI-TOF) m/z*:* [M + H]$^+$ Calcd for $C_{21}H_{19}N_4O$ 343.1553; Found 343.1561.

*5-Phenyl-2-propyl-2H-tetrazole (**1e**):*

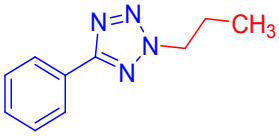

Colorless liquid (80 mg, 43% yield); R_f = 0.36 (0.5:9.5 EtOAc : hexane, Silica gel); ^{1}H NMR (600 MHz, $CDCl_3$): δ 8.15 (d, J = 8.1 Hz, 2H), 7.51–7.44 (m, 3H), 4.62 (t, J = 7.1 Hz, 2H), 2.10 (h, J = 7.3 Hz, 2H), 1.00 (t, J = 7.4 Hz, 3H); ^{13}C{^{1}H} NMR (151 MHz, $CDCl_3$): δ 165.2, 130.4, 129.0, 127.7, 126.9, 54.9, 23.1, 11.1; IR (KBr): 3070, 2967, 2932, 2879, 1528, 1451, 1385, 1354, 1185, 1071, 1027, 807, 787, 732, 693 cm^{-1}; HRMS (ESI-TOF) m/z*:* [M + H]$^+$ Calcd for $C_{10}H_{13}N_4$ 189.1135; Found 189.1139.

*2-Pentyl-5-phenyl-2H-tetrazole (**1f**):*

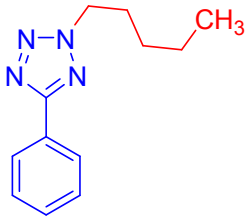

Colorless liquid (160 mg, 74% yield); R_f = 0.46 (0.5:9.5 EtOAc : hexane, Silica gel); ^{1}H NMR (600 MHz, $CDCl_3$): δ 8.17 (d, J = 6.6 Hz, 2H), 7.53–7.45 (m, 3H), 4.66 (t, J = 7.2 Hz, 2H), 2.11–2.04 (m, 2H), 1.43–1.33 (m, 4H), 0.92 (t, J = 7.0 Hz, 3H); ^{13}C{^{1}H} NMR (151 MHz, $CDCl_3$): δ 165.1, 130.3, 129.0, 127.6, 126.9, 53.3, 29.2, 28.6, 22.1, 14.0; IR (KBr): 3130, 2924, 2854, 1625, 1546, 1465, 1400, 1328, 1161, 1128, 1066, 1014, 853, 764, 726, cm^{-1}; HRMS (ESI-TOF) m/z*:* [M + H]$^+$ Calcd for $C_{12}H_{17}N_4$ 217.1448; Found 217.1453.

*2-Heptyl-5-phenyl-2H-tetrazole (**1g**):*

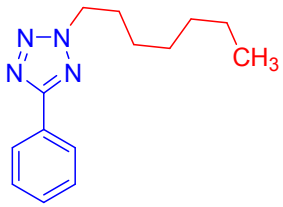

Colorless liquid (183 mg, 75% yield); R_f = 0.36 (0.5:9.5 EtOAc : hexane, Silica gel); ^{1}H NMR (400 MHz, $CDCl_3$): δ 8.15 (d, J = 8.0 Hz, 2H), 7.48 (m, 3H), 4.64 (t, J = 7.2 Hz, 2H), 2.06 (p, J = 7.3 Hz, 2H), 1.41–1.22 (m, 8H), 0.88 (t, J = 6.9 Hz, 3H); ^{13}C{^{1}H} NMR (101 MHz, $CDCl_3$): δ 165.2, 130.3, 129.0, 127.7, 126.9, 53.4, 31.7, 29.5, 28.7, 26.5, 22.6, 14.1; IR (KBr): 3069, 2930, 2861, 1743, 1529, 1456, 1359, 1194, 1035, 924, 787, 732, 695 cm^{-1}; HRMS (ESI-TOF) m/z: [M + H]$^+$ Calcd for $C_{14}H_{21}N_4$ 245.1761; Found 245.1765.

*2-Nonyl-5-phenyl-2H-tetrazole (**1h**):*

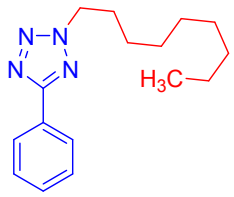

Colorless liquid (215 mg, 79% yield); R_f = 0.24 (1:9 EtOAc : hexane, Silica gel); ^{1}H NMR (400 MHz, $CDCl_3$): δ 8.15 (d, J = 7.9 Hz, 2H), 7.53–7.44 (m, 3H), 4.64 (t, J = 7.2 Hz, 2H), 2.06 (p, J = 7.2 Hz, 2H), 1.37–1.24 (m, 12H), 0.87 (t, J = 6.8 Hz, 3H); ^{13}C{^{1}H} NMR (101 MHz, $CDCl_3$): δ 165.2, 130.3, 129.0, 127.7, 127.0, 53.4, 31.9, 29.5, 29.4, 29.3, 29.0, 26.5, 22.8, 14.2; IR (KBr): 3071, 2927, 2858, 1743, 1529, 1456, 1359, 1282, 1195, 1034, 924, 732, 694 cm^{-1}; HRMS (ESI-TOF) m/z: [M + H]$^+$ Calcd for $C_{16}H_{25}N_4$ 273.2074; Found 273.2077.

*5-Phenyl-2-undecyl-2H-tetrazole (**1i**):*

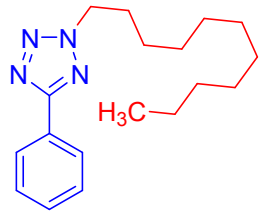

Colorless liquid (240 mg, 80% yield); R_f = 0.24 (1:9 EtOAc : hexane, Silica gel); ^{1}H NMR (600 MHz, $CDCl_3$): δ 8.15 (d, J = 6.6 Hz, 2H), 7.51–7.46 (m, 3H), 4.64 (t, J = 7.2 Hz, 2H), 2.05 (p, J = 7.2 Hz, 2H), 1.30–1.37 (m, 4H), 1.29–1.21 (m, 12H), 0.87 (t, J = 7.0 Hz, 3H); ^{13}C{^{1}H} NMR (151 MHz, $CDCl_3$): δ 165.1, 130.3, 129.0, 127.6, 126.9, 53.3, 32.0, 29.7, 29.6, 29.5, 29.45, 29.41, 29.0, 26.5, 22.8, 14.2; IR (KBr): 3071, 2924, 2855, 1748, 1638, 1451, 1355, 1242, 1194, 1068, 921, 784, 729, 691 cm^{-1}; HRMS (ESI-TOF) m/z: [M + H]$^+$ Calcd for $C_{18}H_{29}N_4$ 301.2387; Found 301.2386.

*5-(4-(tert-Butyl)phenyl)-2-undecyl-2H-tetrazole (**5i**):*

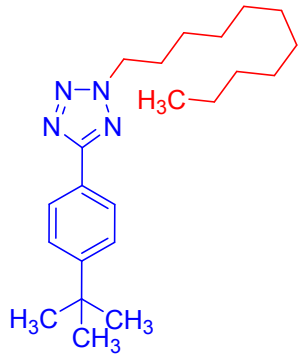

White solid (299 mg, 84% yield); R_f = 0.26 (1:9 EtOAc : hexane, Silica gel); mp 46–48 °C; ^{1}H NMR (600 MHz, $CDCl_3$): δ 8.07 (d, J = 8.4 Hz, 2H), 7.51 (d, J = 8.4 Hz, 2H), 4.63 (t, J = 7.2 Hz, 2H), 2.04 (p, J = 7.1 Hz, 2H), 1.36 (s, 9H), 1.31–1.16 (m, 16H), 0.87 (t, J = 7.0 Hz, 3H); ^{13}C{^{1}H} NMR (151 MHz, $CDCl_3$): δ 165.1, 153.6, 126.7, 125.9, 124.8, 53.3, 35.0, 32.0, 31.6, 29.7, 29.6, 29.53, 29.50, 29.4, 29.0, 26.5, 22.8, 14.3; IR (KBr): 2926, 2858, 1750, 1690, 1621, 1464, 1364, 1269, 1196, 1144, 1038, 844, 766, 725, 561 cm^{-1}; HRMS (ESI-TOF) m/z: [M + H]$^+$ Calcd for $C_{22}H_{37}N_4$ 357.3013; Found 357.3014.

*5-(4-(Trifluoromethyl)phenyl)-2-undecyl-2H-tetrazole (**10i**):*

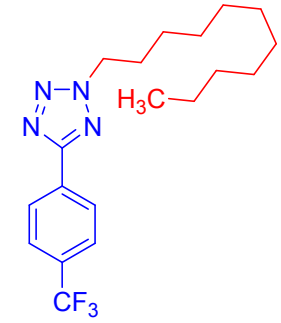

White solid (328 mg, 89% yield); R_f = 0.6 (0.5:9.5 EtOAc : hexane, Silica gel); mp 51–53 °C; ^{1}H NMR (600 MHz, $CDCl_3$): δ 8.28 (d, J = 8.1 Hz, 2H), 7.75 (d, J = 8.2 Hz, 2H), 4.67 (t, J = 7.2 Hz, 2H), 2.07 (p, J = 7.2 Hz, 2H), 1.39–1.34 (m, 4H), 1.29–1.22 (m, 12H), 0.87 (t, J = 7.0 Hz, 3H); ^{13}C{^{1}H} NMR (151 MHz, $CDCl_3$): δ 163.9, 132.1 (q, J = 32.6 Hz), 131.0, 127.4, 126.0 (q, J = 3.75 Hz), 124.0 (q, J = 272.4 Hz), 53.6, 32.0, 29.7, 29.6, 29.49, 29.46, 29.44, 29.0, 26.5, 22.8, 14.3; ^{19}F NMR (565 MHz, $CDCl_3$): –62.84; IR (KBr): 2919, 2852, 1468, 1429, 1328, 1164, 1132, 1069, 850, 762, 726, 597, 510 cm^{-1}; HRMS (ESI-TOF) m/z: [M + H]$^+$ Calcd for $C_{19}H_{28}F_3N_4$ 369.2261; Found 369.2268.

*5-(Naphthalen-2-yl)-2-undecyl-2H-tetrazole (**19i**):*

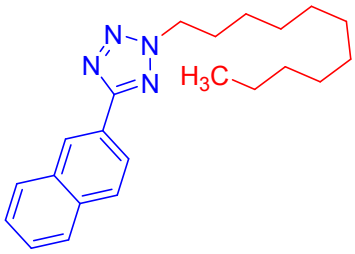

White solid (287 mg, 82% yield); R_f = 0.20 (1:9 EtOAc : hexane, Silica gel); mp 52–54 °C; ^{1}H NMR (400 MHz, $CDCl_3$): δ 8.69 (s, 1H), 8.22 (dd, J = 8.6, 1.6 Hz, 1H), 7.95 (d, J = 8.8 Hz, 2H), 7.90–7.84 (m, 1H), 7.56–7.50 (m, 2H), 4.67 (t, J = 7.2 Hz, 2H), 2.13–2.04 (m, 2H), 1.25 (bs, 16H), 0.87 (t, J = 6.8 Hz, 3H); ^{13}C{^{1}H} NMR (101 MHz, $CDCl_3$): δ 165.3, 134.3, 133.4, 128.8, 128.7, 128.0, 127.2, 126.8, 126.7, 125.0, 124.1, 53.4, 32.0, 29.7, 29.6, 29.5, 29.46, 29.41, 29.0, 26.5, 22.8, 14.2; IR (KBr): 3051, 2919, 2852, 1464, 1404, 1358, 1268, 1237, 1199, 1044,

951, 834, 763 cm^{-1}; HRMS (ESI-TOF) m/z: $[M + H]^+$ Calcd for $C_{22}H_{31}N_4$ 351.2543; Found 351.2547.

*5-(m-Tolyl)-2-undecyl-2H-tetrazole (**20i**):*

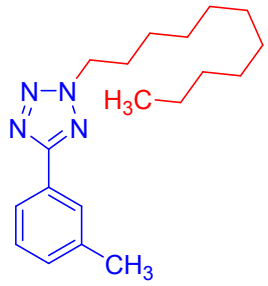

Colorless liquid (233 mg, 74% yield); R_f = 0.58 (0.5:9.5 EtOAc : hexane, Silica gel); ^1H NMR (400 MHz, $CDCl_3$): δ 7.98 (s, 1H), 7.94 (d, J = 7.7 Hz, 1H), 7.37 (t, J = 7.6 Hz, 1H), 7.27 (d, J = 6.9 Hz, 1H), 4.63 (t, J = 7.2 Hz, 2H), 2.43 (s, 3H), 2.05 (p, J = 7.2 Hz, 2H), 1.25 (s, 16H), 0.87 (t, J = 6.9 Hz, 3H); $^{13}C\{^1H\}$ NMR (101 MHz, $CDCl_3$): δ 165.3, 138.7, 131.1, 128.9, 127.6, 127.5, 124.1, 53.3, 32.0, 29.7, 29.6, 29.5, 29.45, 29.41, 29.01, 26.5, 22.8, 21.5, 14.2; IR (KBr): 2956, 2928, 2857, 1660, 1471, 1529, 1465, 1450, 1355, 1194, 1046, 1027, 789, 732, 693 cm^{-1}; HRMS (ESI-TOF) m/z: $[M + H]^+$ Calcd for $C_{19}H_{31}N_4$ 315.2543; Found 315.2550.

*Benzyl 2-phenylacetate (**J**):*[35c]

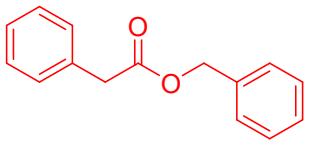

Gummy (349 mg, 77% yield); R_f = 0.42 (0.5:9.5 EtOAc : hexane, Silica gel); ^1H NMR (600 MHz, $CDCl_3$): δ 7.36–7.15 (m, 10H), 5.06 (s, 2H), 3.60 (s, 2H); $^{13}C\{^1H\}$ NMR (151 MHz, $CDCl_3$): δ 171.6, 135.9, 134.0, 129.4, 128.7, 128.67, 128.4, 128.3, 127.3, 66.8, 41.5; IR (KBr): 3076, 2970, 2935, 1768, 1602, 1505, 1415, 1233, 1161, 999, 848, 749, 686 cm^{-1}; HRMS (ESI-TOF) m/z: $[M + H]^+$ Calcd for $C_{15}H_{15}O_2$ 227.1067; Found 227.1069.

*2-(Heptan-3-yl)-5-phenyl-2H-tetrazole (**1k**):*

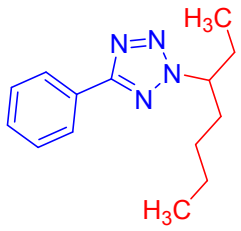

Colorless liquid (188 mg, 77% yield); R_f = 0.59 (0.6:9.4 EtOAc : hexane, Silica gel); ^1H NMR (600 MHz, $CDCl_3$): δ 8.14 (d, J = 6.8 Hz, 2H), 7.48–7.40 (m, 3H), 4.71 (tt, J = 9.5, 4.7 Hz, 1H), 2.11–2.03 (m, 2H), 1.99–1.91 (m, 1H), 1.88 (m, 1H), 1.29–1.16 (m, 3H), 1.07–0.97 (m, 1H), 0.81 (t, J = 5.6 Hz, 3H), 0.79 (t, J = 5.8 Hz, 3H); $^{13}C\{^1H\}$ NMR (151 MHz, $CDCl_3$): δ 165.0, 130.2, 128.9, 127.9, 126.9, 67.2, 34.4, 28.3, 28.1, 22.3, 13.9, 10.5; IR (KBr): 3065, 2935, 2868, 1453, 1351, 1279, 1184, 1030, 928, 931, 788, 731, 695, 514 cm^{-1}; HRMS (ESI-TOF) m/z: $[M + H]^+$ Calcd for $C_{14}H_{21}N_4$ 245.17607; Found 245.1759.

*2-(Heptan-3-yl)-5-(4-methoxyphenyl)-2H-tetrazole (**4k**):*

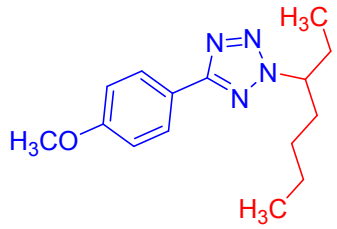

Colorless liquid (162 mg, 71% yield); R_f = 0.42 (0.6:9.4 EtOAc : hexane, Silica gel); ^{1}H NMR (600 MHz, $CDCl_3$): δ 8.06 (d, J = 8.8 Hz, 2H), 6.97 (d, J = 8.8 Hz, 2H), 4.69 (tt, J = 9.5, 4.8 Hz, 1H), 3.84 (s, 3H), 2.09–2.01 (m, 2H), 1.97–1.90 (m, 1H), 1.87 (m, 1H), 1.33–1.15 (m, 3H), 1.07–0.97 (m, 1H), 0.80 (m, 6H); ^{13}C{^{1}H} NMR (151 MHz, $CDCl_3$): δ 164.8, 161.2, 128.4, 120.5, 114.3, 67.1, 55.5, 34.5, 28.3, 28.2, 22.3, 14.0, 10.6; IR (KBr): 2938, 2868, 1614, 1460, 1249, 1176, 1029, 935, 837, 763, 535 cm^{-1}; HRMS (ESI-TOF) m/z*:* $[M + H]^+$ Calcd for $C_{15}H_{23}N_4O$ 275.1866; Found 275.1865.

*5-(2-Chlorophenyl)-2-(heptan-3-yl)-2H-tetrazole (**9k**):*

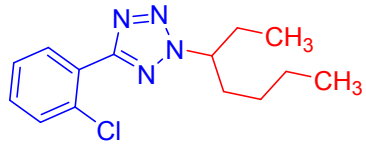

Colorless liquid (204 mg, 73% yield); R_f = 0.52 (0.6:9.4 EtOAc : hexane, Silica gel); ^{1}H NMR (600 MHz, $CDCl_3$): δ 7.89 (d, J = 7.0 Hz, 1H), 7.54–7.43 (m, 1H), 7.38–7.30 (m, 2H), 4.75 (tt, J = 9.5, 4.8 Hz, 1H), 2.11–2.03 (m, 2H), 1.99–1.92 (m, 1H), 1.92–1.86 (m, 1H), 1.31–1.18 (m, 3H), 1.07–0.99 (m, 1H), 0.80 (m, 6H); ^{13}C{^{1}H} NMR (151 MHz, $CDCl_3$): δ 163.1, 133.2, 131.4, 131.0, 130.8, 127.0, 126.9, 67.3, 34.4, 28.3, 28.0, 22.2, 13.9, 10.5; IR (KBr): 3068, 2949, 2865, 1596, 1450, 1345, 1182, 1035, 937, 824, 746, 662, 466 cm^{-1}; HRMS (ESI-TOF) m/z*:* $[M + H]^+$ Calcd for $C_{14}H_{20}ClN_4$ 279.1371; Found 279.1369.

*2-(Heptan-3-yl)-5-(4-(trifluoromethyl)phenyl)-2H-tetrazole (**10k**):*

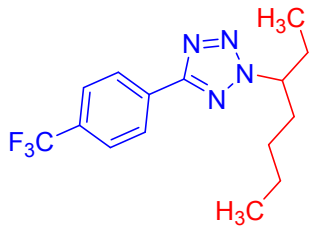

Colorless liquid (256 mg, 82% yield); R_f = 0.5 (0.4:9.6 EtOAc : hexane, Silica gel); ^{1}H NMR (600 MHz, $CDCl_3$): δ 8.28 (d, J = 8.1 Hz, 2H), 7.73 (d, J = 8.2 Hz, 2H), 4.76 (tt, J = 9.5, 4.8 Hz, 1H), 2.13–2.06 (m, 2H), 1.96 (m, 2H), 1.29–1.21 (m, 3H), 1.09–0.98 (m, 1H), 0.82 (m, 6H); ^{13}C{^{1}H} NMR (151 MHz, $CDCl_3$): δ 163.8, 131.97 (q, J = 32.46 Hz), 131.2, 127.2, 125.9 (q, J = 3.62 Hz), 124.0 (q, J = 272.25 Hz), 67.5, 34.4, 28.3, 28.1, 22.2, 13.9, 10.5; ^{19}F NMR (565 MHz, $CDCl_3$): –62.82; IR (KBr): 2956, 2870, 1462, 1321, 1165, 1126, 1065, 934, 851, 766, 598, 462 cm^{-1}; HRMS (ESI-TOF) m/z*:* $[M + H]^+$ Calcd for $C_{15}H_{20}F_3N_4$ 313.1635; Found 313.1633.

*2-(Heptan-3-yl)-5-(4-nitrophenyl)-2H-tetrazole (**11k**):*

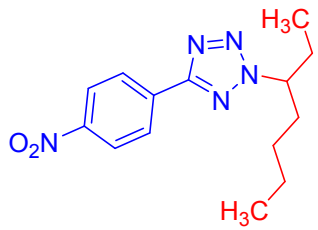

Light yellow solid (246 mg, 85% yield); R_f = 0.48 (0.6:9.4 EtOAc : hexane, Silica gel); mp 42–44 °C; ^{1}H NMR (600 MHz, $CDCl_3$): δ 8.33–8.28 (m, 4H), 4.75 (tt, J = 9.5, 4.8 Hz, 1H), 2.11–2.02 (m, 2H), 2.01–1.94 (m, 1H), 1.91 (m, 1H), 1.30–1.17 (m, 3H), 1.06–0.96 (m, 1H), 0.80 (m, J = 7.3 Hz, 6H); ^{13}C{^{1}H} NMR (151 MHz, $CDCl_3$): δ 163.2, 149.0, 133.8, 127.8, 124.3, 67.7, 34.4, 28.3, 28.1, 22.3, 13.9, 10.5; IR (KBr): 3098, 2935, 2864, 1604, 1518, 1456, 1338, 1105, 1035, 935, 854, 731, 687, 501 cm^{-1}; HRMS (ESI-TOF) m/z: [M + H]$^+$ Calcd for $C_{14}H_{20}N_5O_2$ 290.1612; Found 290.1607.

*2-(Heptan-3-yl)-5-(thiophen-2-yl)-2H-tetrazole (**21k**):*

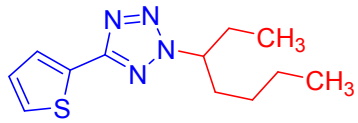

Colorless liquid (185 mg, 74% yield); R_f = 0.56 (0.6:9.4 EtOAc : hexane, Silica gel); ^{1}H NMR (600 MHz, $CDCl_3$): δ 7.77 (dd, J = 3.6, 1.0 Hz, 1H), 7.41 (dd, J = 5.0, 1.0 Hz, 1H), 7.11 (dd, J = 4.9, 3.7 Hz, 1H), 4.69 (tt, J = 9.5, 4.8 Hz, 1H), 2.10–2.00 (m, 2H), 1.97–1.90 (m, 1H), 1.84–1.89 (m, 1H), 1.33–1.15 (m, 3H), 1.05–0.97 (m, 1H), 0.81 (m, 6H); ^{13}C{^{1}H} NMR (151 MHz, $CDCl_3$): δ 161.1, 129.6, 128.0, 127.76, 127.72, 67.4, 34.4, 28.3, 28.1, 22.3, 14.0, 10.6; IR (KBr): 3098, 2955, 2868, 1571, 1468, 1386, 1344, 1223, 1182, 1033, 967, 934, 846, 706, 572 cm^{-1}; HRMS (ESI-TOF) m/z: [M + H]$^+$ Calcd for $C_{12}H_{19}N_4S$ 251.1325; Found 251.1321.

*2-(tert-Butyl)-5-phenyl-2H-tetrazole (**1l**):*[14g]

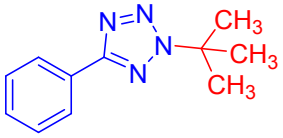

Colorless liquid (176 mg, 87% yield); R_f = 0.53 (0.6:9.4 EtOAc : hexane, Silica gel); ^{1}H NMR (600 MHz, $CDCl_3$): δ 8.20 (dd, J = 7.8, 1.6 Hz, 2H), 7.55–7.45 (m, 3H), 1.84 (s, 9H); ^{13}C{^{1}H} NMR (151 MHz, $CDCl_3$): δ 164.6, 130.1, 128.9, 128.0, 126.9, 64.0, 29.5; IR (KBr): 3070, 2984, 1453, 1369, 1312, 1194, 1028, 926, 789, 731, 694, 595, 514 cm^{-1}; HRMS (ESI-TOF) m/z: [M + H]$^+$ Calcd for $C_{11}H_{15}N_4$ 203.1291; Found 203.1294.

*2-(tert-Butyl)-5-(4-methoxyphenyl)-2H-tetrazole (**4l**):*

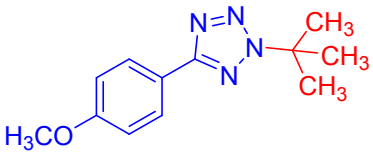

Colorless liquid (188 mg, 81% yield); R_f = 0.39 (0.6:9.4 EtOAc : hexane, Silica gel); ^{1}H NMR (600 MHz, $CDCl_3$): δ 8.06 (d, J = 8.9 Hz, 2H), 6.96 (d, J = 8.8 Hz, 2H), 3.83 (s, 3H), 1.75 (s, 9H); ^{13}C{^{1}H} NMR (151 MHz, $CDCl_3$): δ 164.5, 161.1, 128.4, 120.6, 114.3, 63.8, 55.5, 29.5; IR (KBr): 2983, 2935, 2838, 1614, 1542, 1459, 1368, 1303, 1248, 1182, 1109, 1028, 838, 763, 638, 535 cm^{-1}; HRMS (ESI-TOF) m/z: [M + H]$^+$ Calcd for $C_{12}H_{17}N_4O$ 233.1397; Found 233.1395.

*2-(tert-Butyl)-5-(4-nitrophenyl)-2H-tetrazole (**11l**):*

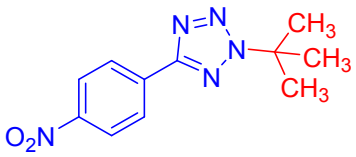

White solid (227 mg, 92% yield); R_f = 0.52 (0.6:9.4 EtOAc : hexane, Silica gel); mp 166–168 °C; ^{1}H NMR (600 MHz, $CDCl_3$): δ 8.38 (s, 4H), 1.85 (s, 9H); ^{13}C{^{1}H} NMR (151 MHz, $CDCl_3$): δ 162.8, 148.8, 133.9, 127.7, 124.3, 64.7, 29.5; IR (KBr): 3103, 2922, 2855, 1602, 1509, 1457, 1332, 1195, 1101, 1030, 856, 729, 599, 497, 437 cm^{-1}; HRMS (ESI-TOF) m/z: [M + H]$^+$ Calcd for $C_{11}H_{14}N_5O_2$ 248.1142; Found 248.1144.

*2-(Adamantan-1-yl)-5-phenyl-2H-tetrazole (**1m**):*[36c]

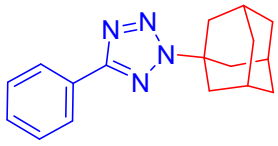

White solid (238 mg, 85% yield); R_f = 0.26 (0.2:9.8 EtOAc : hexane, Silica gel); mp 87–89 °C; ^{1}H NMR (400 MHz, $CDCl_3$): δ 8.13 (dd, J = 7.6, 2.0 Hz, 2H), 7.47–7.40 (m, 3H), 2.37 (d, J = 3.4 Hz, 6H), 2.32–2.20 (m, 3H), 1.80 (t, J = 3.2 Hz, 6H); ^{13}C{^{1}H} NMR (151 MHz, $CDCl_3$): δ 164.3, 130.1, 128.9, 128.1, 126.9, 64.0, 42.3, 36.0, 29.5; IR (KBr): 3055, 2913, 2855, 1449, 1361, 1311, 1179, 1104, 1015, 838, 692, 510 cm^{-1}; HRMS (ESI-TOF) m/z: [M + H]$^+$ Calcd for $C_{17}H_{21}N_4$ 281.1761; Found 281.1758.

*2-(Adamantan-1-yl)-5-(4-(trifluoromethyl)phenyl)-2H-tetrazole (**10m**):*[36c]

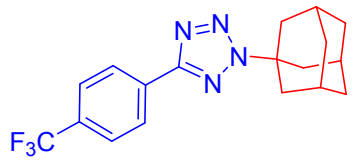

White solid (310 mg, 89% yield); R_f = 0.43 (0.2:9.8 EtOAc : hexane, Silica gel); mp 122–124 °C; ^{1}H NMR (600 MHz, $CDCl_3$): δ 8.31 (d, J = 8.2 Hz, 2H), 7.76 (d, J = 8.4 Hz, 2H), 2.42 (d, J = 3.2 Hz, 6H), 2.37–2.30 (m, 3H), 1.85 (t, J = 3.3 Hz, 6H); ^{13}C{^{1}H} NMR (151 MHz, $CDCl_3$): δ 163.2, 131.86 (q, J = 32.62 Hz), 131.5, 127.2, 125.92 (q, J =

3.7 Hz), 124.08 (q, J = 272.41), 64.4, 42.4, 35.9, 29.5; ^{19}F NMR (565 MHz, $CDCl_3$): –62.78; IR (KBr): 2921, 2858, 1544, 1461, 1419, 1320, 1163, 1110, 1060, 1013, 846, 767, 599, 456 cm^{-1}; HRMS (ESI-TOF) m/z: [M + H]$^+$ Calcd for $C_{18}H_{20}F_3N_4$ 349.1635; Found 349.1630.

*2-(Adamantan-1-yl)-5-(4-nitrophenyl)-2H-tetrazole (**11m**):*[36c]

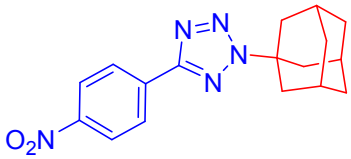

White solid (293 mg, 90% yield); R_f = 0.48 (0.2:9.8 EtOAc : hexane, Silica gel); mp 186–188 °C; ^{1}H NMR (600 MHz, $CDCl_3$): δ 8.38–8.34 (m, 4H), 2.42 (d, J = 3.2 Hz, 6H), 2.38–2.30 (m, 3H), 1.79 (t, J = 3.2 Hz, 6H); ^{13}C{^{1}H} NMR (151 MHz, $CDCl_3$): δ 162.5, 148.8, 134.0, 127.7, 124.3, 64.7, 42.4, 35.9, 29.5; IR (KBr): 3105, 2914, 2853, 1514, 1451, 1335, 1184, 1099, 1017, 853, 734, 684, 509 cm^{-1}; HRMS (ESI-TOF) m/z: [M + H]$^+$ Calcd for $C_{17}H_{20}N_5O_2$ 326.1612; Found 326.1609.

*2,5-Diphenyl-2H-tetrazole (**1n**):*[15c]

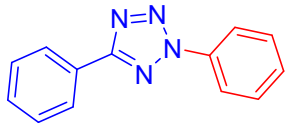

White solid (135 mg, 61% yield); R_f = 0.67 (0.5:9.5 EtOAc : hexane, Silica gel); mp 102–104 °C; ^{1}H NMR (600 MHz, $CDCl_3$): δ 8.16 (d, J = 8.0 Hz, 2H), 8.13 (d, J = 7.4 Hz, 2H), 7.62 (t, J = 7.4 Hz, 1H), 7.59–7.52 (m, 3H), 7.48 (t, J = 7.7 Hz, 2H); ^{13}C{^{1}H} NMR (101 MHz, $CDCl_3$): δ 165.4, 137.1, 130.7, 129.79, 129.76, 129.1, 127.3, 127.2, 120.0; IR (KBr): 3015, 2924, 2851, 1620, 1592, 1530, 1495, 1447, 1367, 1214, 1014, 918, 762, 678 cm^{-1}; HRMS (ESI-TOF) m/z: [M + H]$^+$ Calcd for $C_{13}H_{11}N_4$ 223.0978; Found 223.0977.

*2-Phenyl-5-(p-tolyl)-2H-tetrazole (**3n**):*[15c]

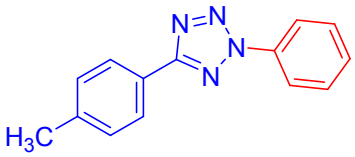

White solid (137 mg, 58% yield); R_f = 0.65 (0.5:9.5 EtOAc : hexane, Silica gel); mp 94–96 °C; ^{1}H NMR (400 MHz, $CDCl_3$): δ 8.20 (d, J = 7.4 Hz, 2H), 8.14 (d, J = 8.1 Hz, 2H), 7.57 (t, J = 7.6 Hz, 2H), 7.49 (t, J = 7.4 Hz, 1H), 7.33 (d, J = 7.9 Hz, 2H), 2.44 (s, 3H); ^{13}C{^{1}H} NMR (101 MHz, $CDCl_3$): δ 165.5, 140.9, 137.1, 129.78, 129.77, 129.7, 127.1, 124.5, 119.9, 21.7; IR (KBr): 3057, 2918, 2848, 1736, 1582, 1552, 1489, 1470, 1447, 1310, 1274, 1198, 1092, 1068, 1016, 965, 875, 805, 725,

687 cm^{-1}; HRMS (ESI-TOF) m/z: $[M + H]^+$ Calcd for $C_{14}H_{13}N_4$ 237.1135; Found 237.1138.

*5-(3-Methoxyphenyl)-2-phenyl-2H-tetrazole (**6n**):*

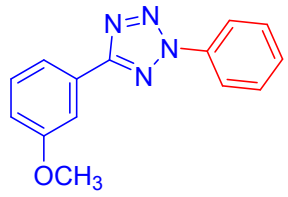

White solid (136 mg, 54% yield); R_f = 0.40 (0.5:9.5 EtOAc : hexane, Silica gel); mp 79–81 °C; ^{1}H NMR (400 MHz, $CDCl_3$): δ 8.20 (d, J = 7.7 Hz, 2H), 7.86 (d, J = 7.6 Hz, 1H), 7.80 (s, 1H), 7.58 (t, J = 7.7 Hz, 2H), 7.51 (t, J = 7.4 Hz, 1H), 7.44 (t, J = 8.0 Hz, 1H), 7.03–7.06 (m, 1H), 3.92 (s, 3H); ^{13}C{^{1}H} NMR (101 MHz, $CDCl_3$): δ 165.3, 160.2, 137.1, 130.2, 129.8, 128.5, 120.0, 119.6, 117.1, 111.9, 55.6; IR (KBr): 3065, 3046, 2934, 2839, 1615, 1499, 1465, 1174, 1019, 907, 879, 752 cm^{-1}; HRMS (ESI-TOF) m/z: $[M + H]^+$ Calcd for $C_{14}H_{13}N_4O$ 253.1084; Found 253.1085.

*5-(4-Bromophenyl)-2-phenyl-2H-tetrazole (**7n**):*[15c]

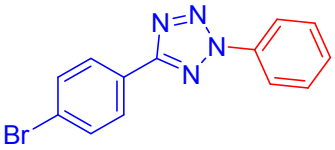

White solid (186 mg, 62% yield); R_f = 0.61 (0.5:9.5 EtOAc : hexane, Silica gel); mp 112–114 °C; ^{1}H NMR (600 MHz, $CDCl_3$): δ 8.19 (d, J = 7.8 Hz, 2H), 8.13 (d, J = 8.4 Hz, 2H), 7.66 (d, J = 8.4 Hz, 2H), 7.58 (t, J = 7.8 Hz, 2H), 7.51 (t, J = 7.4 Hz, 1H); ^{13}C{^{1}H} NMR (151 MHz, $CDCl_3$): δ 164.5, 136.9, 132.4, 129.9, 129.8, 128.7, 126.2, 125.1, 120.0; IR (KBr): 3072, 2954, 2921, 2856, 1597, 1493, 1470, 1454, 1412, 1272, 1216, 1174, 1077, 1008, 994, 833, 751, 696, 676 cm^{-1}; HRMS (ESI-TOF) m/z: $[M + H]^+$ Calcd for $C_{13}H_{10}{}^{79}BrN_4$ 301.0083; Found 301.0086.

*5-(2-Chlorophenyl)-2-phenyl-2H-tetrazole (**9n**):*[37a]

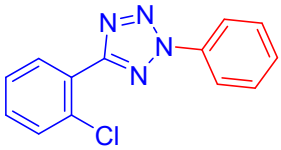

White solid (143 mg, 56% yield); R_f = 0.58 (0.5:9.5 EtOAc : hexane, Silica gel); mp 72–74 °C; ^{1}H NMR (400 MHz, $CDCl_3$): δ 8.14 (d, J = 7.9 Hz, 2H), 8.02–7.96 (m, 1H), 7.51 (t, J = 7.4 Hz, 3H), 7.44 (t, J = 7.4 Hz, 1H), 7.40–7.34 (m, 2H); ^{13}C{^{1}H} NMR (101 MHz, $CDCl_3$): δ 163.6, 137.0, 133.4, 131.6, 131.4, 131.1, 129.9, 129.8, 127.1, 126.5, 120.1; IR (KBr): 3065, 2932, 2853, 1726, 1590, 1549, 1454, 1274, 1263, 1119, 1071, 1043, 779, 705, 688 cm^{-1}; HRMS (ESI-TOF) m/z: $[M + H]^+$ Calcd for $C_{13}H_{10}{}^{35}ClN_4$ 257.0589; Found 257.0593.

*2-Phenyl-5-(4-(trifluoromethyl)phenyl)-2H-tetrazole (**10n**):*

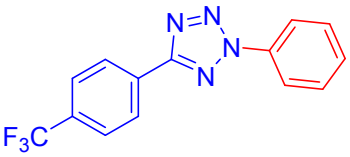

White solid (189 mg, 65% yield); R_f = 0.64 (0.5:9.5 EtOAc : hexane, Silica gel); mp 111–113 °C; ^{1}H NMR (600 MHz, $CDCl_3$): δ 8.39 (d, J = 8.1 Hz, 2H), 8.22 (d, J = 7.8 Hz, 2H), 7.80 (d, J = 8.2 Hz, 2H), 7.60 (t, J = 7.8 Hz, 2H), 7.54 (t, J = 7.4 Hz, 1H); ^{13}C{^{1}H} NMR (101 MHz, $CDCl_3$): δ 164.1, 136.9, 132.4 (q, J = 32.7 Hz), 130.6, 130.0, 129.8, 127.4, 126.0 (q, J = 273.3 Hz), 120.0; ^{19}F NMR (377 MHz, $CDCl_3$): δ –62.90; IR (KBr): 3067, 2916, 1596, 1499, 1425, 1384, 1325, 1210, 1160, 1065, 1015, 991, 920, 854, 765, 728, 685 cm^{-1}; HRMS (ESI-TOF) m/z: [M + H]$^+$ Calcd for $C_{14}H_{10}F_3N_4$ 291.0852; Found 291.0859.

*5-(4-Nitrophenyl)-2-phenyl-2H-tetrazole (**11n**):*[37b]

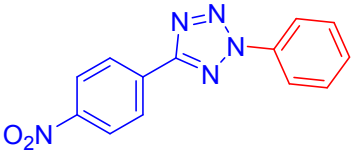

White solid (179 mg, 67% yield); R_f = 0.37 (0.5:9.5 EtOAc : hexane, Silica gel); mp 199–201 °C; ^{1}H NMR (400 MHz, $CDCl_3$): δ 8.45 (d, J = 9.0 Hz, 2H), 8.39 (d, J = 9.0 Hz, 2H), 8.21 (d, J = 7.9 Hz, 2H), 7.61 (t, J = 7.5 Hz, 2H), 7.55 (t, J = 7.3 Hz, 1H); ^{13}C{^{1}H} NMR (151 MHz, $CDCl_3$): δ 163.5, 149.2, 136.8, 133.2, 130.3, 130.0, 128.0, 124.4, 120.1; IR (KBr): 3103, 2920, 2851, 1601, 1519, 1494, 1452, 1423, 1339, 1218, 1105, 1021, 861, 763, 730, 695, 680 cm^{-1}; HRMS (ESI-TOF) m/z: [M + H]$^+$ Calcd for $C_{13}H_{10}N_5O_2$ 268.0829; Found 268.0831.

*2-Phenyl-5-(thiophen-2-yl)-2H-tetrazole (**21n**):*[37c]

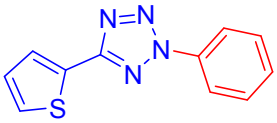

Yellow solid (144 mg, 63% yield); R_f = 0.55 (0.5:9.5 EtOAc : hexane, Silica gel); mp 132–134 °C; ^{1}H NMR (400 MHz, $CDCl_3$): δ 8.15–8.19 (m, 2H), 7.91 (dd, J = 3.6, 1.1 Hz, 1H), 7.59–7.54 (m, 2H), 7.52–7.46 (m, 2H), 7.18 (dd, J = 5.0, 3.7 Hz, 1H); ^{13}C{^{1}H} NMR (101 MHz, $CDCl_3$): δ 161.5, 136.9, 129.84, 129.81, 128.9, 128.4, 128.2, 120.0; IR (KBr): 3107, 3067, 2923, 2852, 1594, 1571, 1493, 1463, 1374, 1226, 1204, 1003, 848, 763, 674 cm^{-1}; HRMS (ESI-TOF) m/z: [M + H]$^+$ Calcd for $C_{11}H_9N_4S$ 229.0542; Found 229.0546.

*5-(2-Bromo-4-methylphenyl)-2-phenyl-2H-tetrazole (**22n**):*

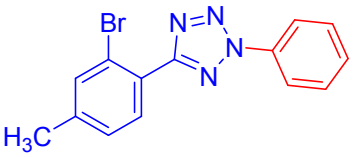

White solid (183 mg, 58% yield); R_f = 0.43 (0.5:9.5 EtOAc : hexane, Silica gel); mp 99–101 °C; ^{1}H NMR (600 MHz, $CDCl_3$): δ 8.10–8.13 (m, 2H), 7.78 (d, J = 7.9 Hz, 1H), 7.50 (s, 1H), 7.48 (t, J = 7.9 Hz, 2H), 7.40 (t, J = 7.4 Hz, 1H), 7.15–7.19 (m, 1H), 2.31 (s, 3H); ^{13}C{^{1}H} NMR (151 MHz, $CDCl_3$): δ 164.3, 142.2, 137.0, 134.8, 131.5, 129.8, 129.7, 128.5, 125.4, 121.9, 120.0, 21.1; IR (KBr): 3067, 3045, 2915, 2851, 1609, 1596, 1499, 1471, 1457, 1351, 1218, 1205, 1078, 1016, 992, 825, 755, 701, 678 cm^{-1}; HRMS (ESI-TOF) m/z: [M + H]$^+$ Calcd for $C_{14}H_{12}{}^{79}BrN_4$ 315.0240; Found 315.0241.

*5-Phenyl-2-(o-tolyl)-2H-tetrazole (**1o**):*[15a]

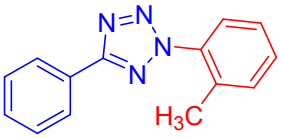

White solid (87.3 mg, 54% yield); R_f = 0.59 (0.5:9.5 EtOAc : hexane, Silica gel); mp 48–50 °C; ^{1}H NMR (400 MHz, $CDCl_3$): δ 8.24–8.27 (m, 2H), 7.67 (d, J = 8.0 Hz, 1H), 7.56–7.48 (m, 3H), 7.48–7.37 (m, 3H), 2.44 (s, 3H); ^{13}C{^{1}H} NMR (101 MHz, $CDCl_3$): δ 165.1, 136.6, 133.2, 132.0, 130.6, 130.5, 129.1, 127.4, 127.1, 127.0, 125.4, 18.9; IR (KBr): 3048, 2923, 2854, 1580, 1494, 1457, 1362, 1284, 1207, 1011, 756, 726, 693 cm^{-1}; HRMS (ESI-TOF) m/z: [M + H]$^+$ Calcd for $C_{14}H_{13}N_4$ 237.1135; Found 237.1138.

*2-(4-Methoxyphenyl)-5-phenyl-2H-tetrazole (**1p**):*[15a]

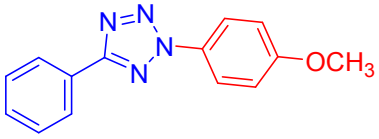

White solid (134 mg, 53% yield); R_f = 0.40 (0.5:9.5 EtOAc : hexane, Silica gel); mp 100–102 °C; ^{1}H NMR (400 MHz, $CDCl_3$): δ 8.24 (dd, J = 7.8, 1.8 Hz, 2H), 8.11 (d, J = 9.1 Hz, 2H), 7.55–7.48 (m, 3H), 7.07 (d, J = 9.1 Hz, 2H), 3.90 (s, 3H); ^{13}C{^{1}H} NMR (101 MHz, $CDCl_3$): δ 165.1, 160.6, 130.6, 130.5, 129.1, 127.5, 127.1, 121.6, 114.8, 55.8; IR (KBr): 3013, 2923, 2850, 1595, 1512, 1454, 1258, 1182, 1020, 830, 725, 692 cm^{-1}; HRMS (ESI-TOF) m/z: [M + H]$^+$ Calcd for $C_{14}H_{13}N_4O$ 253.1084; Found 253.1089.

*2-(4-Ethylphenyl)-5-phenyl-2H-tetrazole (**1q**):*

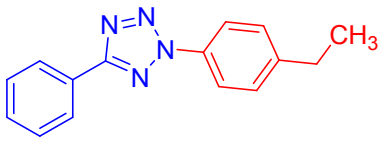

Orange solid (143 mg, 57% yield); R_f = 0.67 (0.5:9.5 EtOAc : hexane, Silica gel); mp 39–41 °C; ^{1}H NMR (400 MHz, $CDCl_3$): δ 8.25 (dd, J =

7.8, 1.8 Hz, 2H), 8.10 (d, J = 8.6 Hz, 2H), 7.51 (dd, J = 5.5, 3.5 Hz, 3H), 7.39 (d, J = 8.6 Hz, 2H), 2.75 (q, J = 7.6 Hz, 2H), 1.30 (t, J = 7.6 Hz, 3H); $^{13}C\{^1H\}$ NMR (101 MHz, $CDCl_3$): δ 165.2, 146.3, 135.0, 130.6, 129.2, 129.1, 127.5, 127.2, 120.0, 28.7, 15.5; IR (KBr): 3038, 2963, 2929, 2867, 1513, 1453, 1285, 1211, 1013, 835, 730, 693 cm^{-1}; HRMS (ESI-TOF) m/z: [M + H]$^+$ Calcd for $C_{15}H_{15}N_4$ 251.1291; Found 251.1293.

*2-(4-Fluorophenyl)-5-phenyl-2H-tetrazole (**1r**):*[37d]

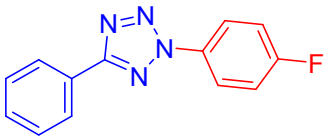

White solid (144 mg, 60% yield); R_f = 0.63 (0.5:9.5 EtOAc : hexane, Silica gel); mp 129–131 °C; ^1H NMR (600 MHz, $CDCl_3$): δ 8.23 (dd, J = 7.8, 1.5 Hz, 2H), 8.18 (dd, J = 9.0, 4.6 Hz, 2H), 7.52 (dt, J = 13.8, 4.5 Hz, 3H), 7.26 (t, J = 8.5 Hz, 2H); $^{13}C\{^1H\}$ NMR (101 MHz, $CDCl_3$): δ 165.5, 163.1 (d, J = 251.2 Hz), 133.1, 130.8, 129.1, 127.2, 121.9 (d, J = 8.7 Hz), 116.8, 116.7; ^{19}F NMR (377 MHz, $CDCl_3$): δ –102.30; IR (KBr): 3087, 2924, 1598, 1506, 1451, 1362, 1288, 1229, 1154, 1071, 836, 726, 689 cm^{-1}; HRMS (ESI-TOF) m/z: [M + H]$^+$ Calcd for $C_{13}H_{10}FN_4$ 241.0884; Found 241.0889.

*2-(4-Bromophenyl)-5-phenyl-2H-tetrazole (**1s**):*[37e]

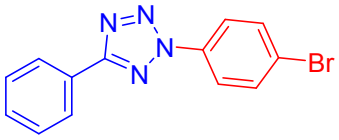

White solid (184 mg, 61% yield); R_f = 0.6 (0.1:9.5 EtOAc : hexane, Silica gel); mp 121–123 °C; ^1H NMR (600 MHz, $CDCl_3$): δ 8.23 (dd, J = 7.7, 1.8 Hz, 2H), 8.07 (d, J = 8.9 Hz, 2H), 7.69 (d, J = 8.9 Hz, 2H), 7.59–7.42 (m, 3H); $^{13}C\{^1H\}$ NMR (151 MHz, $CDCl_3$): δ 165.5, 135.9, 133.0, 130.8, 129.1, 127.2, 127.0, 123.6, 121.3; IR (KBr): 3054, 2923, 2856, 1547, 1481, 1446, 1282, 1084, 1023, 967, 773, 721, 693 cm^{-1}; HRMS (ESI-TOF) m/z: [M + H]$^+$ Calcd for $C_{13}H_{10}{}^{79}BrN_4$ 301.0083; Found 301.0091.

*2,2,6,6-Tetramethyl-1-(undecyloxy)piperidine (**bi**):*[38]

Colorless liquid (448 mg, 72% yield); R_f = 0.6 (0.2:9.8 EtOAc : hexane, Silica gel); ^1H NMR (600 MHz, $CDCl_3$): δ 3.68 (t, J = 6.7 Hz, 2H), 1.50–1.45 (m, 2H), 1.44–1.37 (m, 4H), 1.33–1.19 (m, 18H), 1.11 (s, 6H), 1.06 (s, 6H), 0.85 (t, J = 7.0 Hz, 3H); $^{13}C\{^1H\}$ NMR

(151 MHz, $CDCl_3$): δ 77.1, 59.8, 39.8, 33.2, 32.1, 29.88, 29.79, 29.78, 29.76, 29.5, 28.9, 26.6, 22.8, 20.3, 17.3, 14.3; IR (KBr): 2923, 2857, 1459, 1365, 1254, 1132, 1041, 962, 714, 586, 507 cm^{-1}; HRMS (ESI-TOF) m/z: $[M + H]^+$ Calcd for $C_{20}H_{42}NO$ 312.3261; Found 312.3258.

*5-(m-Tolyl)-2H-tetrazol-2-yl benzoate (**20n'**):*

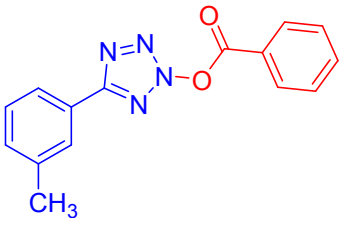

Gummy (205 mg, 73% yield); R_f = 0.58 (0.5:9.5 EtOAc : hexane, Silica gel); ^1H NMR (600 MHz, $CDCl_3$): δ 8.15 (dd, J = 7.8, 1.7 Hz, 2H), 7.97 (s, 1H), 7.94 (d, J = 7.7 Hz, 1H), 7.57–7.51 (m, 3H), 7.42 (t, J = 7.6 Hz, 1H), 7.36 (d, J = 7.6 Hz, 1H), 2.46 (s, 3H); $^{13}C\{^1H\}$ NMR (151 MHz, $CDCl_3$): δ 164.9, 164.6, 139.1, 132.7, 131.8, 129.2, 129.1, 127.6, 127.1, 124.2, 124.1, 123.9, 21.5; IR (KBr): 3065, 2929, 2856, 1724, 1592, 1547, 1447, 1274, 1122, 1084, 1028, 964, 774, 729, 689, 449 cm^{-1}

*2-Phenyl-5-(m-tolyl)-2H-tetrazole (**20n**):*

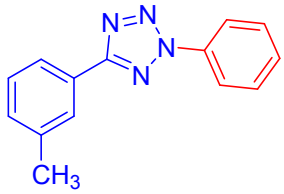

White solid (77 mg, 51% yield); R_f = 0.64 (0.5:9.5 EtOAc : hexane, Silica gel); ^1H NMR (600 MHz, $CDCl_3$): δ 8.17 (d, J = 7.6 Hz, 2H), 8.06 (s, 1H), 8.03 (d, J = 7.7 Hz, 1H), 7.54 (t, J = 7.8 Hz, 2H), 7.47 (t, J = 7.4 Hz, 1H), 7.39 (t, J = 7.6 Hz, 1H), 7.29 (d, J = 7.5 Hz, 1H), 2.43 (s, 3H); $^{13}C\{^1H\}$ NMR (151 MHz, $CDCl_3$): δ 165.4, 138.9, 137.0, 131.5, 129.8, 129.7, 129.0, 127.7, 127.1, 124.3, 119.9, 21.5; IR (KBr): 3067, 2920, 2857, 2343, 1599, 1488, 1206, 1072, 999, 913, 803, 757, 987 cm^{-1}; HRMS (ESI-TOF) m/z: $[M + H]^+$ Calcd for $C_{14}H_{13}N_4$ 237.1135; Found 237.1137.

AUTHOR INFORMATION

Corresponding Author

*E-mail: patel@iitg.ac.in

*E-mail: sugumarv@iisermohali.ac.in

Supporting Information Available

The Supporting Information is available free of charge on the ACS Publications website at http://pubs.acs.org. X-ray data's for **7a** and **1s** (CIF), spectral and analytical data of all products.

ACKNOWLEDGMENT

B. K. P acknowledges the support of this research by the Department of Science and Technology (DST/SERB) (EMR/2016/007042) and MHRD: 5-5/2014-TS-VII (SB/S1/OC-53/2013), New Delhi and CIF for instrumental facilities. SV is thankful to IISERM and the Science and Engineering Research Board (SERB), New Delhi (CRG/2019/005744) for the financial support and providing computational facilities. RS thanks Dr. Ganesh Majji, Dr. Sourav Kumar Santra, Dr. R. Elan Cheran, S. Muruganantham and Neelam Sarmah for their help and valuable suggestion to improve the manuscript quality. We are also thankful to IITG central instrument facilities for the spectroscopic support.

REFERENCES

(1) (a) Zard, S. Z. Recent Progress in the Generation and Use of Nitrogen-Centred Radicals. *Chem. Soc. Rev.* **2008**, *37*, 1603–1618, DOI: 10.1039/B613443M. (b) Faulkner, A.; Race, N. J.; Scott, J. S.; Bower, J. F. Copper Catalyzed Heck-Like Cyclizations of Oxime Esters. *Chem. Sci.* **2014**, *5*, 2416–2421, DOI: 10.1039/C4SC00652F. (c) Guindon, Y.; Guérin, B.; Landry, S. R. Intramolecular Aminyl and Iminyl Radical Additions to α,β-Unsaturated Esters. Diastereoselective Tandem Cyclofunctionalization and Hydrogen Transfer Reactions. *Org. Lett.* **2001**, *3*, 2293–2296, DOI: 10.1021/ol0160809.

(2) (a) Wolff, M. E. Cyclization of N–Halogenated Amines the Hofmann-Löffler Reaction. *Chem. Rev*. **1963**, *63*, 55–64, DOI: 10.1021/cr60221a004. (b) Hofmann, A. W. Knowledge of Piperidine and Pyridine. *Ber. Dtsch. Chem. Ges*. **1879**, *12*, 984–990, DOI: 10.1002/cber.187901201254. (c) Hofmann, A. W. To know the Coniin group. *Ber. Dtsch. Chem. Ges*. **1885**, *18*, 5–23, DOI: 10.1002/cber.18850180103. (d) Löffler, K.; Freytag, C. On a New Way of Forming *N*-Alkylated Pyrrolidines. *Ber. Dtsch. Chem. Ges*. **1909**, *42*, 3427–3431, DOI: 10.1002/cber.19090420377. (e) Hu, X.; Zhang, G.; Bu, F.; Nie, L.; Lei, A. Electrochemical-Oxidation-Induced Site-Selective Intramolecular C(sp^3)–H Amination. *ACS Catal*. **2018**, *8*, 9370–9375, DOI: 10.1021/acscatal.8b02847.

(3) (a) Chen, J.-R.; Hu, X.-Q.; Lu, L.-Q.; Xiao, W.-J. Visible Light Photoredox-Controlled Reactions of N-Radicals and Radical Ions. *Chem. Soc. Rev.* **2016**, *45*, 2044–2056, DOI: 10.1039/C5CS00655D. (b) Kärkäs, M. D. Photochemical Generation of Nitrogen-Centered Amidyl, Hydrazonyl, and Imidyl Radicals: Methodology Developments and Catalytic

Applications. *ACS Catal*. **2017**, *7*, 4999−5022, DOI: 10.1021/acscatal.7b01385. (c) Davies, J.; Svejstrup, T. D.; Reina, D. F.; Sheikh, N. S.; Leonori, D. Visible-Light-Mediated Synthesis of Amidyl Radicals: Transition-Metal-Free Hydroamination and N-Arylation Reactions. *J. Am. Chem. Soc*. **2016**, *138*, 8092−8095, DOI: 10.1021/jacs.6b04920.

(4) Aruri, H.; Singh, U.; Kumar, M.; Sharma, S.; Aithagani, S. K.; Gupta, V. K.; Mignani, S.; Vishwakarma, R. A.; Singh, P. P. Metal-free Cross-Dehydrogenative Coupling of HN-azoles with α-C(sp^3)-H Amides via C–H Activation and Its Mechanistic and Application Studies. *J. Org. Chem*. **2017**, *82*, 1000−1002, DOI: 10.1021/acs.joc.6b02448.

(5) (a) Myznikov, L. V.; Hrabalek, A.; Koldobskii, G. I. Drugs in the Tetrazole Series. *Chem. Heterocycl. Compd*. **2007**, *43*, 1−9, DOI: 10.1007/s10593-007-0001-5. (b) Klapötke, T. M.; Piercey, D. G. 1,1′-Azobis(tetrazole): A Highly Energetic Nitrogen-Rich Compound with a N_{10} Chain. *Inorg. Chem.* **2011**, *50*, 2732−2734, DOI: 10.1021/ic200071q. (c) Singh, H.; Chawla, A. S.; Kapoor, V. K.; Paul, D.; Malhotra, R. K. Medicinal Chemistry of Tetrazoles. *Prog. Med. Chem.* **1980**, *17*, 151−183, DOI: 10.1016/S0079-6468(08)70159-0. (d) Wittenberger, S.-J. Recent Developments in Tetrazole Chemistry. A Review. *Org. Prep. Proced. Int.* **1994**, *26*, 499−531, DOI: 10.1080/00304949409458050.

(6) (a) Massi, M.; Stagni, S.; Ogden, M. I. Lanthanoid Tetrazole Coordination Complexes. *Coord. Chem. Rev*. **2018**, *375*, 164−172, DOI: 10.1016/j.ccr.2017.11.017. (b) Giraud, M.; Andreiadis, E. S.; Fisyuk, A. S.; Demadrille, R.; Pecaut, J.; Imbert, D.; Mazzanti, M. Efficient Sensitization of Lanthanide Luminescence by Tetrazole-Based Polydentate Ligands. *Inorg. Chem.* **2008**, *47*, 3952−3954, DOI: 10.1021/ic8005663.

(7) (a) Monk, B. C.; Keniya, M. V.; Sabherwal, M.; Wilson, R. K.; Graham, D. O.; Hassan, H. F.; Chen, D.; Tyndall, J. D. A. Azole Resistance Reduces Susceptibility to the Tetrazole Antifungal VT-1161. *Antimicrob. Agents Chemother.* **2019**, *63*, 2114−2118, DOI: 10.1128/AAC.02114-18. (b) Christian, I.; Grosjean-Cournoyer, M.-C.; Hutin, P.; Rinolfi, P.; Tuch, A.; Vidal, J. Fungicide. Hydroximoyl-Tetrazole Dervatives. WO/2008/006875 A1, 2008. (c) Upadhayaya, R. S.; Jain, S.; Sinha, N.; Kishore, N.; Chandra, R.; Arora, S. K. Synthesis of Novel Substituted Tetrazoles having Antifungal Activity. *Eur. J. Med. Chem*. **2004**, *39*, 579−592, DOI:10.1016/j.ejmech.2004.03.004.

(8) Frija, L. M. T.; Ismael, A.; Cristiano, M. L. S. Photochemical Transformations of Tetrazole Derivatives: Applications in Organic Synthesis. *Molecules* **2010**, *15*, 3757–3774, DOI: 10.3390/molecules15053757.

(9) (a) Herr, R. J. 5-Substituted-1*H*-tetrazoles as Carboxylic Acid Isosteres: Medicinal Chemistry and Synthetic Methods. *Bioorg. Med. Chem*. **2002**, *10*, 3379–3393, DOI: 10.1016/S0968-0896(02)00239-0. (b) Ballatore, C.; Huryn, D. M.; Smith, A. B., III. Carboxylic Acid (Bio)Isosteres in Drug Design. *ChemMedChem* **2013**, *8*, 385–395, DOI: 10.1002/cmdc.201200585. (c) Patani, G. A.; LaVoie, E. J. Bioisosterism: A Rational Approach in Drug Design. *Chem. Rev*. **1996**, *96*, 3147–3176, DOI: 10.1021/cr950066q.

(10) (a) Madasu, S. B.; Vekariya, N. A.; Koteswaramma, C.; Islam, A.; Sanasi, P. D.; Korupolu, R. B. An Efficient, Commercially Viable, and Safe Process for Preparation of Losartan Potassium, an Angiotensin II Receptor Antagonist. *Org. Process Res. Dev*. **2012**, *16*, 2025–2030, DOI: 10.1021/op300179u. (b) Suseendharnath, A.; Joshi, V. M.; Beeram, S. R.; Vobalaboina, V.; Bhagwatwar, H. P.; Chawla, M. Candesartan Pharmaceutical Compositions. WO/2012/033983 A2, 2012. (c) Muszalska, I.; Sobczak, A.; Dołhań, A.; Jelińska, A. Analysis of Sartans: A Review. *J. Pharm. Sci.* **2014**, *103*, 2–28, DOI: 10.1002/jps.23760. (d) NisnevichIgor, G.; Rukhman, I.; Pertsikov, B.; Kaftanov, J.; Dolitzky, B.-Z. Novel Synthesis of Irbesartan. WO/2004/007482 A2, 2004. (e) Yanagihara, Y.; Kasai, H.; Kawashima, T.; Ninomiya, K. Immunopharmacological Studies on TBX, a New Antiallergic Drug Effects on Type II to IV Allergic Reactions and Immunological Functions in Animal Models. *Jpn. J. Pharmacol.* **1989**, *51*, 93–100, DOI: 10.1254/jjp.51.93. (f) Suh, O. K.; Kim, S. H.; Lee, M. G. Pharmacokinetics and Pharmacodynamics of Azosemide. *Biopharm. Drug Dispos*. **2003**, *24*, 275–297, DOI: 10.1002/bdd.365.

(11) Szimhardt, N.; Wurzenberger, M. H. H.; Beringer, A.; Daumann, L.; Stierstorfer, *J. Coord. Chem.* with 1-Methyl-5*H*-tetrazole: Cocrystallization, Laser-Ignition, Lead-Free Primary Explosives – One Ligand, Three Goals. *J. Mater. Chem. A* **2017**, *5*, 23753–23765, DOI: 10.1039/C7TA07780G.

(12) (a) Ronald G. Hall II, Smith, W. J.; Putnam, W. C.; Pass, S. E. An Evaluation of Tedizolid for the Treatment of MRSA Infections. *Expert Opin. Pharmacother*. **2018**, *19*, 1489–1494, DOI: 10.1080/14656566.2018.1519021. (b) McCool, R.; Gould, I. M.; Eales, J.; Barata, T.; Arber, M.;

Fleetwood, K.; Glanville, J.; Kauf, T. L. Systematic Review and Network Meta-Analysis of Tedizolid for the Treatment of Acute Bacterial Skin and Skin Structure Infections Caused by MRSA. *BMC Infect. Dis*. **2017**, *17*, 39–49, DOI: 10.1186/s12879-016-2100-3. (c) Bayer, A. S.; Abdelhady, W.; Li, L.; Gonzales, R.; Xiong. Y. Q. Comparative Efficacies of Tedizolid Phosphate, Linezolid, and Vancomycin in a Murine Model of Subcutaneous Catheter-Related Biofilm Infection Due to Methicillin-Susceptible and -Resistant Staphylococcus Aureus. *Antimicrob. Agents Chemother*. **2016**, *60*, 5092−5096, DOI: 10.1128/AAC.00880-16. (d) Im, W. B.; Choi, S. H.; Park, J.-Y.; Choi, S. H.; Finn, J.; Yoon, S.-H. Discovery of Torezolid as a Novel 5-Hydroxymethyl-Oxazolidinone Antibacterial Agent. *Eur. J. Med. Chem.* **2011**, *46,* 1027−1039, DOI: 10.1016/j.ejmech.2011.01.014. (e) Flick, A. C.; Ding, H. X.; Leverett, C. A.; Kyne, R. E.; Liu, K. K.-C.; Fink, S. J.; O'Donnell, C. J. Synthetic Approaches to the 2014 New Drugs. *Bioorg. Med. Chem*. **2016**, *24*, 1937−1980, DOI: 10.1016/j.bmc.2016.03.004.

(13) Köhler, S. C.; Wiese, M. HM30181 Derivatives as Novel Potent and Selective Inhibitors of the Breast Cancer Resistance Protein (BCRP/ABCG2). *J. Med. Chem.* **2015**, *58*, 3910–3921, DOI: 10.1021/acs.jmedchem.5b00188.

(14) (a) Jo, Y. W.; Im, W. B.; Rhee, J. K.; Shim, M. J.; Kim, W. B.; Choi, E. C. Synthesis and Antibacterial Activity of Oxazolidinones Containing Pyridine Substituted with Heteroaromatic Ring. *Bioorg. Med. Chem.* **2004**, *12*, 5909–5919, DOI: 10.1016/j.bmc.2004.08.025. (b) Mahy, W.; Leitch, J. A.; Frost, C. G. Copper Catalyzed Assembly of N-Aryloxazolidinones: Synthesis of Linezolid, Tedizolid, and Rivaroxaban. *Eur. J. Org. Chem*. **2016**, 1305−1313, DOI: 10.1002/ejoc.201600033. (c) Prhavc, M.; Kobe, J. Novel Regioselective *N*-Alkylations of 5-Substituted *2H*-Tetrazoles. *Tetrahedron Lett*. **1990**, *31*, 1925–1928, DOI: 10.1016/S0040-4039(00)98819-1. (d) Wang, L.; Zhu, K.; Chen, Q.; He, M. –Y. Transition-Metal-Free Direct Alkylation of Aryl Tetrazoles via Intermolecular Oxidative C–N Formation. *J. Org. Chem.* **2014**, *79*, 11780−11786, DOI: 10.1021/jo502283h. (e) Rajamanickam, S.; Majji, G.; Santra, S. K.; Patel, B. K. Bu_4NI Catalyzed C–N Bond Formation via Cross-Dehydrogenative Coupling of Aryl Ethers (Csp^3–H) and Tetrazoles (N–H). *Org. Lett*. **2015**, *17*, 5586, DOI: 10.1021/acs.orglett.5b02749. (f) Wang, L.; Zhu, K.-Q.; Wu, W.-T.; Chen, Q.; He, M.-Y. *n*-Bu_4NI-Catalyzed Direct Amination of Ethers with Aryl Tetrazoles and Triazoles via Cross-Dehydrogenative Coupling Reaction. *Catal. Sci. Technol*. **2015**, *5*, 2891−2896, DOI: 10.1039/C5CY00229J. (g) Zhu, K.; Wang, L.; Chen, Q.; He, M. Iron-Catalyzed Oxidative

Dehydrogenative Coupling of Ethers with Aryl Tetrazoles. *Tetrahedron Lett*. **2015**, *56*, 4943–4946, DOI: 10.1016/j.tetlet.2015.06.091.

(15) (a) Li, Y.; Gao, L.-X.; Han, F.-S. Efficient Synthesis of 2,5-Disubstituted Tetrazoles via the Cu_2O-Catalyzed Aerobic Oxidative Direct Cross-Coupling of N–H Free Tetrazoles with Boronic Acids. *Chem. Commun*. **2012**, *48*, 2719–2721, DOI:10.1039/C2CC17894J. (b) Liu, C.-Y.; Li, Y.; Ding, J.-Y.; Dong, D.-W.; Han, F.-S. The Development of Copper-Catalyzed Aerobic Oxidative Coupling of H-Tetrazoles with Boronic Acids and an Insight into the Reaction Mechanism. *Chem. - Eur. J.* **2014**, *20*, 2373–2381, DOI: 10.1002/chem.201302857. (c) Onaka, T.; Umemoto, H.; Miki, Y.; Nakamura, A.; Maegawa, T. $[Cu(OH)(TMEDA)]_2Cl_2$-Catalyzed Regioselective 2-Arylation of 5-Substituted Tetrazoles with Boronic Acids under Mild Conditions. *J. Org. Chem*. **2014**, *79*, 6703–6707, DOI: 10.1021/jo500862t.

(16) (a) Davydov, D. V.; Beletskaya, I. P.; Semenov, B. B.; Smushkevich, Y. I. Regioselective Arylation of *N*-Tributylstannylated 5-Substituted Tetrazoles by Diaryliodonium Salts in the Presence of $Cu(OAc)_2$. *Tetrahedron Lett*. **2002**, *43*, 6217–6219, DOI: 10.1016/S0040-4039(02)01326-6. (b) Beletskaya, I. P.; Davydov, D. V.; Gorovoy, M. S. Palladium- and Copper-Catalyzed Selective Arylation of 5-Aryltetrazoles by Diaryliodonium Salts. *Tetrahedron Lett*. **2002**, *43*, 6221–6223, DOI: 10.1016/S0040-4039(02)01325-4.

(17) Zhu, Y.; Yan, H.; Lu, L.; Liu, D.; Rong, G.; Mao, J. Copper-Catalyzed Methyl Esterification Reactions via C–C Bond Cleavage. *J. Org. Chem*. **2013**, *78*, 9898–9905, DOI: 10.1021/jo4016387.

(18) (a) Rueda-Becerril, M.; Sazepin, C. C.; Leung, J. C.; Okbinoglu, T.; Kennepohl, P.; Paquin, J. F.; Sammis, G. M. Fluorine Transfer to Alkyl Radicals. *J. Am. Chem. Soc*. **2012**, *134*, 4026–4029, DOI: 10.1021/ja211679v. (b) Babu, K. R.; Zhu, N.; Bao, H. Iron-Catalyzed C–H Alkylation of Heterocyclic C–H Bonds. *Org. Lett*. **2017**, *19*, 46–49, DOI: 10.1021/acs.orglett.6b03287. (c) Jian, W.; Ge, L.; Jiao, Y.; Qian, B.; Bao, H. Iron-Catalyzed Decarboxylative Alkyl Etherification of Vinylarenes with Aliphatic Acids as the Alkyl Source. *Angew. Chem., Int. Ed.* **2017**, *56*, 3650, DOI: 10.1002/anie.201612365. (d) Qian, B.; Chen, S.; Wang, T.; Zhang, X.; Bao, H. Iron-Catalyzed Carboamination of Olefins: Synthesis of Amines and Disubstituted β-Amino Acids. *J. Am. Chem. Soc*. **2017**, *139*, 13076–13082, DOI: 10.1021/jacs.7b06590. (e) Ye, C.; Qian, B.; Li, Y.; Su, M.; Li, D.; Bao, H. Iron-Catalyzed Dehydrative Alkylation of Propargyl Alcohol with Alkyl Peroxides to Form Substituted 1,3-Enynes. *Org. Lett*. **2018**, *20*, 3202–3205, DOI:

10.1021/acs.orglett.8b01043. (f) Li, Y.; Ge, L.; Muhammad, T. M.; Bao, H. Recent Progress on Radical Decarboxylative Alkylation for Csp^3–C Bond Formation. *Synthesis* **2017**, *49*, 5263−5284, DOI: 10.1055/s-0036-1590935, and references cited therein.

(19) (a) Henry, R. A. Methylation of 5-Phenyltetrazole. *J. Am. Chem. Soc*. **1951**, *73*, 4470–4470, DOI: 10.1021/ja01153a517. (b) Xie, A.; Zhang, Q.; Liu, Y.; Feng, L.; Hu, X.; Dong, W. An Environmentally Friendly Method for *N*-Methylation of 5-Substituted 1*H*-Tetrazoles with a Green Methylating Reagent: Dimethyl Carbonate. *J. Heterocycl. Chem*. **2015**, *52*, 1483−1487, DOI: 10.1002/jhet.2179. (c) Butler, R. N.; Garvin, V. C. A Study of Annular Tautomerism, Interannular Conjugation, and Methylation Reactions of ortho-Substituted-5-Aryltetrazoles Using Carbon-13 and Hydrogen-1 N.M.R. Spectroscopy. *J. Chem. Soc., Perkin Trans. I*, **1981**, 390–393, DOI: 10.1039/P19810000390. (d) Fraser, R. R.; Haque, K. E. Nuclear Magnetic Resonance and Mass Spectral Properties of 5-Aryltetrazoles. *Can. J. Chem.* **1968**, *46*, 2855–2859, DOI: 10.1139/v68-471. (e) Imai, T.; Harigae, R.; Moriyama, K.; Togo, H. Preparation of 5-Aryl-2-Alkyltetrazoles with Aromatic Aldehydes, Alkylhydrazine, Di-*tert*-butyl Azodicarboxylate, and [Bis(trifluoroacetoxy)iodo]benzene. *J. Org. Chem*. **2016**, *81*, 3975−3980, DOI: 10.1021/acs.joc.6b00606.

(20) Wei, W.; Zhang, C.; Xu, Y.; Wan, X. Synthesis of *tert*-Butyl Peresters from Aldehydes by Bu_4NI-Catalyzed Metal-Free Oxidation and its Combination with the Kharasch–Sosnovsky Reaction. *Chem. Commun*. **2011**, *47*, 10827−10829, DOI: 10.1039/C1CC14602E.

(21) (a) Bao, X.; Yokoe, T.; Ha, T. M.; Wang, Q.; Zhu, J. Copper-Catalyzed Methylative Difunctionalization of Alkenes. *Nat. Commun*. **2018**, *9*, 3725–3732, DOI: 10.1038/s41467-018-06246-6. (b) Zhang, P.-Z.; Li, J.-A.; Zhang, L.; Shoberu, A.; Zou, J.-P.; Zhang, W. Metal-Free Radical C–H Methylation of Pyrimidinones and Pyridinones with Dicumyl Peroxide. *Green Chem*. **2017**, *19*, 919–923, DOI: 10.1039/C6GC03355E.

(22) (a) Foresman, J. B.; Frisch, Æ. Exploring Chemistry with Electronic Structure Methods, 3rd ed. Gaussian, Inc., Wallingford, CT, 2015. (b) Barckholtz, C.; Barckholtz, T. A.; Hadad, C. M. C−H and N−H Bond Dissociation Energies of Small Aromatic Hydrocarbons. *J. Am. Chem. Soc*. **1999**, *121*, 491−500.

(23) (a) Shi, E. B.; Shao, Y.; Chen, S. L.; Hu, H. Y.; Liu, Z. J.; Zhang, J.; Wan, X. B. Tetrabutylammonium Iodide Catalyzed Synthesis of Allylic Ester with *tert*-Butyl Hydroperoxide

as an Oxidant. *Org. Lett*. **2012**, *14*, 3384−3387, DOI: 10.1021/ol3013606. (b) Wong, Y.-C.; Tseng, C.-T.; Kao, T.-T.; Yeh, Y.-C.; Shia, K.-S. Tandem Cyclization of α-Cyano α-Alkynyl Aryl Ketones Induced by *tert*-Butyl Hydroperoxide and Tetrabutylammonium Iodide. *Org. Lett*. **2012**, *14*, 6024−6027, DOI: 10.1021/ol3028972. (c) Meesin, J.; Pohmakotr, M.; Reutrakul, V.; Soorukram, D.; Leowanawat, P.; Saithong, S.; Kuhakarn, C. TBAI/TBHP-Mediated Cascade Cyclization toward Sulfonylated Indeno[1,2-c]quinolines. *Org. Lett*. **2017**, *19*, 6546−6549, DOI: 10.1021/acs.orglett.7b03246. (d) Liu, Z.; Zhang, J.; Chen, S.; Shi, E.; Xu, Y.; Wan, X. Cross Coupling of Acyl and Aminyl Radicals: Direct Synthesis of Amides Catalyzed by Bu_4NI with TBHP as an Oxidant. *Angew. Chem., Int. Ed*. **2012**, *51*, 3231−3235, DOI: 10.1002/anie.201108763. (e) Majji, G.; Rajamanickam, S.; Khatun, N.; Santra, S. K.; Patel, B. K. Generation of *bis*-Acyl Ketals from Esters and Benzyl Amines Under Oxidative Conditions. *J. Org. Chem*. **2015**, *80*, 3440−3446, DOI: 10.1021/jo502903d. (f) Chen, R.; Chen, J.; Zhang, J.; Wan, X. Combination of Tetrabutylammonium Iodide (TBAI) with *tert*-Butyl Hydroperoxide (TBHP): An Efficient Transition-Metal-Free System to Construct Various Chemical Bonds. *Chem. Rec.* **2018**, *18*, 1292−1305, DOI: 10.1002/tcr.201700069. (g) Majji, G.; Rout, S. K.; Rajamanickam, S.; Guin, S.; Patel, B. K. Synthesis of Esters via sp^3 C–H Functionalisation. *Org. Biomol. Chem*. **2016**, *14*, 8178−8211, DOI:10.1039/C6OB01250G.

(24) We could not obtain the corresponding transition state for (**1x**) even after several attempts. During the searches for the transition state (TS) in (**1x**), we observed deviations from the coplanarity of the phenyl tetrazole radical, and also a rotational motion corresponding to the methyl group that hindered our attempts. However, we were able to estimate the barriers for the H-abstraction by iodine atom in both (**1**) and (**1x**) (23.6 and 25.4 kcal/mol, respectively) (Figure S6). These barriers clearly indicate a marginal preference for the abstraction of N^2-H (kinetically favourable) than N^1-H leading to the same NCR.

(25) (a) Sah, C.; Yadav, A. K.; Venkataramani, S. Deciphering Stability of Five-Membered Heterocyclic Radicals: Balancing Act Between Delocalization and Ring Strain. *J. Phys. Chem. A*. **2018**, *122*, 5464−5476, DOI: 10.1021/acs.jpca.8b03145. (b) Mukhopadhyay, A.; Jacob, L.; Venkataramani, S. Dehydro-Oxazole, Thiazole and Imidazole Radicals: Insights into the Electronic Structure, Stability and Reactivity Aspects. *Phys. Chem. Chem. Phys.* **2017**, *19*, 394−407, DOI: 10.1039/C6CP05677F. (c) Lu, D.; Wu, C.; Li, P. 3-Center-5-Electron Boryl Radicals with $\sigma^0\pi^1$ Ground State Electronic Structure. *Org. Lett*. **2014**, *16*, 1486−1489, DOI:

10.1021/ol500296a. (d) Lv, Y.; Li, Y.; Xiong, T.; Lu, Y.; Liu, Q.; Zhang, Q. *n*Bu_4NI-Catalyzed Oxidative Imidation of Ketones with Imides: Synthesis of α-Amino Ketones. *Chem. Commun*. **2014**, *50*, 2367–2369, DOI: 10.1039/C3CC48887J.

(26) Greene, F. D.; Kazan, J. Preparation of Diacyl Peroxides with *N,N'*-Dicyclohexylcarbodiimide. *J. Org. Chem*. **1963**, *28*, 2168–2171, DOI: 10.1021/jo01044a002.

(27) (a) Walling, C.; Waits, H. P.; Milovanovic, J.; Pappiaonnou, C. G. Polar and Radical Paths in the Decomposition of Diacyl Peroxides. *J. Am. Chem. Soc*. **1970**, *92*, 4927–4932, DOI: 10.1021/ja00719a028. (b) Bartlett, P. D.; Leffler, J. E. Acid Catalysis and the Mechanism of Decomposition of *Bis*-Phenylacetyl Peroxide. *J. Am. Chem. Soc*. **1950**, *72*, 3030–3035, DOI: 10.1021/ja01163a064. (c) Hey, D. H.; Walker, E. W. Union of Aryl Nuclei. Part VII. Reactions with Acyl Peroxides. *J. Chem. Soc*. **1948**, 2213–2220, DOI: 10.1039/JR9480002213.

(28) Beckwith, A. L. J.; Cross, R. T.; Gream, G. E. *Aust. J. Chem*. **1974**, *27*, 1673–1692, DOI: 10.1071/CH9741673.

(29) Yu, W.-Y.; Sit, W. N.; Zhou, Z.; Chan, A. S.-C. Palladium-Catalyzed Decarboxylative Arylation of C−H Bonds by Aryl Acylperoxides. *Org. Lett*. **2009**, *11*, 3174–3177, DOI: 10.1021/ol900756g.

(30) (a) Tokumaru, K. Does Reduction of Organic Peroxides by Iodide Really Proceed via Single Electron Transfer? *Chem. Lett.* **1992**, 523−526, DOI: 10.1246/cl.1992.523. (b) Perrin, C. L.; Wang, J.; Szwarc, M. Two-Electron Transfer from Potassium Anion to Peroxides: Simultaneous or Stepwise? *J. Am. Chem. Soc*. **2000**, *122*, 4569–4572, 10.1021/ja9937369. (c) Tsuchihashi, G.; Miyajima, S.; Otsu, T.; Simamura, O. The Kinetics of the Reactions of Acyl Peroxides with Alkali Iodides-I; The Reactions of Aroyl Peroxides with Potassium Iodide. *Tetrahedron*, **1965**, *21*, 1039–1048, DOI: 10.1016/0040-4020(65)80043-6. (d) Hammond, G. S. The Decomposition of Benzoyl Peroxide in the Presence of Iodine. I. Aromatic Solvents. *J. Am. Chem. Soc*. **1950**, *72*, 3737–3743, DOI: 10.1021/ja01164a115. (e) Kochi, J. K.; Graybill, B. M.; Kurz, M. Reactions of Peroxides with Halide Salts. Electrophilic and Homolytic Halogenations. *J. Am. Chem. Soc*. **1964**, *86*, 5257–5264, DOI: 10.1021/ja01077a043. (f) Bunce, N. J.; Tanner, D. D. Benzoyl Hypochlorite, an Intermediate in the Oxidation of Ionic Chlorides and Hydrogen Chloride by Benzoyl Peroxide. *J. Am. Chem. Soc*. **1969**, *91*, 6096–6102, DOI: 10.1021/ja01050a028.

(31) (a) Okumura, S.; Lin, C.-H.; Takeda, Y.; Minakata, S. J. Oxidative Dimerization of (Hetero)aromatic Amines Utilizing *t*-BuOI Leading to (Hetero)aromatic Azo Compounds: Scope and Mechanistic Studies. *J. Org. Chem*. **2013**, *78*, 12090–12105, DOI: 10.1021/jo402120w. (b) Minakata, S.; Okumura, S.; Nagamachi, T.; Takeda, Y. Generation of Nitrile Oxides from Oximes using *t*-BuOI and their Cycloaddition. *Org. Lett*. **2011**, *13*, 2966–2969, DOI: 10.1021/ol2010616. (c) Barton, D. H. R.; Faro, H. P.; Serebryakov, E. P.; Woolsey, N. F. Photochemical Transformations. Part XVII. Improved Methods for the Decarboxylation of Acids. *J. Chem. Soc*. **1965**, 2438–2444, DOI: 10.1039/JR9650002438. (d) Glover, S. A.; Golding, S. L.; Goosen, A.; McCleland, C. W. Intramolecular Cyclisations of Biphenyl-2-carboxyl Radicals: Evidence for a II-State Aroyloxyl Radical. *J. Chem. Soc., Perkin Trans. 1*, **1981**, 842–848, DOI: 10.1039/P19810000842. (e) Feigl, F.; Anger, V. Spot Tests in Inorganic Analysis 6th editions; Elsevier, pp. 169. (f) Wang, L.; Ren, X.; Yu, J.; Jiang, Y.; Cheng, J. Base-Promoted Formal Arylation of Benzo[d]oxazoles with Acyl Chloride. *J. Org. Chem*. **2013**, *78*, 12076–12081, DOI: 10.1021/jo402106q.

(32) (a) Johnson, R. G.; Ingham, R. K.; The Degradation of Carboxylic Acid Salts by Means of Halogen the Hunsdiecker Reaction. *Chem. Rev*. **1956**, *56*, 219–269, DOI: 10.1021/cr50008a002. (b) Trost, B. M.; Fleming, I. The Hunsdiecker and Related Reactions, Comprehensive Organic Synthesis, Pergamon Press, Oxford, **1991**, *7*, 717. (c) Wang, Z. Hunsdiecker Reaction. Comprehensive Organic Name Reactions and Reagents. John Wiley & Sons, Inc. **2010**, 1511–1515, DOI: 10.1002/9780470638859.

(33) (a) Demko, Z. P.; Sharpless, K. B. Preparation of 5-Substituted 1*H*-Tetrazoles from Nitriles in Water. *J. Org. Chem*. **2001**, *66*, 7945–7950, DOI: 10.1021/jo010635w. (b) Kumar, S.; Dubey, S.; Saxena, N.; Awasthi, S. K. $(NH_4)_2Ce(NO_3)_6$ as an Inexpensive, Eco-Friendly, Efficient Catalyst for the Synthesis of 5-Substituted 1*H* Tetrazoles from Nitriles. *Tetrahedron Lett*. **2014**, *55*, 6034–6038, DOI: 10.1016/j.tetlet.2014.09.010. (c) Vignesh, A.; Bhuvanesh, N. S. P.; Dharmaraj, N. Conversion of Arylboronic Acids to Tetrazoles Catalyzed by ONO Pincer-Type Palladium Complex. *J. Org. Chem.* **2017***, 82*, 887−892*,* DOI: 10.1021/acs.joc.6b02277. (d) Palde, P. B.; Jamison, T. F. Safe and Efficient Tetrazole Synthesis in a Continuous-Flow Microreactor. *Angew. Chem., Int. Ed*. **2011**, *50*, 3525–3528, DOI: 10.1002/anie.201006272. (e) Reddy, M.; Gowd, M. B.; Pasha, M. A. A Versatile and an Efficient Synthesis of 5-Substituted-1*H*-tetrazoles. *J. Chem. Sci.,* **2011,** *123,* 75–79, DOI: 10.1007/s12039-011-0065-8. (f) Zarghani,

M.; Akhlaghinia, B. Magnetically Separable Fe_3O_4@chitin as an Ecofriendly Nanocatalyst with High Efficiency for Green Synthesis of 5-Substituted-1*H*-tetrazoles under Solvent-Free Conditions. *RSC Adv*. **2016**, *6*, 31850, DOI: 10.1039/c6ra07252f.

(34) (a) Becke, A. D. Density-Functional Thermochemistry. III. The Role of Exact Exchange. *J. Chem. Phys.* **1993**, *98*, 5648−5652, DOI: 10.1063/1.464913. (b) Dunning, T. H., Jr. Gaussian Basis Sets for Use in Correlated Molecular Calculations. I. The Atoms Boron through Neon and Hydrogen. *J. Chem. Phys*. **1989**, *90*, 1007–1023, DOI: 10.1063/1.456153. (c) Woon, D. E.; Dunning, T. H., Jr Gaussian Basis Sets for Use in Correlated Molecular Calculations. III. The Atoms Aluminum Through Argon. *J. Chem. Phys.* **1993**, *98*, 1358−1371, DOI: 10.1063/1.464303. (d) Halgren, T. A.; Lipscomb, W. N. The Synchronous-Transit Method for Determining Reaction Pathways and Locating Molecular Transition States. *Chem. Phys. Lett*. **1977**, *49*, 225−232, DOI: 10.1016/0009-2614(77)80574-5. (e) Ayala, P. Y.; Schlegel, H. B. A Combined Method for Determining Reaction Paths, Minima and Transition State Geometries. *J. Chem. Phys.* **1997**, *107*, 375–384, DOI: 10.1063/1.474398. (f) Barone, V. Vibrational Zero-point Energies and Thermodynamic Functions Beyond the Harmonic Approximation. *J. Chem. Phys*. **2004**, *120*, 3059−3065, DOI: 10.1063/1.1637580. (g) Frisch, M. J.; Trucks, G. W.; Schlegel, H. B.; Scuseria, G. E.; Robb, M. A.; Cheeseman, J. R.; Scalmani, G.; Barone, V.; Petersson, G. A.; Nakatsuji, H.; et al. *Gaussian 09*, revision C. 01; Gaussian, Inc.: Wallingford, CT, 2009.

(35) (a) Her, B.; Jones, A.; Wollack, J. W. A Three-Step Synthesis of Benzoyl Peroxide. *J. Chem. Educ*. **2014**, *91*, 1491–1494, DOI: 10.1021/ed400240k. (b) Yao, X.; Weng, X.; Wang, K.; Xiang, H.; Zhou, X. Transition Metal Free Oxygenation of 8-Aminoquinoline Amides in Water. *Green Chem*. **2018**, *20*, 2472–2476, DOI: 10.1039/C8GC00191J. (c) Milne, J. E.; Murry, J. A.; King, A.; Larsen, R. D. Pd-Catalyzed Deoxygenation of Mandelate Esters. *J. Org. Chem*. **2009**, *74*, 445–447, DOI: 10.1021/jo8021499.

(36) (a) Singh, D.; Silakari, O. Sodium Hydrogen Exchanger Inhibitory Activity of Benzotriazole Derivatives. *Eur. J. Med. Chem.* **2017**, *126*, 183–189, DOI: 10.1016/j.ejmech.2016.10.005. (b) Tan, D.; Friščić, T. Carbodiimide Insertion into Sulfonimides: One-Step Route to Azepine Derivatives via a Two-Atom Saccharin Ring Expansion. *Chem. Commun*. **2017**, *53*, 901–904, DOI:10.1039/C6CC07331J. (c) Seliverstova, D. V.; Suslonov, V. V.; Zarubaev, V. V.; Trifonov. R. E. Synthesis, Structure, and Anti-influenza Activity of 2-(Adamantan-1-yl)-5-aryl-1,3,4-

oxadiazoles and 2-(Adamantan-1-yl)-5-aryltetrazoles. *Russ. J. Org. Chem.* **2018**, *54*, 633–638, DOI: 10.1134/S107042801804019X.

(37) (a) Stewart, S.; Harris, R.; Jamieson, C. Regiospecific Synthesis of N2-Aryl 1,2,3-Triazoles from 2,5-Disubstituted Tetrazoles via Photochemically Generated Nitrile Imine Intermediates. *Synlett* **2014**, *25*, 2480–2484, DOI: 10.1055/s-0034-1379010. (b) Li, J.; Huang, L.; Xiao, X.; Chen, Y.; Wang, X.; Zhou, Z.; Zhang, C.; Zhang, Y. Photoclickable MicroRNA for the Intracellular Target Identification of MicroRNAs. *J. Am. Chem. Soc*. **2016**, *138*, 15943–15949, DOI: 10.1021/jacs.6b08521. (c) Shawali, A. S.; Fahmi, A. A.; Eweiss, N. F. Azo Coupling of Benzenesulfonylhydrazones of Heterocyclic Aldehydes. *J. Heterocycl. Chem*. **1979**, *16*, 123–128, DOI: 10.1002/jhet.5570160123. (d) Ramanathan, M.; Wang, Y. H.; Liu, S.-T. One-Pot Reactions for Synthesis of 2,5-Substituted Tetrazoles from Aryldiazonium Salts and Amidines. *Org. Lett*. **2015**, *17*, 5886–5889, DOI: 10.1021/acs.orglett.5b03068. (e) Suketaka, I.; Yumo, T.; Akikazu, K. Synthesis of 2,5-Diaryltetrazoles from N-Phenylsulfonylbenzhydrazidoyl Chlorides and Arylhydrazines. *Bull. Chem. Soc. Jpn.* **1976**, *49*, 762–766, DOI: 10.1246/bcsj.49.762.

(38) Li, Y.; Han, Y.; Xiong, H.; Zhu, N.; Qian, B.; Ye, C.; Kantchev, E. A.; Bao, H. Copper-Catalyzed Regioselective 1,2-Alkylesterification of Dienes to Allylic Esters. *Org. Lett*. **2016**, *18*, 392–395, DOI: 10.1021/acs.orglett.5b03399.